ISTANBUL TECHNICAL UNIVERSITY ★ GRADUATE SCHOOL OF SCIENCE ENGINEERING AND TECHNOLOGY

EFFECTS OF POLYHEDRAL OLIGOMERIC SILSESQUIOXANE REINFORCED POLYPROPYLENE (PP) NANOCOMPOSITES ON THE THERMAL, MECHANICAL, AND OPTICAL PROPERTIES OF PP

M.Sc. THESIS

Sevil KAYNAR

Department of Polymer Science and Technology

Polymer Science and Technology Programme

MAY 2016

ISTANBUL TECHNICAL UNIVERSITY ★ GRADUATE SCHOOL OF SCIENCE ENGINEERING AND TECHNOLOGY

EFFECTS OF POLYHEDRAL OLIGOMERIC SILSESQUIOXANE REINFORCED POLYPROPYLENE (PP) NANOCOMPOSITES ON THE THERMAL, MECHANICAL, AND OPTICAL PROPERTIES OF PP

M.Sc. THESIS

Sevil KAYNAR
(515141023)

Department of Polymer Science and Technology

Polymer Science and Technology Programme

Thesis Advisor : Prof. Dr. Nurseli UYANIK
Co-advisor : Prof. Dr. Mükerrem ÇAKMAK

MAY 2016

İSTANBUL TEKNİK ÜNİVERSİTESİ ★ FEN BİLİMLERİ ENSTİTÜSÜ

POLİHEDRAL OLİGOMERİK SİLSESKUİOKZAN KATKILI POLİPROPİLEN (PP) NANOKOMPOZİTLERİN PP ÜZERİNDEKİ TERMAL, MEKANİK VE OPTİK ÖZELLİKLERİNİN İNCELENMESİ

YÜKSEK LİSANS TEZİ

Sevil KAYNAR
(515141023)

Polimer Bilim ve Teknolojileri Bölümü

Polimer Bilim ve Teknolojileri Programı

Tez Danışmanı : Prof. Dr. Nurseli UYANIK
Tez Eş Danışmanı : Mükerrem ÇAKMAK

MAYIS 2016

Sevil KAYNAR, a M.Sc. student of ITU Graduate School of Science Engineering and Technology student ID 515141023, successfully defended the thesis/dissertation entitled "Effects of Polyhedral Oligomeric Silsesquioxane Reinforced Polypropylene (PP) Nanocomposites on the Thermal, Mechanical, and Optical Properties of PP", which she prepared after fulfilling the requirements specified in the associated legislations, before the jury whose signatures are below.

Thesis Advisor :	**Prof. Dr. Nurseli UYANIK** Istanbul Technical University	.....
Co-advisor :	**Prof.Dr. Mükerrem ÇAKMAK** University of Akron	.....
Jury Members :	**Prof. Dr. Nilgün KIZILCAN** İstanbul Technical University	.....
	Assoc.Prof. Dr. Nurcan TÜZÜN Istanbul Technical University	.....
	Assoc.Prof. Dr. Ali DURMUŞ Istanbul University	.....

Date of Submission : 8 July 2016
Date of Defense : 8 June 2016

FOREWORD

Words stay short in expressing my sincere appreciation and gratitude to my thesis supervisor, ***Prof. Dr. Nurseli UYANIK*** for her infinite support, guidance and helpful suggestions throughout my research. It was a great honor and pleasure to work with her and benefit from her experience.

I am extremely grateful to my co-advisor ***Prof. Dr. Mükerrem ÇAKMAK*** from University of Akron, Department of Polymer Engineering, who inspired me in so many ways. I truly appreciate his patience, helpfulness and encouragement in every aspect of life.

I would like to thank ***Assoc. Prof. Dr. Ali DURMUŞ*** from Istanbul University, Department of Chemical Engineering, providing me to their laboratory facilities.

I would like to show deeply appreciation to ***Assoc. Prof. Dr. H. Ökkeş DEMİR, Gamze Sultan BAŞ*** and ***Dr. Murat BAKAN*** for their all support and helpfullness during my stay at University of Akron.

I want to express great appreciation to ***Ido OFFENBACH, Chao WANG, Enmin WANG***, ***Gustavo GUZMAN*** and all Çakmak group for their support. Also, ***Semih ŞAŞMAZ*** and ***Refik ARAT*** from ITU, for their friendship and support.

I would like to express my thanks to managers of Elkim Rubber Company ***Murat and Gülşen ÖZKILIÇ*** (my uncle and his wife) for their financial support.

I would like to thank to ***Alaettin ŞENKAYA*** for his help to TGA analysis.

I would like to thank all of my other friends for all their emotional assists and motivation during this extremely difficult accomplishment.

My special thanks to ***Aykut TÜRKOĞLU***. He will remain my inspiration forever.

I appreciate my family, my father ***Mehmet KAYNAR*** my mother ***Ayşe KAYNAR***, and my brothers ***Semih and Onur KAYNAR*** for supporting me all my life.

June 2016

Sevil KAYNAR
(Metallurgical and Material Engineer)

TABLE OF CONTENTS

Page

ABBREVIATIONS

PP : Polypropylene
POSS : Polyhedral Oligomeric Silsesquioxanes
PNC : Polymer Nanocomposites
MW : Molecular Weight
Tg : Glass Transition Temperature
Tm : Melting Temperature
DSC : Differential Scanning Calorimeter
TGA : Thermogravimetric Analysis
SEM : Scanning Electron Microscope
SAXS : Small Angle X-ray Scattering
POM : Polarized optical microscope
MFR : Melt Flow Rate
Rpm : Revolutions per minute
MWD : Molecular weight distribution
L/D : Length to diameter ratio

SYMBOLS

Δn_{12} : Birefringence
ΔG_m : Gibbs free energy of mixing
T_m : Melting temperature
T_c : Crystallisation temperature
X_c : Degree of crystallinity
ΔH_m : Fusion enthalpy
ΔH_c : Crystallization enthalpy

LIST OF TABLES

Page

LIST OF FIGURES

Page

EFFECTS OF POLYHEDRAL OLIGOMERIC SILSESQUIOXANE REINFORCED POLYPROPYLENE (PP) NANOCOMPOSITES ON THE THERMAL, MECHANICAL, AND OPTICAL PROPERTIES OF PP

SUMMARY

Polymeric hybrids and nanocomposites containing polyhedral oligomeric silsesquioxanes (POSS) - general formula $(RSiO_{1.5})_n$ where R is an organic group – as dispersed inorganic phase offer the opportunity to design advanced materials with enhanced thermal and mechanical performances. The incorporation of POSS or its derivatives into polymers can lead to some improved properties, such as the increase in use temperature, oxidation resistance, surface hardening and mechanical strengths, as well as reductions in flammability, heat evolution, and viscosity during processing. It has been pointed out that the morphology, the thermal stability and tensile properties of thermoplastics (polyolefins, polyesters, polyamides, etc.) containing POSS can be largely affected by the chemical structure, concentration and dispersion degree of POSS nanoparticles. It is possible to obtain dispersion of POSS particles to the scale of individual molecules with size approximately 1-2 nm. In view of this, POSS molecules are nearly equivalent in size to most polymer segments and, therefore, potentially can exert dramatic reinforcement effects. In contrast to other nanofillers, such as layered silicates which are platy and carbon nanotubes which are cylindrical, the shape of the POSS molecules is isotropic. In addition, POSS molecules can be easily functionalized by chemically altering the R groups. This presents opportunities for copolymerization or grafting reactions with functional groups on polymer chains and for defining and controlling the nature of interactions between POSS molecules and the polymer chains.

Polypropylene (PP) is a versatile member of polyolefins and this thermoplastic polymer is used in a wide variety of applications including packaging, textiles, stationery, plastic parts and reusable containers of various types, laboratory equipment, loudspeakers and automotive components. PP has been used as the matrix material in a commercial form because of its many attractive properties, such as low weight, relatively low cost, excellent heat distortion temperature (above 100 °C) and its recycling ability. But its toughness, strength and stiffness are not sufficient for applications as an engineering plastic. To reinforce PP, polymer nanocomposite technique by adding rigid polymers, is used.

In this study, 1, 3, 5, 8, 10 wt-% POSS containing PP nanocomposites PP/POSS nanocomposites (PP/POSS NC) were prepared by melt blending via extrusion. Methyl-POSS reinforced polypropylene (PP) nanocomposite was used as POSS carrier material (or as a masterbatch) and the effects of methyl-polyhedral oligomeric silsesquioxanes (methyl-POSS) on the rheological, and thermal behavior of polypropylene (PP) were investigated.

Rheological studies of PP/POSS NC pellets were operated by using parallel plate rheometry at three different temperatures. For all samples, it can be observed that complex viscosity (η*) decreases with increasing frequency, both storage modulus (G') and loss modulus (G") progressively increase with increasing frequency. Complex viscosity showed large increase with reduction of temperature at high frequency. The

increase of frequency causes the restriction of chain movements and a stiffer behavior was observed.

Thermal behaviors of nanocomposites were characterized by DSC and TGA. The fusion enthalpy of the nanocomposites (obtained by peak integration) decreases with increasing of POSS content. 5% and 10% weight loss temperatures obtained from TGA curves. It was observed that increasing of POSS content increased these degredation temperatures and also the thermal stability of nanocomposites.

The prepared PP/POSS nanocomposites and PP pellets were also subjected to melt spinning process by using capillary rheometer with 6 take up speed and 3 plunger speed to produce 97 fiber samples. Draw down ratio ($DDR=D_{die}^2/D_{fiber}^2$) of fibers were calculated and the effects of draw down ratio on the strength, and polymer chain orientation were investigated by mechanically, optically and morphologically.

Mechanical properties of prepared fiber samples measured by universal testing machine. It was observed that POSS composition and DDR of the nanocomposites had a pronounced effect on the tensile properties of these materials. Tensile data shows that the modulus increase with increasing of take up speed and decreasing by increasing of POSS content. Addionally, the maximum load, tensile strain at maximum load, and tensile strain at break decreases with increasing of take up speed.

Morphological characterizations were made by using polarized optical microscope (POM) and small angle X-ray scattering (SAXS). Birefringence data of fibers calculated by using POM images and DDR of samples. For all fibers, increasing of DDR lead to increase birefringence. The other result was that increasing of POSS content caused the decrease of birefringence values with the comparison of neat PP.

SAXS pattern clearly showed that isotropy of fibers increases with increasing of POSS content. On the other side, increasing of take up speed increases anisotropy. Increasing of take up speed also increased the fiber orientation. Furthermore, it was observed that high POSS content fibers have more isotropic structure. In consideration of this observation it is clearly seen that POSS content effects the morphology of fibers significantly.

POLİHEDRAL OLİGOMERİK SİLSESKUİOKZAN KATKILI POLİPROPİLEN (PP) NANOKOMPOZİTLERİN PP ÜZERİNDEKİ TERMAL, MEKANİK VE OPTİK ÖZELLİKLERİNİN İNCELENMESİ

ÖZET

Polihedral oligomerik silseskuiokzan (POSS), genel formülü R organik grup olmak üzere (RSiO1.5)n, içeren polimerik hibritler ve nanokompozitler, dağılmış inorganik faz sayesinde termal ve mekanik performansı gelişmiş malzeme tasarımına olanak sağlamaktadır. POSS veya türevlerinin polimere katılımı ile kullanım sıcaklığı, oksidasyon dayanımı, yüzey sertliği ve mekanik dayanımı, yanma özelliği, ısı ölçümü, proses esnasındaki viskozitesi gibi bir çok özelliğinin önemli ölçüde değişimine neden olmaktadır. Morfolojilerine dikkat edecek olursak, POSS nanopartiküllerin kimyasal yapısı, konsantrasyonu ve dağılma derecesi POSS içeren termoplastiklerin (poliolefinler, polyesterler, poliamidler) ısıl kararlılığını ve çekme özelliğini önemli ölçüde etkilemektedir. POSS partiküllerinin dağılımını, her bir molülünün ölçüsü yaklaşık 1-2 nm olacak şekilde sağlayabilmek mümkündür. Görüldüğü üzere, POSS molekülleri birçok polimer bölümüyle hemen hemen eşit boyuta sahiptir ve bu yüzden önemli ölçüde takviye etkisi gösterebilmektedir. Yassı katmanlı silikatlar ve silindirik yapıdaki karbon nanotüpler gibi diğer nanodolguların aksine, POSS moleküllerinin şekli izotropiktir. Bununla beraber POSS molekülleri kimyasal olarak R gruplarının değiştirilmesiyle kolay bir şekilde işlevsel hale getirilebilmektedir. R gruplarının işlevselliği de polimer zincirindeki fonksiyonel gruplar ile kopolimerizasyon veya aşılama reaksiyonlarına ve POSS molekülleri ile polimer zincirleri arasındaki etkileşiminin belirlenmesine ve ayrıca POSS molekülleri ile polimer zincirleri arasındaki tepkimelerin kontrol edilmesine olanak sağlar.

Polipropilen (PP) poliolefinlerin çok yönlü bir üyesidir ve bu termoplastik polimer ambalaj, tekstil, kırtasiye, plastik bölümler ve çeşitli yeniden kullanılabilir konteynırlar, laboratuvar ekipmanları, hoparlörler ve otomobil parçaları gibi çok çeşitli uygulamalarda kullanılır. PP hafif oluşu, düşük maliyeti, mükemmel ısıl bozulma sıcaklığı (yaklaşık 100 °C) ve geri dönüştürülebilme özelliği dolayısıyla ticarette matris malzemesi olarak kullanılmaktadır. Fakat PP'nin dayanımı, tokluğu ve sertliği mühendislik plastiği uygulamalarında kullanılmak için yeterli değildir. PP'nin kullanım alanını arttırmak ve özelliklerini iyileştirmek için modern teknolojide yaygın olan sert nanokatkılar ekleme yöntemi kullanılabilir. Bu nanokatkılar organik olabileceği gibi inorganik de olabilirler.

Bu çalışmada, %10'a kadar metil-POSS bileşeninden oluşan PP/POSS nanokompozitler çift vidalı ekstrüderde eriyik halde karıştırılarak hazırlanmıştır. %10 metil-POSS katkılı polipropilen (PP), nanokompozitte POSS taşıyıcı malzeme olarak kullanılmıştır. Bu maddenin PP ile eriyik karıştırma yöntemi ile %1, %3, %5, %8 POSS katkılı PP/POSS nanokompozitleri hazırlanmıştır. Saf PP ve saf %10 PP/POSS örnekleri ile beraber toplam 5 farklı yüzdeli PP/POSS nanokompozitleri ve referans PP örneklerinde, POSS'un PP'nin reolojik ve termal davranışları üzerine olan etkileri detaylı bir şekilde araştırılmıştır. Reolojik incelemeler paralel düzlem reometresi ve termal özellikleri de diferansiyel taramalı kalorimetre ve termal gravimetrik analiz ile incelenmiştir.

Reolojik incelemeler için üç farklı (180°C, 205°C ve 230°C) sıcaklıkta yapılan çalışmalarda, tüm örnekler için yüksek frekanslarda kompleks viskozitenin düştüğü (η*), depolama modülü (G') ve kayıp modülün (G") yükseldiği gözlemlenmiştir. Yine yüksek frekanslarda sıcaklık düşüşünün kompleks viskoziteyi önemli ölçüde arttırdığı görülmüştür. Ayrıca 180°C'de kompleks viskozite değerleri 205°C ve 230°C' ye kıyasla önemli bir azalma göstermiştir. Sonuç olarak frekansın yükselmesi zincir hareketlerini kısıtlayarak daha sert (düşük elastikiyet) davranışlar görülmesine sebep olmuştur.

Nanokompozitlerin ısıl özellikleri diferansiyel taramalı kalorimetre (DSC) ve termal gravimetrik analiz (TGA) ile karakterize edilmiştir. Karışımların DSC termogramlarında tepe noktası integrasyonu ile elde edilmiş olan erime entalpisi (ΔHm) değerleri, POSS içeriğinin artmasıyla azalmaktadır. POSS içeriğinin artmasıyla erime ve kristalizasyon sıcaklığı değerleri de azalmış, erime piklerinin genişlikleri ise artmıştır. Yine POSS ilavesi kristalizasyon derecesini düşürmüştür. Buradan hareketle POSS moleküllerinin zincir hareketlerini kısıtladığı söylenebilir. Diğer taraftan elyaf nanokompozitlerde film örneklere oranla daha yüksek kristallenme oranı değerleri hesaplanmıştır. TGA eğrisinden %5 ve 10% kütle kayıplarının meydana geldiği sıcaklıklar ölçülmüştür. Saf PP nitrojen atmosferinde 350°C civarında bozulmaya başlarken POSS içeren nanokompozitlerde 400°C'ye kadar kütle kaybı görülmemiştir. Sonuç olarak artan POSS katkısının nanokompozitlerin bozunma sıcaklıklarını yukarı çektiği ve ısıl kararlılığı arttırdığı açıkça görülmüştür.

Bu nanokompozit peletlerden daha sonra rpm cinsinden 6 farklı fiber çekme hızı (20- 40- 60- 80- 100- 120) ve mm/min cinsinden 3 farklı piston basma hızı (0,5- 1- 2) uygulanarak eriyik eğirme yöntemi ile 97 çeşit fiber örneği üretilmiştir. Üretilen elyafların aşağı çekme oranı (draw down ratio/DDR $DDR=D_{kalıp}^2/D_{elyaf}^2$) hesaplanarak, DDR'ın dayanım ve polimer zincir yönlenmesi üzerindeki etkileri araştırılmıştır.

Hazırlanan elyafların mekanik ölçümleri universal test makinesi kullanılarak yapılmıştır. DDR ve POSS içeriğinin çekme özellikleri üzerinde çok etkili olduğu gözlemlenmiştir. POSS içeriğinin artmasıyla birlikte modülün düştüğü, fiber çekme oranının (rpm) artması birlikte ise modülün arttığı görülmüştür. Ayrıca maksimum yük, maksimum yükteki çekme uzaması ve kopmadaki çekme uzaması artan fiber çekme hızı ile azalmıştır.

Morfolojik analizler polarize optik mikroskobu (POM) ve küçük açılı X-ışını saçılması (SAXS) kullanılarak yapılmıştır. POM görüntüleri ve DDR kullanılarak çift kırılım değerleri hesaplanmıştır. Hesaplamalar sonucunda DDR'ın artması ile tüm elyafların çift kırılım (birefringence) değerlerinin arttığı gözlemlenmiştir. Diğer bir bulgu ise artan POSS miktarının saf PP'ye oranla çift kırılım değerlerinde düşmeye neden olduğudur. Diğer taraftan POSS katkısının PP'nin moleküler oryantasyonunu azalttığı gözlemlenmiştir. Saf PP elyafları POSS katkılı nanokompozitlere oranla yüksek molekül ağırlığına sahip olduğu için zincir hareketlerini kısıtlayarak daha viskoz davranış göstermiştir.

SAXS görüntülerinde POSS miktarı artışın fiberlerin izotropisini arttırıcı bir etki gösterdiği açıkça görülmektedir. Diğer taraftan fiber çekme hızındaki artış fiberlerin anizotropisini arttırmıştır. Artan fiber çekme hızının ayrıca elyafların oryantasyonunu da arttırıcı bir etki yapmıştır. Yine SAXS analizlerinden yüksek miktarda POSS içeren fiberlerin daha izotropik yapıda olduğu görülmüştür. Saçılma yoğunlukları ve komşu

düzlemler arası mesafeler Bragg yasasından hesaplanmıştır. Bu gözlemler ve hesaplamalar sonucu POSS miktarının yapının morfolojisini önemli ölçüde etkilediği açıkça görülmüştür.

1. INTRODUCTION

Polymeric materials are appreciated for their physical, chemical and economical qualities. The successful use of plastic materials is substantially attributable to the incorporation of additives, such as plasticizers, antioxidants, colorants, impact modifiers, heat/UV stabilizers, flame retardants, and extenders.

In order to obtain better properties of polymeric materials, polymer nanocomposites can be widely used as a versatile method in the industry because of their ability to tailor materials for specific applications, at a relatively low cost when compared with the development of a new polymer. Using this approach, the polymer properties can be efficiently improved while maintaining its inherently low density and high ductility. Improvements in mechanical properties are often found even at relatively low filler content. The nanofillers may have spherical (metal or semi-conductive nanoparticles (NPs)), layered (clay), or fibrous (nanofibers and carbon nanotubes) shapes. Such polymer nanocomposites are diverse and versatile functional materials, with applications in systems ranging from electronic devices to biosensors and catalysts. The field of polymer nanocomposite materials has attracted great consideration from polymer scientists and engineers in especially last two decades. The simple premise involves using building blocks of nanosize dimensions to create new polymeric materials exhibiting improved physical properties [1].

Nanotechnology is the understanding and control of matter at dimensions of roughly 1 to 100 nanometers, where unique phenomena enable novel applications [2]. As the filler is decreased to smaller than 100 nm, the resulting composites, termed nanocomposites, may achieve dramatic improvements in such physical properties as gas barrier, thermal stability, elastic modulus, and ultimate mechanical properties. [3]. Nanofillers exist in various shapes, such as spherical (metallic particles and semi-conductive particles), layered silicate, and fibrous (nanofibers and carbon nanotubes). Applications ranging from automotive components to food packaging and to biomaterials have been pursued.

Isotactic polypropylene (iPP) is one of the most important commodity thermoplastics, accounting for about 20% of the world polyolefin production [4]. PP has been used in various applications for human daily life thanks to its low density, excellent thermal and mechanical properties and good processability with its appropriate price. However, its toughness, strength and stiffness are not sufficient for applications as an engineering plastic. In order to reinforce PP, nano-sized inorganic particles such as polyhedral oligomeric silsesquioxane (POSS) was used [1].

Polyhedral oligomeric silsesquioxane (POSS) are a family of compounds with general formula $(RSiO_{1,5})_n$ where R is hydrogen or an organic group (alkyl, aryl or any of their derivatives), and are characterized by a size in the range 1–3 nm and by high chemical versatility and capability to form nanostructureswith tailored dimensionality [5].

The crystallization behavior of polymer melts under shear is an important subject in polymer processing that directly affects the final properties. Compared with quiescent crystallization, the shear-induced crystallization of polymers can be much faster, resulting in very different morphologies [6].

The order or arrangement of the polymer structure is called morphology. The morphology of the nanocomposite systems are examined by various techniques like scanning electron microscopy (SEM) and transmission electron microscope (TEM). One of the other important morphology characterization technique is "birefringence". For isotropic materials, the refraction indexes remain constant for all directions. However, for deformed polymer films which show anisotropic behavior the refraction indexes change. When uniaxial stress was applied, the macromolecules of polymer film will extend and arrange, known as orientation, which leads to anisotropy and different refraction indexes. The material now shows double refraction or, in other word, is birefringent. Birefringence is caused by the difference of indexes of refractions of a media setting between two orthogonal polarization planes. Amedia's index of refraction is defined as the ratio of the speed of light in vacuum divided by the speed of light in the media. Retardation will generate when a polarized lightpasses through the birefringent materials because of the phase difference of the light. Later, the different of refraction index was found as a function of principal stress. This gave rise to the stress-optical (Brewster's) law.

In this study, different compositions of PP-POSS nanocomposites without compatibilizer prepared by melt blending via extrusion. These nanocomposite pellets then were subjected to melt spinning to measure the effect of draw down ratio on the strength, crystallinity, and polymer chain orientation. The effects of methyl-polyhedral oligomeric silsesquioxanes (methyl-POSS) up to 10% on the thermal, mechanical, and optical behavior of polypropylene (PP) were investigated, in detail.

2. THEORY

2.1 Polymer Nanocomposites

Polymer nanocomposites have attracted a considerable scientific and technological interest because of their extraordinary properties such as unique electronic, optical, and mechanical properties when compared to the conventional composites [7-9]. Therefore, the polymer nanocomposites have been investigated by combining various nanofillers such as carbon nanotubes, nanoparticles, nanoclay with common polymers [10-12]. In recent times, polymer nanocomposites with polyhedral oligomeric silsesquioxane (POSS) have presented much interest due to its unlimited surface modification and the relatively excellent compatibility with organic materials differentiating from typical nanofillers [13-15]. The polymer nanocomposites containing POSS have been fabricated by various techniques including copolymerization [16,17], grafting [18], and melt blending [19,20].

Composite material is multicomponent material including multiple, different (non-gaseous) phase domains in which at least one type of phase domain is a continuous phase [21].

Nanotechnology is the study and control of matter at dimensions of roughly 1 to 100 nanometers (nm), where unique phenomena enable novel applications. Nanotechnology is also the design, fabrication, and application of nanostructures or nanomaterials. The studies surrounding nanoscale science and technology gives us unique opportunities to develop revolutionary materials. Nanoscale science and technology is a young field that covers nearly every discipline of science and engineering. Nanophase and nanostructured materials, a new branch of materials research, are attracting a great deal of attention because of their potential applications in areas such as electronics, optics, catalysis, ceramics, magnetic data storage, and polymer nanocomposites.

Polymer nanocomposites (PNs) includes a polymeric material (e.g., thermoplastics, thermosets, or elastomers) and a reinforcing nanoscale material (nanoparticle). The nanoparticle has at least one dimension in nanometer scale. Polymer nanocomposites show major improvements in mechanical properties, gas barrier properties, thermal stability, fire retardancy, and other areas.

There are different types of commercially available nanoparticles that can be incorporated into the polymer matrix to form polymer nanocomposites. Depending on the application, the researcher must determine the type of nanoparticle needed to provide the desired effect. A brief discussion will include the most commonly used nanoparticles in the literature:

• Montmorillonite organoclays (MMT)

• Carbon nanofibers (CNFs)

• Polyhedral oligomeric silsesquioxane (POSS)

• Carbon nanotubes [multiwall (MWNTs), small-diameter (SDNTs), and single-wall (SWNTs)]

• Nanosilica (N-silica)

• Nanoaluminum oxide ($A1_20_3$)

• Nanotitanium oxide (TiO_2)

• Others [2].

Such polymer nanocomposites are diverse and versatile functional materials, with applications in systems ranging from electronic devices to biosensors and catalysts. The field of polymer nanocomposite materials has excides great consideration from polymer scientists and engineers in last years. The simple premise involves using building blocks of nanosize dimensions to create new polymeric materials demonstrated improved physical properties [1].

POSS derivatives can be effectively incorporated into polymers by copolymerization, grafting, or even simple physical blending to produce polymeric hybrids or nanocomposites because of a large variety of organic substituents. It has been observed that the phase structure, morphology, thermal stability, and mechanical performance of POSS-modified thermoplastics (such as polyolefins, polyesters, or polyamides) can

be largely affected by the chemical structure, concentration, and dispersion degree of POSS [22].

In the field of inorganic-organic composite materials, many research interests are oriented to polyhedral oligomeric silsesquioxane (POSS) based materials, both as organic-inorganic hybrids and as polymer nanocomposites. The dispersion of POSS nanoparticles in polymeric matrices - such as polyacrylates, polyesters, polyimides, polystyrene and its copolymers - allows to obtain advanced composite materials with high thermal, mechanical and oxidative performances [23]. The compatibility of these materials is expected to be markedly enhanced due to the possibility of modifying the chemical/ physical interactions at polymer-filler interface through introduction of functional groups on the POSS molecules.

2.2 Nanocomposites Preparation

In general, POSS-based nanostructured materials can be obtained following two different strategies. The first one is based on a chemical approach. Following this strategy, POSS molecules can be chemically inserted into the polymeric chains by in situ copolymerization. A large number of matrices, such as polyolefins , polyimides , polyamides and epoxy resins have been used in the formation of organic/inorganic hybrid systems with high thermal, mechanical and oxidation resistance performances [24]. The second one is a physical approach, based on a melt blending process in which POSS are dispersed into polymer matrices in the molten state.

For liquid thermosetting reactive prepolymers or thermoplastic polymers with solid nanoparticles, the following processing methods are recommended:

• In-situ polymerization

• Emulsion polymerization

• High-shear mixing [2].

2.2.1 In-situ polymerization

In-situ polymerization presents a unique opportunity to prepare well-dispersed polyolefin nanocomposites. This is done by first dispersing nanoparticles in a polymerization solvent, followed by homogeneous polymerization within the dispersion through addition of catalyst and monomer. For polyolefins, homogeneous

polymerization is achievable with single site metallocene catalysts. In principle, any single site catalyst or combination of catalysts can be applied to an in-situ polymerization, enabling control of the morphology and properties of synthesized PNCs [25].

The in situ copolymerization of POSS to produce hybrid organic-inorganic polymers with pendant POSS groups has been widely studied for both thermoplastics and thermosets, showing frequently improved thermal stability and physical properties [22].

2.2.2 Emulsion polymerization

Emulsion polymerization is a complex process in which the radical addition polymerization proceeds in a heterogeneous system. This process involves emulsification of the relatively hydrophobic monomer in water by an oil-in-water emulsifier, followed by the initiation reaction with either a water-soluble or an oil-soluble free radical initiator. At the end of the polymerization, a milky fluid called "latex", "synthetic latex" or "polymer dispersion" is obtained. Latex is defined as "colloidal dispersion of polymer particles in an aqueous medium". The polymer may be organic or inorganic. In general, latexes contain 40-60 % polymer solids and comprise a large population of polymer particles dispersed in the continuous aqueous phase (about 1015 particles per mL of latex). The particles are within the size range 10 nm to 1000 nm in a diameter and are generally spherical. A typical of particle is composed of 1-10000 macromolecules, and each macromolecule contains about 100–106 monomer units [26].

A typical emulsion polymerization formulation comprises four basic ingredients: 1) monomer, 2) dispersion medium, 3) emulsifier, 4) initiator. Further auxiliaries, such as chain transfer agents, buffers, acids, bases, anti-aging agents, biocids, etc., can be used. In emulsion polymerization process, a monomer or a mixture of monomers is emulsified in the presence of an aqueous solution of an emulsifier in a suitable container. The monomer is thus present almost entirely as emulsion droplets dispersed in water. The initiator causes the monomer molecules to polymerize within a certain temperature range. When the polymerization is complete, a stable colloidal dispersion of polymer particles in an aqueous medium (the latex) will remain.

2.2.3 High shear mixing/extrusion

Extrusion is a process where the feed is homogeneously conveyed to the die to take a desired shape product by being pushed forward with sufficient heat and pressure through the extruder [27]. In batch extrusion systems, the purpose is only to take a desired shape product so the feed is already uniform. On the other side, in continuous extrusion processes, the ingredients are fed together to the extruder and besides taking the shape of the die, homogeneous mixing of the ingredients is also very important.

In many extrusion applications, some prior and downstream operations are also necessary. Polymers which are hygroscopic need drying to prevent degradation because of moisture before being fed. In most cases, the polymer will be fed not alone but with some other ingredients such as additives, if a blend is point at issue, the other blend component, compatibilizer etc. So a feed preparation step is usually necessary. After the preparation of true and dry formulation, it is fed to and extruded in the extruder to be melted, mixed, conveyed to the die homogeneously and shaped. Then, the product, namely extrudate or throughput or output, is usually cooled by such means as air or water cooling, and collected pullers. Further operations such as printing, annealing may be necessary in some cases. Finally, the product quality is checked before packaging step [28].

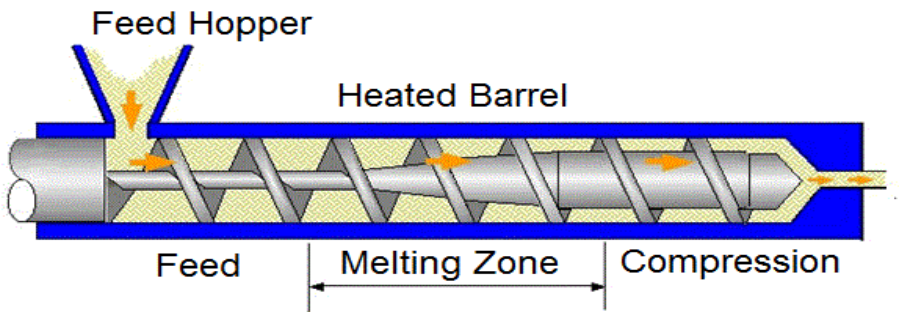

Figure 2.1 : Single screw polymer extruder. Showing three main sections: feed zone, melting zone, and compression zone.

In a screw extrusion process, polymer is fed from the hopper, and mechanically pushed forward by the rotation of the screw as shown in Figure 2.1. Along its travel to die, the fed polymer is heated to certain temperatures by the heater bands within the barrel and mainly by the shear created within the extruder to be melted and mixed homogeneously. After reaching to the die by a pumping action, the homogeneous melt is forced through a die orifice that relates to the shape of the product's cross section.

The formed melt (extrudate) is cooled as it is being drawn away from the die exit through downstream equipment. Products produced include films, sheets, profiles, pipes, tubes, rods, wire/cable coverings, coatings, filaments, blown shapes, and others. Each step in this whole extrusion line is very important for the product to be in the desired spec. Any deviation from the determined conditions in any step, for example a change in the extruder temperature profile, screw speed, or cooling temperature, puller speed, drawing ratio, will result in very big differences in the product properties. For instance if screw speed is changed, a homogeneous mixing may not be obtained depending on the residence time, screw itself etc. If the temperature of the cooling bath deviates, a very different product will be obtained depending on different crystallization kinetics [28]. It is convenient to classify extruders as continuous-processing and discontinuous processing according to their mode of operation. Namely, there are continuous extruders with single-screws or multi screws; continuous disk or drum extruders, which use viscous drag melt actions or elastic melt actions and discontinuous extruders, which use ram and reciprocating actions [29]. Since a twin screw extruder is employed in this thesis, only this type of extruder will be mentioned from now on.

The are many twin screw extruder commercially available. The choice should depend on end-use application. Different models have two parallel screw shafts that either rotate in the same direction (called corotating) or rotate in opposite directions (called counterrotating), with varying distances between the screw shafts as shown in Figure 2.2. If the centerline distance between the shafts is less than the screw diameter, the screws are called intermeshing, whereas screws with a distance between the shafts equal to the screw diameter are called non-inter-meshing.

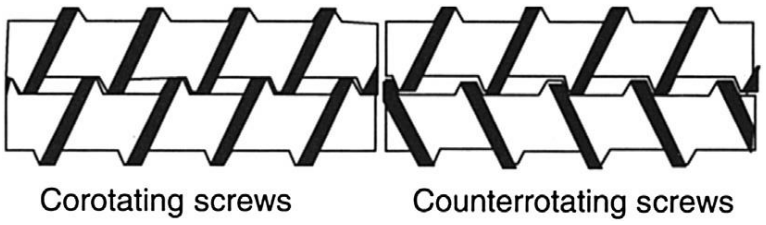

Figure 2.2 : Corotating and counterrotating fully intermeshing screws.

Major equipment components (drive motor and gearbox, feed, screw and barrel, and the die or head) of a parallel twin screw extruder are identified by Figure 2.3. The fifth component is the control cabinet. The drive system is composed of a direct current

(DC) motor, cooling system for the motor, coupling between the motor and gear box, thrust bearing, gear box, oil lubrication and cooling for the gear box, and shaft coupling between the gear box and the extruder screws. One feed port is located at the rear of the extruder in the first barrel section. Additional feed streams can be added in numerous locations along the barrel length through gravity from a volumetric or gravimetric feeder, liquid feed using a pump with a liquid injection nozzle, and/or a side feed extruder or stuffer to add polymer, additives, fillers, or reinforcements at locations along the barrel. Screw and barrel sections are both modular. Barrel sections can be added or removed to make the extruder barrel longer or shorter to increase or decrease compounding capabilities, depending on the product application. A set of screw shafts is required for each extruder length. Additional barrel sections are normally added to increase process flexibility for downstream feeding or venting. Each barrel section is normally cooled with water and heated with cast heaters to control barrel temperature. Screws are modular, with different elements combined in a strategic design to localize the feeding, melting, conveying, mixing, pumping, and venting at specific locations along the extruder barrel.

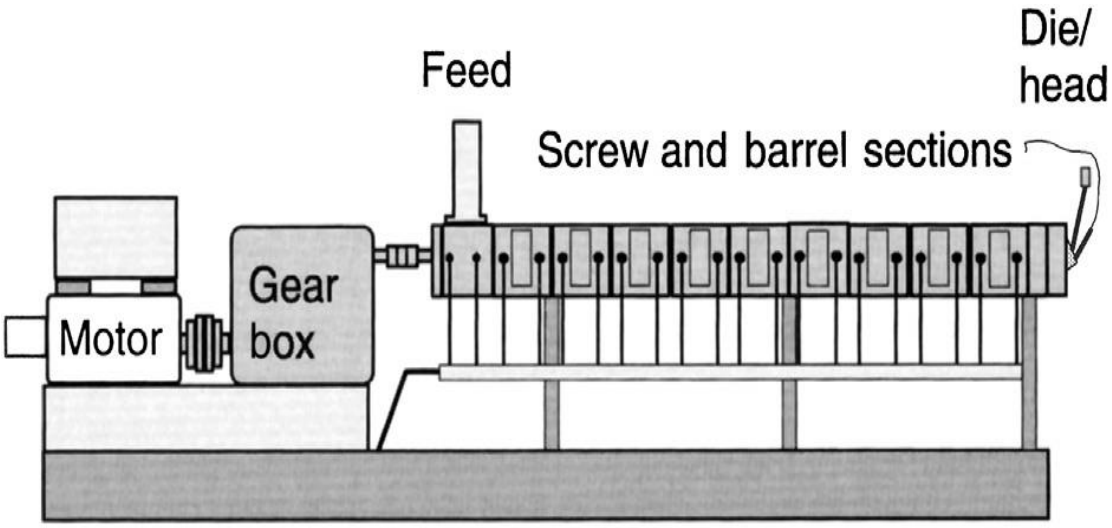

Figure 2.3 : Corotating and counterrotating fully intermeshing screws.

2.3 PP/POSS Nanocomposites

2.3.1 Polypropylene (PP)

Polypropylene is a polyolefin with the formula show in Figure 2.4 which is readily formed by polymerizing propylene with suitable catalysts, generally aluminum alkyl and titanium tetrachloride. Polypropylene properties change according to molecular weight, method of production, and the copolymers involved. Generally polypropylene has showed certain advantages in improved strength, stiffness and higher temperature capability over polyethylene. Polypropylene has been very successfully applied to the forming of fibers because of its good specific strength which is why it is the single largest use of polypropylene. Polypropylene also happens to be one of the lightest plastics available with a density of 0.905 g/cm^3.

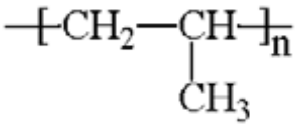

Figure 2.4 : Structure of polypropylene.

Polypropylene is a versatile member of polyolefins which are profoundly affected by stereoregularity (Figure 2.5). PP has been used as the matrix material in a commercial form because of its many attractive properties, such as low weight, relatively low cost, excellent heat distortion temperature (above 100 °C) and its recycling ability [30].

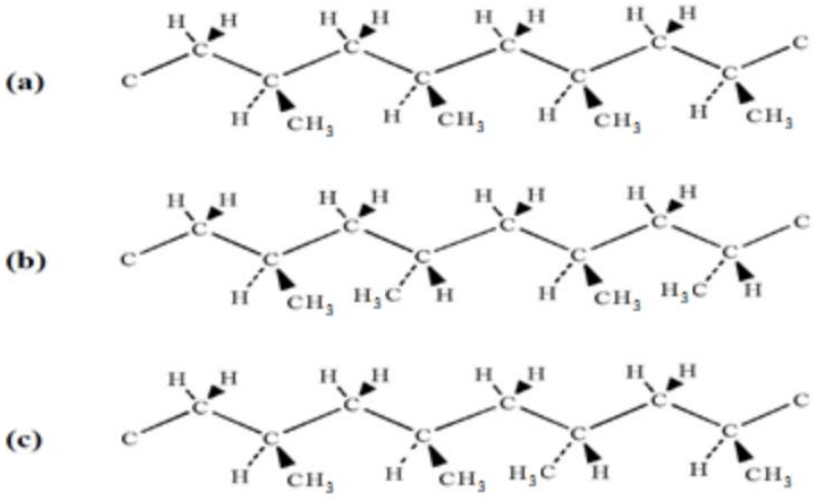

Figure 2.5 : Structure of (a) isotactic, (b) syndiotactic, (c) atactic polypropylene.

Polypropylene with an isotactic, syndiotactic, or atactic configuration can be obtained by using C_2 , C_{2v}, or C_s symmetric zirconocenes [31]. The isotactic polypropylene is prepared with various modifications of Ziegler-Natta coordination catalysis, producing polymers with varying degrees of stereoregular order with isotacticity up to 98%.

Syndiotactic polypropylene is prepared with soluble coordination catalysis and the stereoregularity achieved is generally lower than that of isotactic polymers. Atactic polypropylene can be obtained by extraction with boiling n-heptane from isotactic polypropylene of lower stereoregularity [32].

Polypropylene has had a outstanding growth over the past years [33] due to its inertness to acids and alkali, ability for modification, its overall balance of physical, mechanical, electrical, chemical, and thermal properties, and above all a competitive price. Additionally, PP-based materials exhibits very good thermal stability over a wide range of temperature. The other attribute is excellent retention of mechanical properties after recycling.

2.3.1.1 Properties of polypropylene

The mechanical and thermal properties of polypropylene can vary based on the isotacticity, the molecular weight and its distribution and % crystallinity. Since PP is a viscoelastic material like other thermoplastics, its mechanical properties are strongly dependent on time, temperature and stress.

- Density

Polypropylene is the lightest among the commonly used thermoplastics and has a density of 0.9 g/cm3.

- Thermal properties

Polypropylene has a glass transition temperature and a crystalline melting point of -10ºC and 160-170ºC, respectively. Moreover, it has a maximum continuous use temperature of 100ºC, which is importantly higher than those of the other commodity plastics and some other engineering plastics.

- Mechanical properties

The mechanical properties of isotactic PP depend on its % crystallinity. The crystalline phase maintains mechanical strength up to rather high temperatures because of its relatively high melting temperature,. It has high tensile strength, stiffness and hardness due to its crystallinity. However, an increase in molecular weight causes a reduction in tensile strength, stiffness, hardness but an increase in impact strength of polypropylene.

- Electrical properties

Polypropylene demonstrates great electrical insulating property. It has outstandingly high resistivity, low dielectric constant and negligible power factor.

- Solubility

Polypropylene is soluble only at elevated temperatures due to its crystalline character. Isotactic PP is soluble in "good" solvents such as xylene, tetralin, chlorinated aromatic and aliphatic hydrocarbons, etc. above 80ºC [34].

2.3.2 Polyhedral oligomeric silsesquioxane (POSS)

Polyhedral oligomeric silsesquioxane (POSS) is one of many kinds of silsesquioxane molecules. The term silsesquioxane refers to themolecules, whose chemical structure follows the basic composition of $R_nSi_nO_{1.5n}$ (Figure 2.6). Here, the R-group, also called the vertex group for polyhedral molecules, may be hydrogen, alkyl, alkylene, aryl arylene, among others. Such silsesquioxanes can form oligomeric organosilsesquioxanes $(CH_3SiO_{1.5})_n$ through chemical reactions and the chemical structures of the derivative silsesquioxanes are quite versatile and the interested readers are referred to the review by [35] which focuses on the preparation, structures, and applications of such silsesquioxanes.

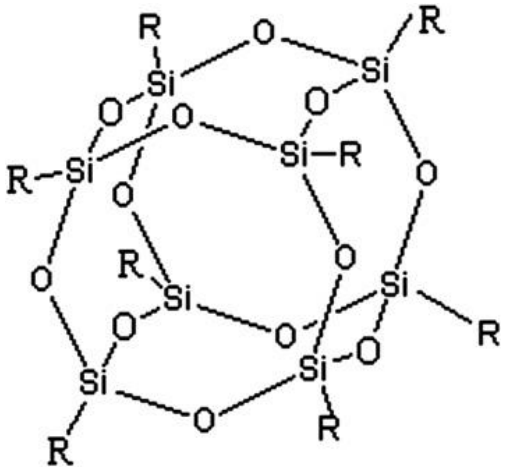

Figure 2.6 : Structure of polyhedral oligomeric silsesquioxane.

The molecular architecture of silsesquioxanes can be classified into two categories: noncaged structure and caged structure, each shown in Figure 2.7. As shown in Figure 2.7, the caged silsesquioxane molecules can be further classified into: (c) T8 structure; (d) T10 structure and (e) T12 structure. Non-caged silsesquioxane molecules can also

be further classified into: (a) random structure; (b) ladder structure, and (f) partial-cage structure.

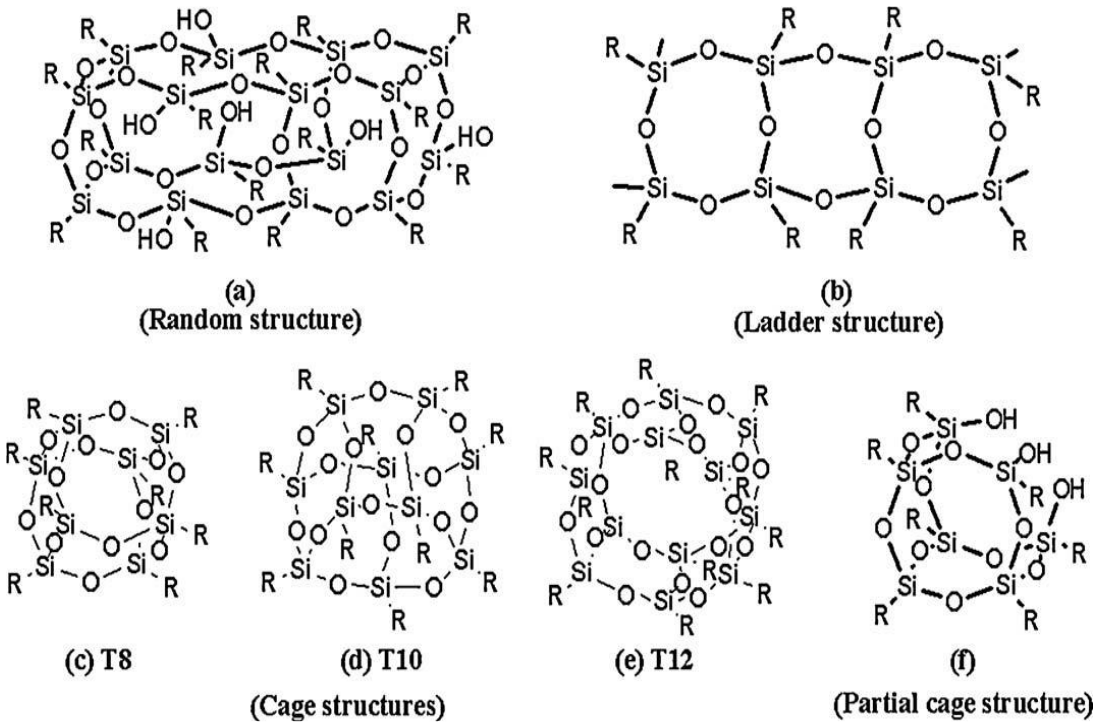

Figure 2.7 : Structures of various types of silsesquioxanes [3].

2.3.3 PP/POSS literature

A wide range of POSS amounts was incorporated in polyolefin POSS copolymers as Coughlin et al. [36] indicated. They prepared hybrid norbornylene-substituted POSS/polyolefin copolymers using single site catalysts. These copolymers exhibited enhanced thermooxidative stability. In another work of Coughlin et al. [37-40], his team demonstrated a visual model of a POSS-copolymer based on the morphology of POSS-polybutadiene and polyethylene copolymers. These polymers were synthesized by ring-opening metathesis copolymerization, which shows a hybrid inorganic/organic structure and single site catalysts, both allowing for good control of POSS incorporation. In their article, they argued that two-dimensional networks are the highest possible architecture that a POSS-copolymer can adopt due to the constraints of the polymer chain, while three-dimensional structures can be expected for most POSS-polymer blends.

Furthermore, Fu et al. [41] studied the rheological behavior of ethylene-propylene (EP) copolymers containing POSS molecules. They look through under oscillatory shear

and DMA. They reported that EP/POSS nanocomposites exhibited a solid-like rheological behavior which suggests cause of inducing physical gelation of EP in the presence of POSS molecules.

In another work of Fu et al. [42],they performed crystallization studies of isotactic polypropylene (iPP) blends with octamethyl POSS under inert condition and under shear. In this work, the DSC traces shows that octamethyl-POSS crystals acted as nucleating agents in quiescent crystallization of iPP. The addition of POSS also significantly increased the crystallization rate during shear compared with the rate for the neat polymer which is totally opposite of Zheng's work [36]. So, these articles accepted that dispersed POSS molecules behaved as weak crosslinkers in polymer melts and thus increased the relaxation time of the polymer chains after shear. Consequently, polymer chains retained orientation longer and hence faster polymer crystallization rate was observed in the presence of POSS.

Additionally Zhang et al. [43] prepared polypropylene-POSS nanocomposites using a C_2 symmetric ansa-metallocene catalyst in conjunction with a modified MAO. Their PP/POSS copolymers exhibited improved thermal stabilities with higher degradation temperature and charyields, revealing that inclusion of the inorganic POSS NPs made the organic polymer matrix more thermally robust.

Hsiao and coworkers [44] used DSC to investigate a series of isotactic polypropylene (iPP) melt-blended with nanostructured OM-POSS molecules to study the quiescent melt crystallization behavior and shear-induced crystallization behavior. They observed that the addition of OM-POSS molecules increased the crystallization rate of iPP under both isothermal and non-isothermal conditions, implying that POSS crystals acted as nucleating agents, a finding that is similar to that with PE systems.

Fina et al. [45,46] studied the influence of functional groups of POSS cages on the properties of PP/POSS nanocomposite blends. POSS with different side chain lengths, e.g., octamethyl-, octaisobutyl- and octaisooctyl-POSS were considered and melt mixed with PP. It was observed that octamethyl-POSS acted as a nucleating agent although poor dispersion was produced. On the other hand, octaisobutyl-POSS did not act as a nucleating agent, but produced good dispersion. However, in the latter case, the POSS aggregates were of a few micrometer in size. The thermoxidative properties

of the PP matrix improved and the peak weight loss temperature increased in the presence of POSS.

3. EXPERIMENTAL

3.1 Materials

3.1.1 Polypropylene

PP homopolymer was the commercial LubanTM isotactic PP supplied from Oman Polypropylene LLC company. The melt flow rate (190°C/2.16 kg) and heat deflection temperature (under 0.45 MPa) are 5.4 g/10 min and 85ºC respectively. The density is declared 910 kg/m3 by the company.

3.1.2 Polyhedral oligomeric silsesquioxane

PP-POSS nanocomposite is a commercial grade material purchased from Aldrich, product number of 565628. It is an isotactic polypropylene (i-PP) based nanocomposite reinforced with 10 wt% of methyl-polyhedral oligomeric silsesquioxanes (methyl-POSS).

3.2 Material Preparation Equipments

3.2.1 Extruder

Samples were prepared by melt processing in a lab-scale twin screw extruder (Rondol Technology Ltd. Micro Lab., UK, D:10 mm, L/D: 20) with a screwspeed of 75 rpm. Screws of the extruder were configured as including 3D of 4 x 60° followed by 2D of 4 x 90° kneading segments. A temperature profile of 110°C / 170°C / 190°C / 190°C / 190°C was applied throughout the barrel from the feeding zone to die.

3.2.2 Pelletizer

Extruded samples were cut by using Rondol Technology Ltd. Microlab pelletizer after extrusion process to make granular shape to samples.

3.2.3 Compression press

Carver compression press whose maximum pressure and temperature values are 4000 Psi and 300°C respectively, was used to prepare circular shaped samples to use in discovery hybrid rheometer. Hot press process parameters are shown in Table 3.1.

Table 3.1 : The parameters used in hot press process.

Temperature (°C)	Pressure (Psi)	Pre-heating time (min)	Press time (min)
190	2000	15	10

3.2.4 Capillary rheometer for melt spinning process

The pellets containing PP and POSS were melt-spun as monofilament through a capillary die using a Bohlin Instruments-Rosand- Advanced Capillary Rheometer RH7 and a takeup device schematically shown in Figure 3.1.

Spinning is the process of extruding polymer melts or solutions through a metal plate having a number of symmetrically arranged small holes, to form a corresponding number of continuous fluid strands. This capillary rheometer was used to spin fibers for the following reasons. First, the flow through the capillary is purely pressure-driven flow. Second reason is that the polymer melt temperature could be controlled easily. Thirdly, the exit strand diameter was easily controlled using a constant diameter long capillary die. Monofilament fibers were obtained by extruding through a capillary die. 18 types fiber samples for each composition of polymer nanocomposites were prepared by varying the plunger speed (0.5 and 2 mm/min) and take-up velocity (20 to 120 rpm) at constant melt temperature (190 °C). A critical part of fiber production is understanding the draw down ratio, DDR. This gives a sense of the degree of elongation of the polymer melt. In this case, the draw down ratio (DDR) was determined as ($DDR= D_{die}^2/D_{fiber}^2$) ranging from 50 to 600. Here D_{die} and D_{fiber} are the die and the fiber diameters, respectively. Important parameters used in fiber spinning process are given in the Table 3.2.

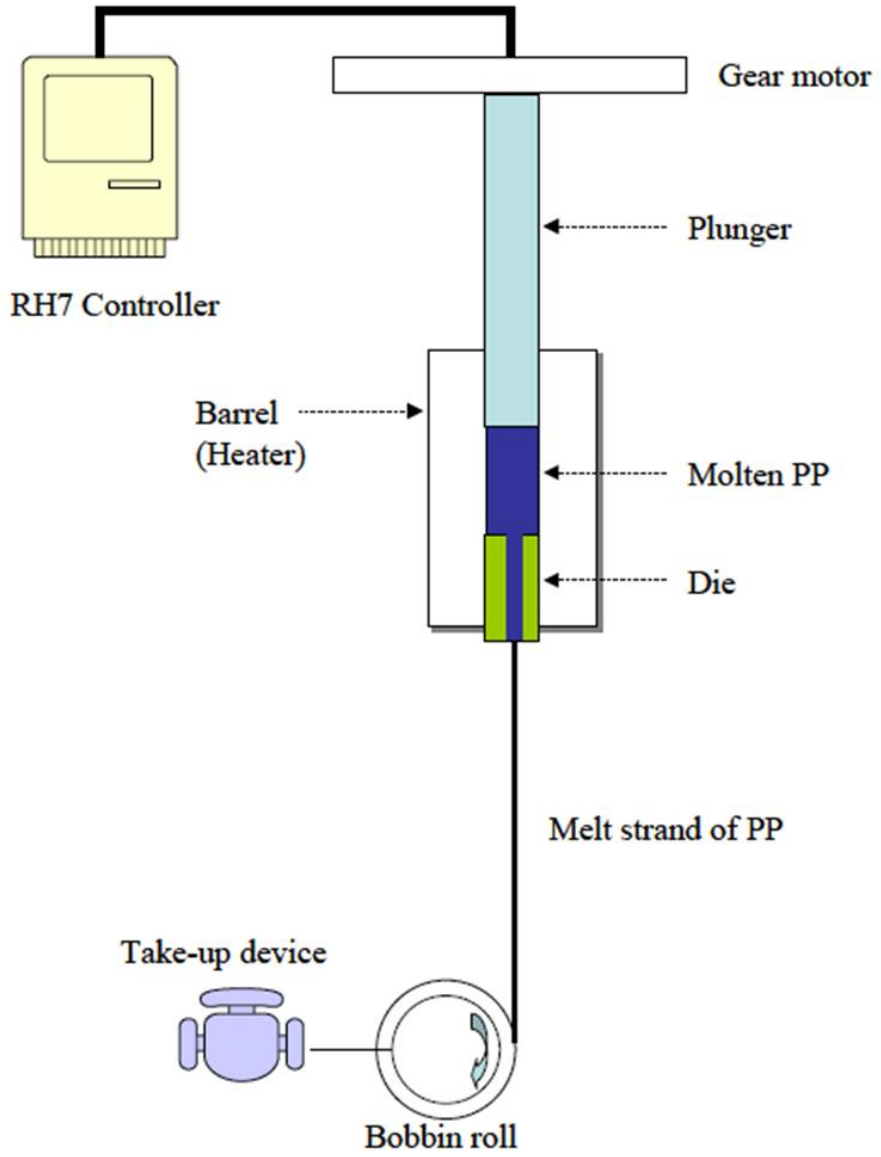

Figure 3.1 : Schematic diagram of melt spinning process using capillary rheometer and take-up device [47].

Table 3.2 : Important process parameters in fiber spinning.

Take up speed (rpm)	Capillary die (mm)	Temperature (°C)	Capillary length/diameter (L/D)	Cross head speed (mm/min)
20-120	1	190	4	0.5 – 2

3.3 Nanocomposite Preparation

In this study, 50 grams of polymer was prepared from each composition for melt mixing in extruder. Then 1%, 3 %, 5%, 8%, and 10% POSS reinforced PP nanocomposites without compatibilizer were extruded at 75 rpm.

The PP and POSS pellets were premixed by shaking for 5 minutes before being fed to the extruder. Temperatures of the zone 1, zone 2, zone 3, and die were 110°C / 170°C / 190°C / 190°C / 190°C respectively. The strands from the die were collected on a metal plate and pelletized after complete solidification. The mixtures prepared in extruder were collected from die and the middle of these productions was taken as samples of the mixtures, because effective mixing takes place at this point.

After the pelletized nanocomposites were prepared, the samples were shaped depending on the characterization methods. 4mm diameter circular shaped samples were prepared by using compression molding for rheological tests at parallel plate rheometer. For all the other characterizations the melt spinning of the nanocomposites were prepared by using Rosand capillary rheometer. This allowed precise control of temperature and uniform flow of melt to the fiber spinning operation. L/D ratio of fibers were taken as 4 with a capillary die of 1mm. The polymer pellets were loaded into the preheated capillary barrel. The barrel remained at 190 °C during all runs. The pellets were packed and then the extrusion began once the pellets were allowed to heat for 20 minutes. An plunger speed of 2 mm/min, 1 mm/min, 0.5 mm/min with a diameter of 15 mm, was used in all spinning.

Once the extrudate had extruded partially it was pulled to the bobbin spinning at ~ 10 rpm. Once the fiber was firmly attached and had reached steady state elongation, then the fiber spinning process began. The bobbin was allowed to collect sufficient fibers for testing, and then the rpm was increased to the next level. This was done for each fiber system produced. The take up rpm of 20, 40, 60, 80, 100, and 120 was used for the bobbin of diameter 90 mm. After spinning fibers were removed and prepared for DSC, X-ray diffraction, tensile, and birefringence measurements. Labeling methodology of nanofibers can be seen from Figure 3.2.

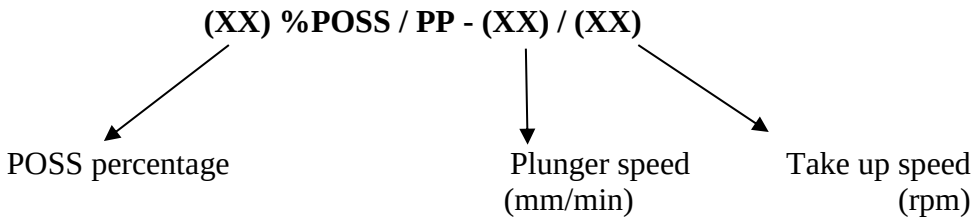

Figure 3.2 : Labeling methodology for nanofibers.

3.4 Nanocomposite Characterization

3.4.1 Tensile testing machine

For tensile measurements, fibers were taped to a holder to reduce bending. This was loaded into the clamps of a Instron Universal Tester 567. A 100 N load cell was used with an extrion rate of 100 mm/min for all samples. Once the sample was loaded, the paper sample holder was cut. Then the measurement was started and the load was recorded until breaking of the samples.

3.4.2 Rheological analysis

An advanced rheometric expansion system (ARES) from TA Instruments, operated with parallel plates was used to measure the rheological properties – such as storage modulus (G′), loss modulus (G″), and loss tangent (tan δ) of the samples. 180°C, 205°C, and 230°C were applied as process temperature to recorded complex viscosity (η*) of various PP /POSS blends. Disk-shaped 97 specimens of 25 mm diameter and 1.5 mm thickness were molded using the compression molding machine. For tensile measurements, fibers were taped to a holder to reduce bending. This was loaded into the clamps of a Instron Universal Tester 567. A 100 N load cell was used with an extrion rate of 100 mm/min for all samples. Once the sample was loaded, the paper sample holder was cut. Then the measurement was started and the load was recorded until break age of the samples.

3.4.3 Differential scanning calorimetry (DSC)

For DSC SII Nanotechnology ExStar 6200 was used. Fibers were cut into very small lengths the fit comfortably into the DSC pan. A heating rate of 10 °C/min from room

temperature to past the melting peak was used. Once full melting had been seen in the sample, the run was stopped. Using TA Universal analysis software, the DSC data was then analyzed for melting and crystallization enthalpies, to determine the crystallinity of the samples from the known crystallization enthalpies.

3.4.4 Thermogravimetric analysis (TGA)

Thermogravimetric analysis (TGA) was performed with a TA Instruments SDT 2960 simultaneous TG/DSC system. The scans were recorded at a heating rate of 10°C/min in a temperature range from 20 to 600° C. Experiments were done under nitrogen atmosphere. The onset of the degradation (Tonset) was calculated as the intersection between the starting mass line and the line of maximum gradient tangent to the TG curve.

3.4.5 Morphological analysis

Micrographs of the crystallites of PP and the self-assembled structure of POSS in the cross-sections of the spun fibers were observed.

3.4.5.1 Polarized optical microscope (POM)

For birefringence measurements a polarized optical microscope was used with Berec compensators of 30^{th} order. To measure the sample birefringence, the fibers were first taped to a glass slide. Then optical fluid was added to the region of interest. This helped to reduce the lens effect the round fiber has on the light passing through it. With no compensator in place, the region of most cross polarization of the sample was found. The sample was then rotated 45 degrees to the axis of highest polarizability of the polymer chain to be perpendicular with the gamma direction of the compensator. This insured that the compensator was indeed compensating for the polarization of the light passing through the sample, and not adding to the retardation if gamma was parallel to the axis of highest polarizability. For PP the highest polarization axis is 90 degrees to the chain axis, and for POSS the highest polarization occurs along the chain axis. The compensator was then adjusted from black to red retardation levels matching the location of the black polarization line. This was repeated at 5 times for each fiber. Also, the fiber was measured optically used a calibrated standard. This increased the precision of the birefringence measurement.

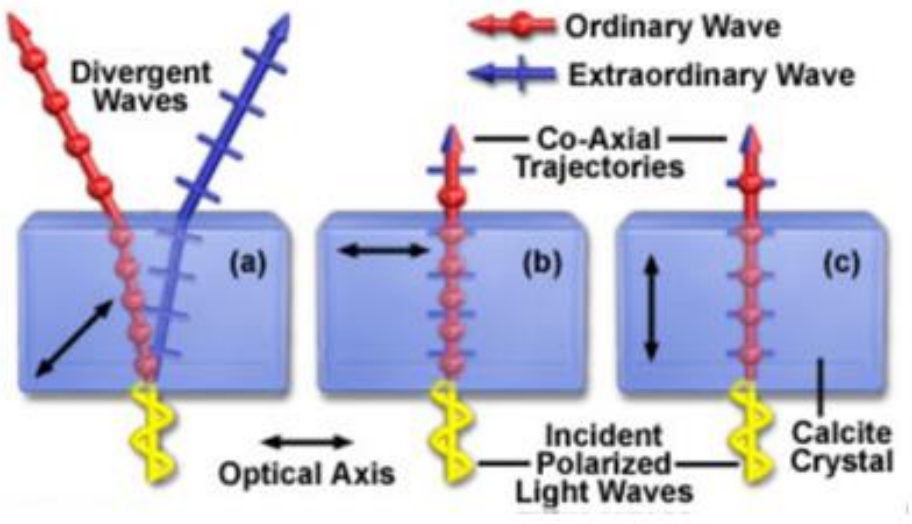

Figure 3.3 : Seperation of light waves by a birefringent crystal.

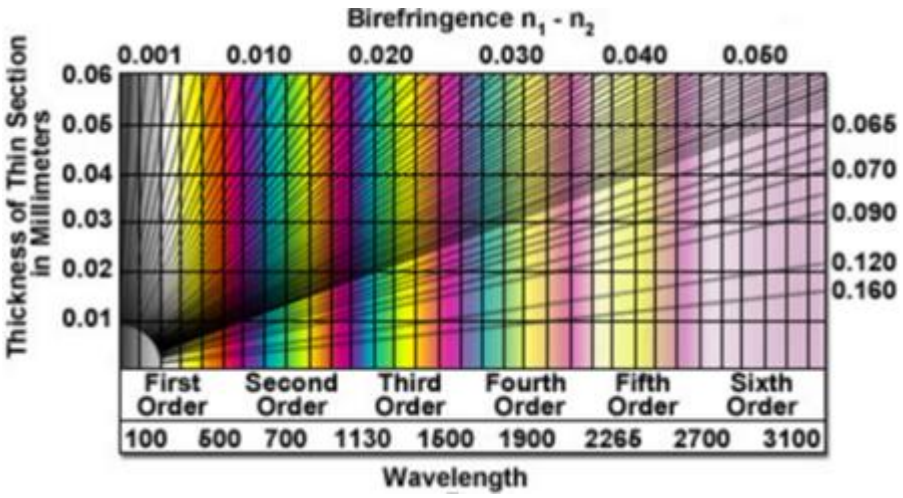

Figure 3.4 : Michel-Levy birefringence chart.

3.4.6 Small angle x-ray scattering (SAXS)

Crystallization studies of isotactic polypropylene (iPP) containing nanostructured polyhedral oligomeric silsesquioxane (POSS) molecules were performed with Kapton Window small-angle x-ray scattering (SAXS).

4. RESULT AND DISCUSSIONS

In this study, PP/POSS nanocomposites (NC) were prepared according to the procedure given in the Section 3.3. 97 fiber samples were produced by using 6 take up speed and 3 plunger speed to 6 different nanocomposites then they were characterized. The measurements results of the mechanical, thermal and morphological properties of the nanocomposites were given.

4.1 Tensile Properties

The tensile properties of the samples were measured using an Instron Universal Tester 567 at room temperature (Section 3.4.1). At least three measurements were performed for each sample. The maximum load (N), tensile stress at maximum load (in MPa), tensile strain at maximum load (in MPa), tensile stress at break (in MPa), strain at break (in %), the stress at yield (in MPa), and Young's modulus (in MPa) have been measured changing take up speed (rpm) for every samples and plunger speed.

The sample tensile properties of the materials are shown in Table 4.1 and the average data of samples is plotted on Figures from 4.1 to 4.3. From these results, it is clear that composition and DDR of the samples have a pronounced effect on the mechanical properties of these materials. Tensile data for all fibers were given in Appendix B.

Table 4.1 : Tensile data for 1%POSS/PP samples at 2 mm/min plunger speed.

rpm	Maximum Load (N)	Tensile stress at Max. Load (MPa)	Tensile strain at Max.	Tensile strain at Break (%)	Tensile stress at Yield (MPa)	Modulus (E-modulus) (MPa)
20	1.39	30	1128	1300	24	636
40	0.68	28	672	1075	26	1079
60	0.58	34	661	915	27	1024
80	0.62	48	778	1059	27	1392
100	0.38	37	595	926	25	965
120	0.35	48	574	854	27	1127

The maximum tensile strengths, tensile stress at maximum load, the stress at yield, and Young's modulus (in MPa) increase by increasing of take up speed (rpm) of almost all samples. Afterwards, the maximum load, tensile strain at maximum load, and tensile strain at break decreases with increasing of take up speed.

Young's Modulus (modulus of elasticity) equals to the ratio of the applied load per unit area of cross section to the increase in length per unit length. PP can be considered a tough material at room temperature. Addition of POSS to the PP decrease the modulus of elasticity so it is clearly seen that increasing of POSS content decreases the Young's modulus of the POSS/PP nanocomposites in almost all investigated samples.

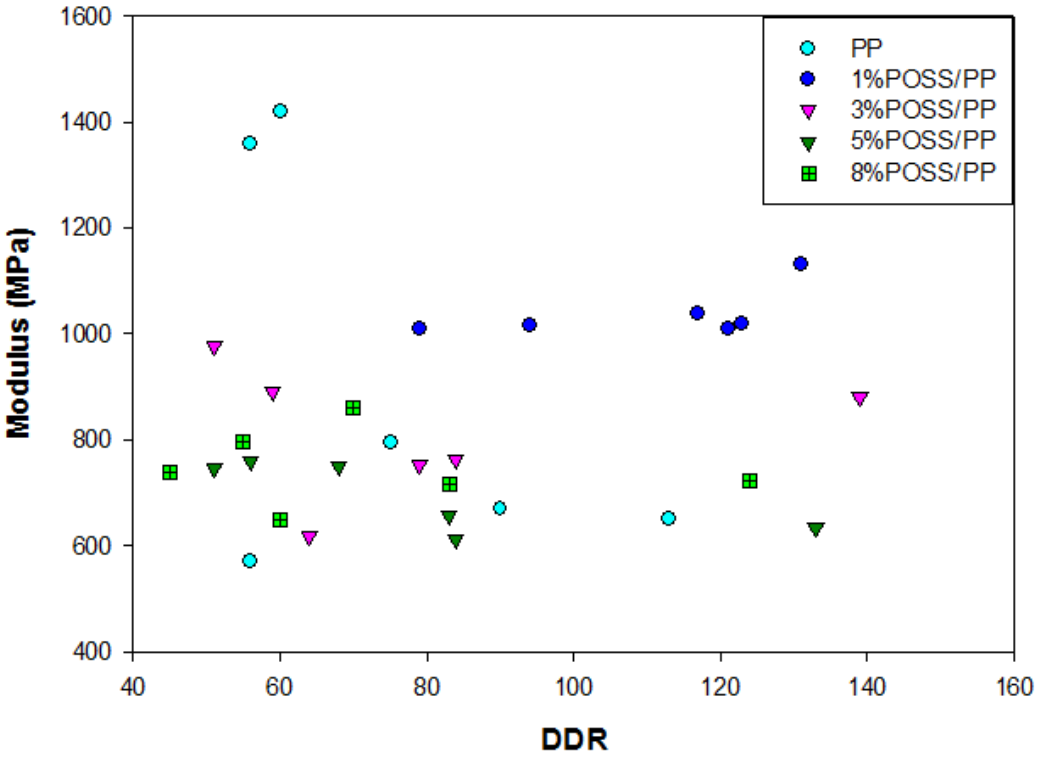

Figure 4.1 : Young's modulus for melt spun fibers of all samples with 0.5 mm/min plunger speed.

For nearly all samples, increased DDR led to decreased elasticity and plasticity of the fibers. As the plunger speed increase the modulus of fibers also increase that can be easily seen on Figures from 4.1 to 4.3.

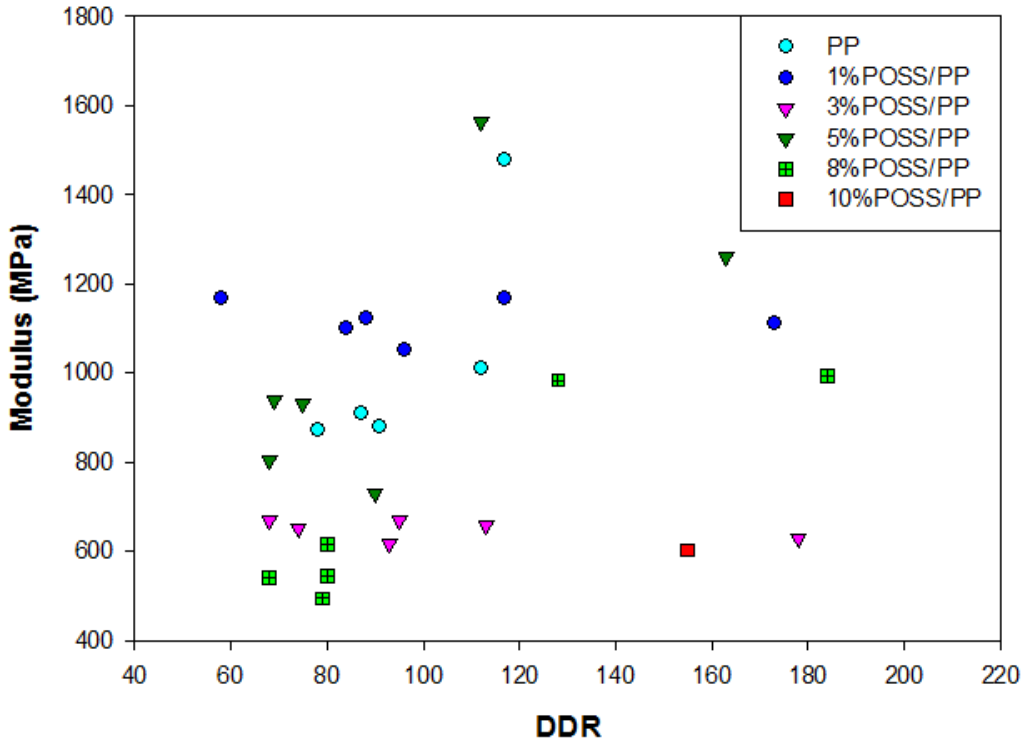

Figure 4.2 : Young's modulus for melt spun fibers of all samples with 1 mm/min plunger speed.

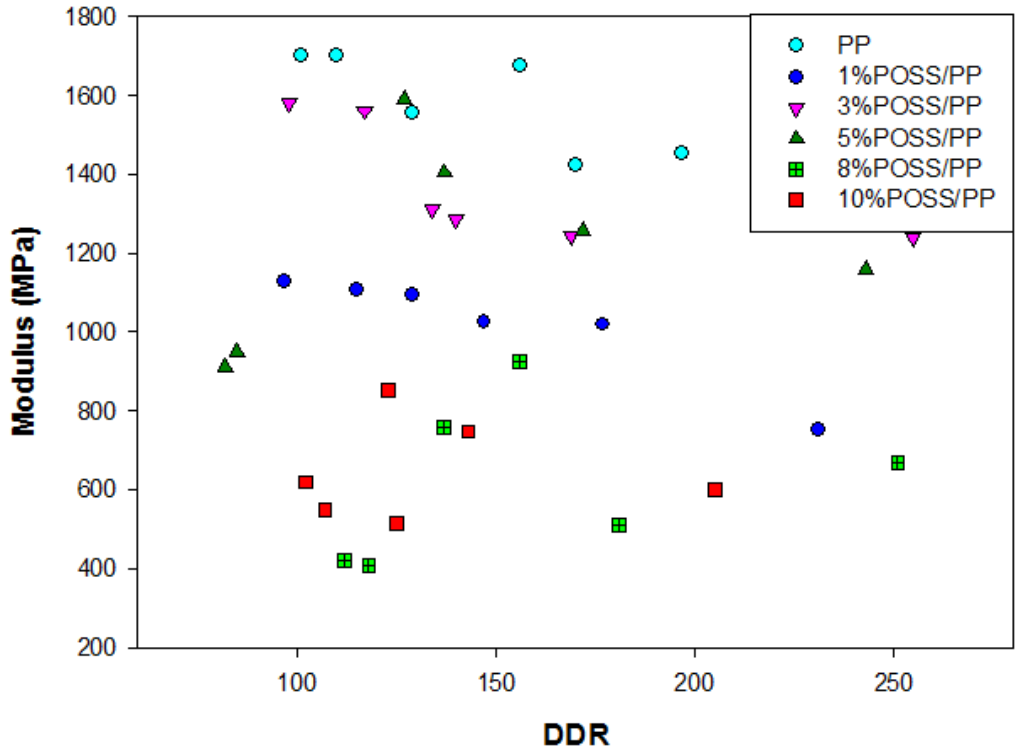

Figure 4.3 : Young's modulus for melt spun fibers of all samples with 2 mm/min plunger speed.

4.2 Rheological Test Results

Frequency sweep test were operated on disk shaped six nanocomposite samples at three process temperature (180°C, 205°C, and 230°C) according to the procedure given in the Section 3.4.2. Storage Modulus (G') and loss Modulus (G") and complex viscosity (η*) were plotted against frequency in log-log scale can be shown in Figure 4.4, Figure 4.5 and Figure 4.6.

For all temperatures, it can be observed that both storage modulus and loss modulus progressively increase with increase of frequency. However, loss modulus (G") takes higher value than (G') at low frequency. On the other side, complex viscosity (η*) decreases with increasing frequency.

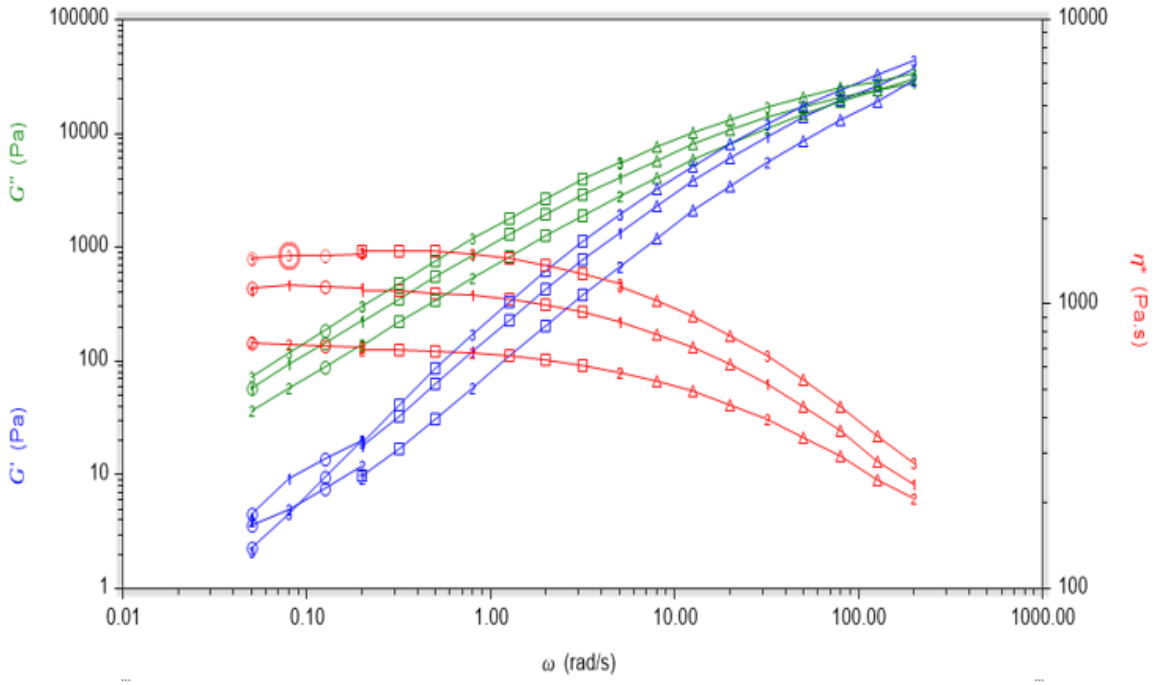

Figure 4.4 : Storage modulus (G'), loss modulus (G") and complex viscosity (η*) of (1) 3%POSS-PP , (2) 5%POSS-PP and (3)10%POSS-PP samples at 180ºC.

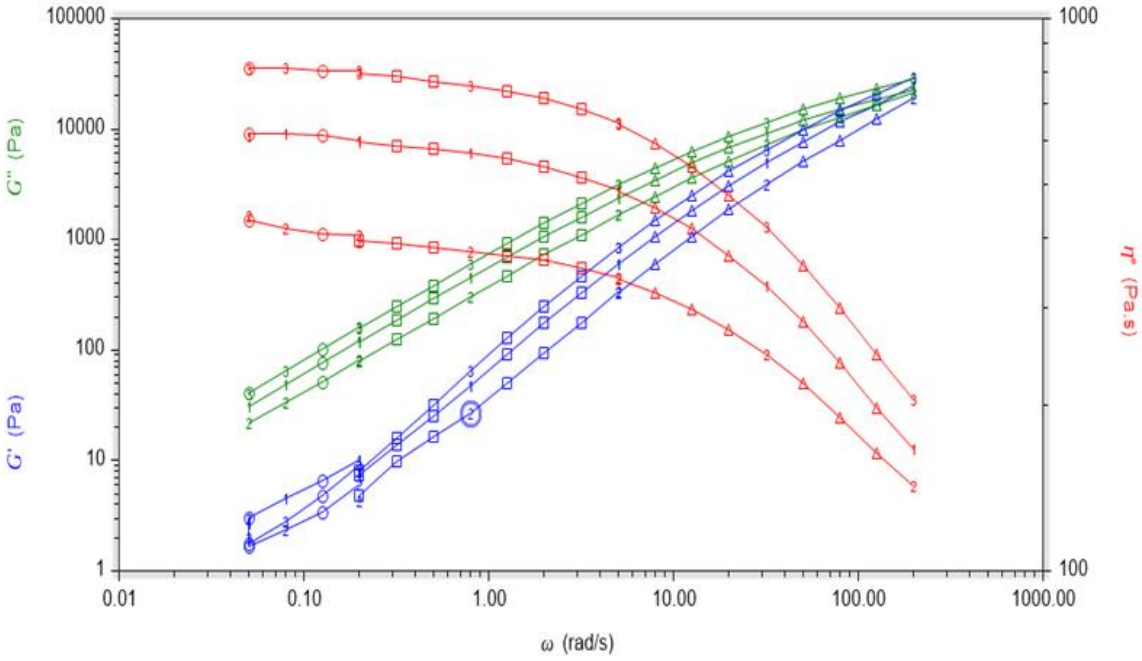

Figure 4.5 : Storage modulus (G'), loss modulus (G") and complex viscosity (η*) of (1) 3%POSS-PP , (2) 5%POSS-PP and (3)10%POSS-PP samples at 205ºC.

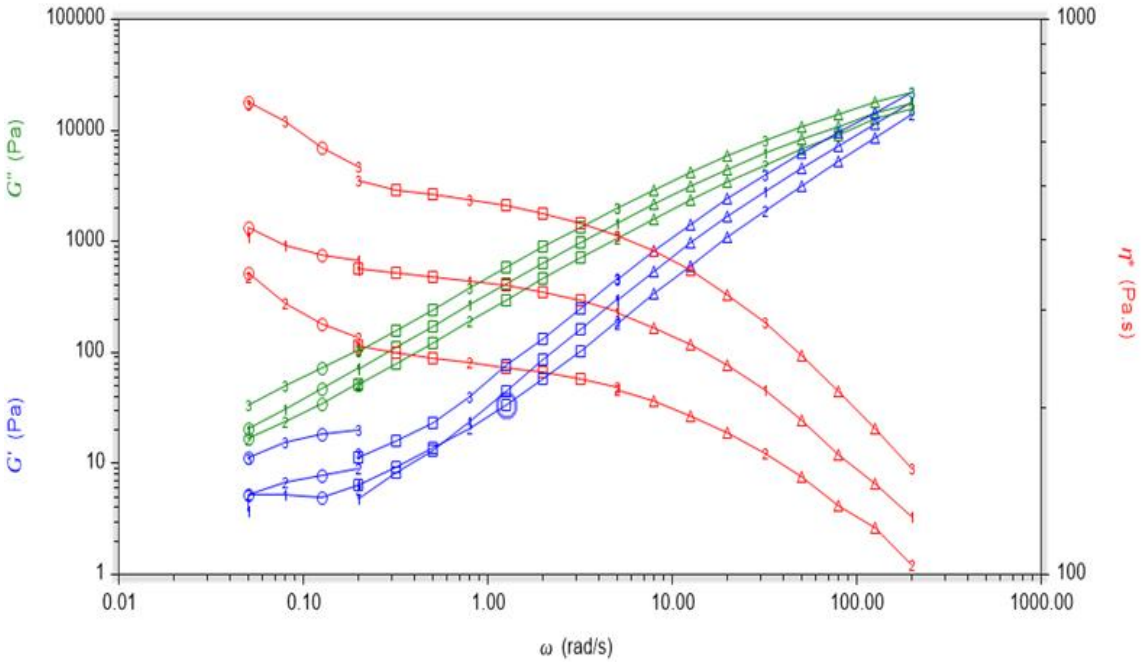

Figure 4.6 : Storage modulus (G'), loss modulus (G") and complex viscosity (η*) of (1) 10%POSS-PP , (2) 5%POSS-PP and (3)1%POSS-PP samples at 230ºC.

The value of complex viscosity showed large increase with reduction of temperature at high frequency. For instance, complex viscosity values measured at 205 °C and 230 °C were very close to each other for ω >10 rad/s. However, complex viscosity measured at 180 °C showed much larger deviations than what was seen in Figure 4.4

The increase of frequency “freezes” the chain movements and a stiffer behavior was observed. This temperature shifted to higher values with increasing frequency, indicating that at higher frequency, more movement of the atoms will be required to match the imposed frequency, which can be attained with higher temperature [48].

4.3 Differential Scanning Calorimetry (DSC)

The thermal transition behaviors of PP/POSS nanocomposites were analyzed by differential scanning calorimetry. The heating and cooling curves for the PP with different POSS percentage were shown in Figures from 4.7 to 4.11.

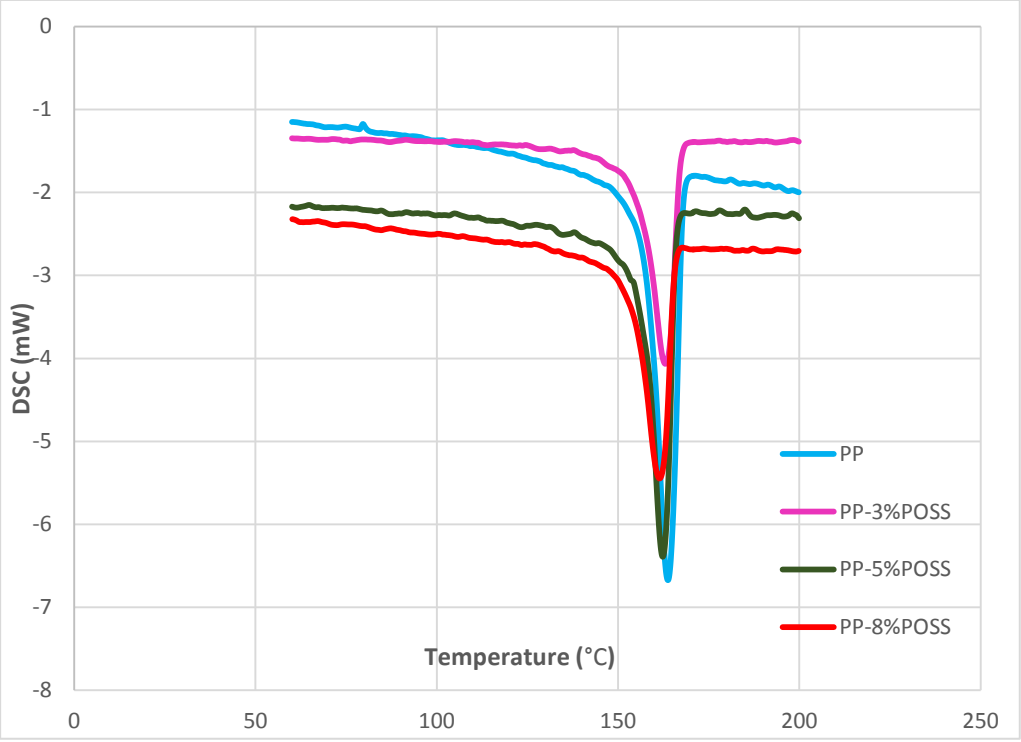

Figure 4.7 : Melting peaks of endothermic DSC curves of PP/POSS nanocomposite fibers.

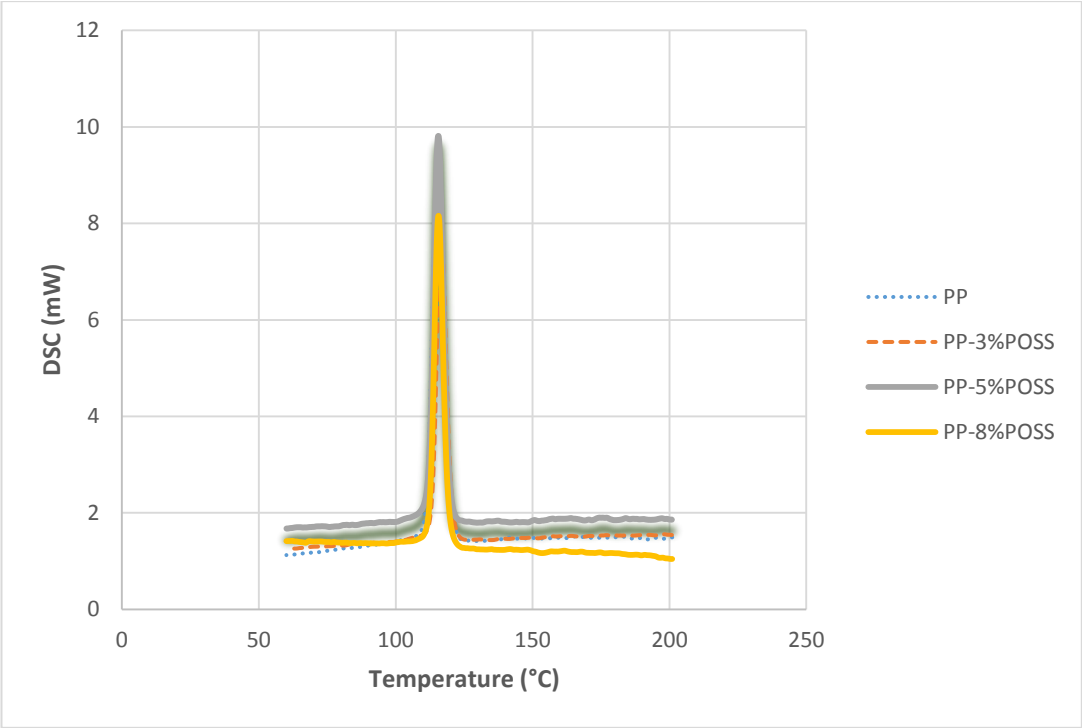

Figure 4.8 : Crystallisation peaks of exothermic DSC curves of PP/POSS nanocomposite fibers.

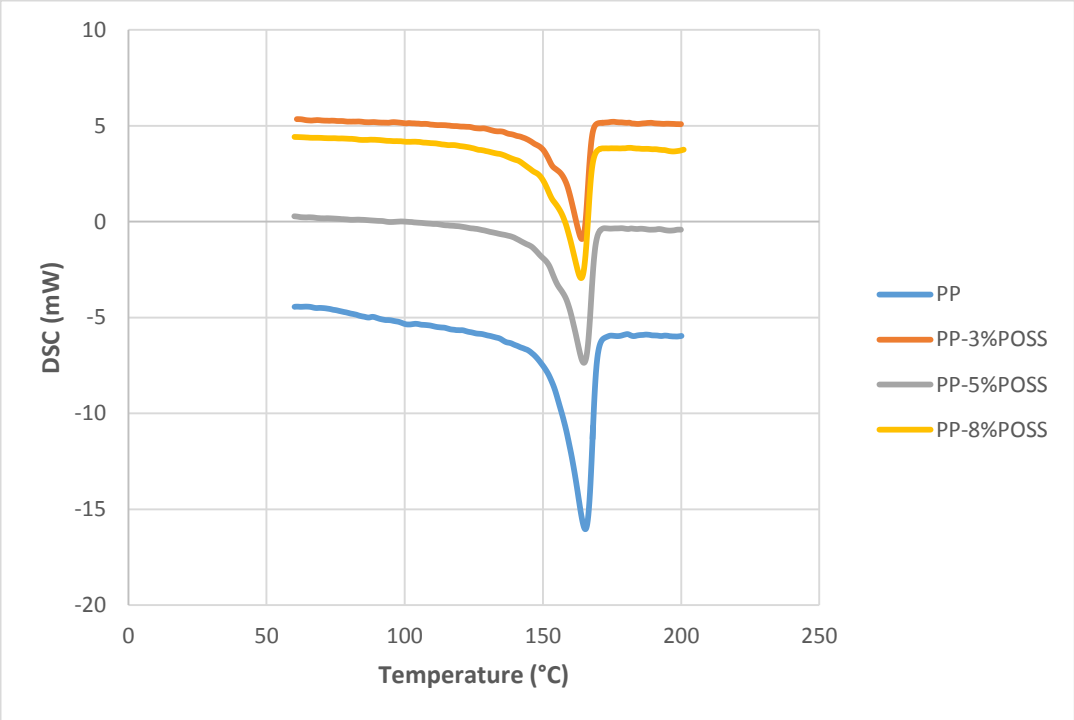

Figure 4.9 : First melting peaks of endothermic DSC curves of PP/POSS nanocomposite films.

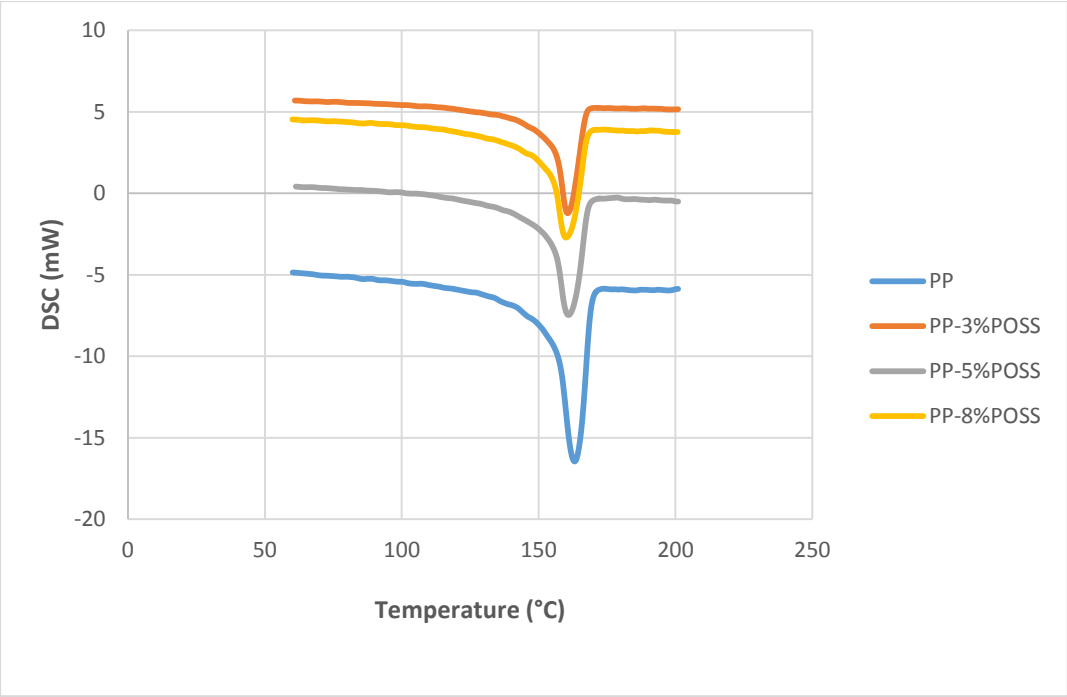

Figure 4.10 : Second melting peaks of endothermic DSC curves of PP/POSS nanocomposite films.

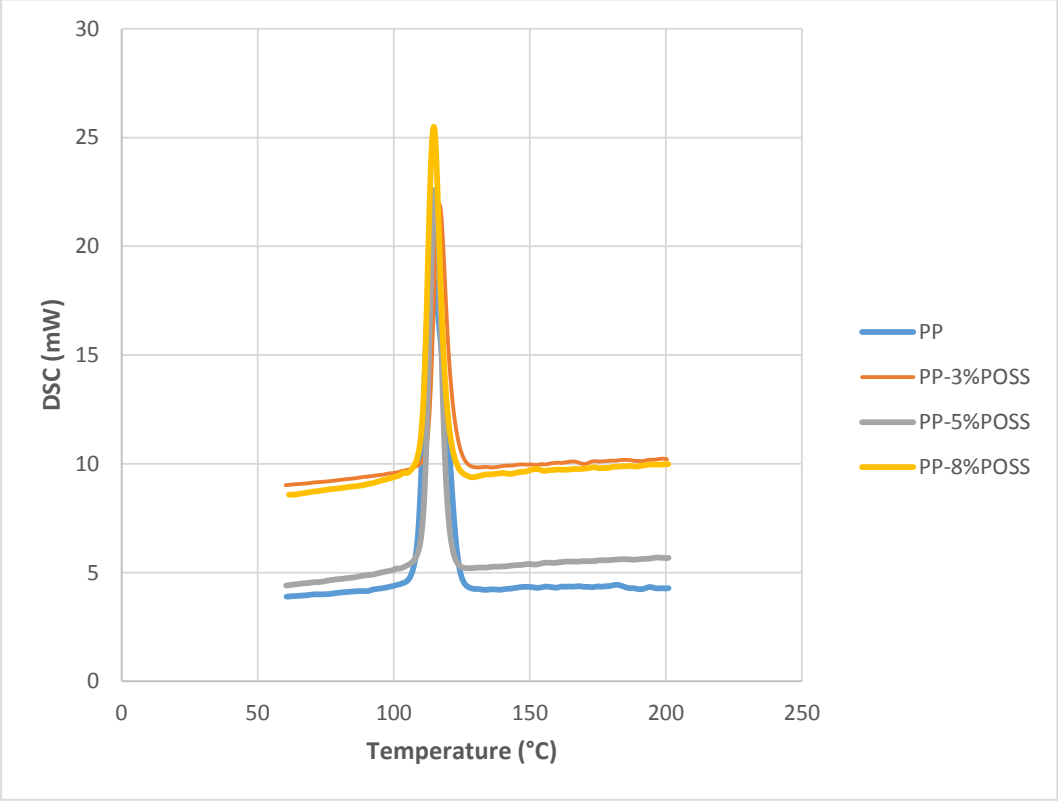

Figure 4.11 : Crystallisation peaks of exothermic DSC curves of PP/POSS nanocomposite films.

Degree of crystallinity (Xc) values determined from the enthalpy values of melting obtained from the second heating run using the following equation [49] :

$$X_c(\%) = \frac{\Delta H_m}{(1-\alpha)\Delta H_m^o} \times 100 \quad (1)$$

where ΔHm is the enthalpy of melting in the second heating scan of the samples (Jg^{-1}), ΔHm is the enthalpy value of melting of a 100% crystalline form of a matrix polymer and α is the weight fraction of nano-POSS or PP-POSS nanocomposite. Values of ΔHm were taken as 209 Jg^{-1} for i-PP.

Table 4.2 : Second melting temperature, enthalpy and degree of crystallinity values of the film samples crystallized at a particular crystallization temperature.

Samples	Tcry (°C)	Tm (°C)	ΔHm (J/g)[a]	ΔHc (J/g)	Xc (%)[b]
PP	116.4	162.9	120	-132	57.4
3%POSS/PP	116.1	163.1	105	-105	51.7
5%POSS/PP	115.9	161.6	93	-100	46.8
8%POSS/PP	115.3	160.3	89	-96.6	46.3

[a] Enthalpy of second melting endotherm recorded at the heating rate of 10 °C min^{-1}.

[b] Degree of crystallinity calculated with the Eq. (1) by using the enthalpy values of second melting.

Table 4.3 : First melting temperature, enthalpy and degree of crystallinity values of the film samples crystallized at a particular crystallization temperature.

Samples	Tcry (°C)	Tm (°C)	ΔHm (J/g)[a]	ΔHc (J/g)	Xc (%)[b]
PP	116.4	165.4	110	-132	52.6
3%POSS/PP	116.1	164.1	104	-105	51.2
5%POSS/PP	115.9	164.6	86	-100	43.4
8%POSS/PP	115.3	164.1	81	-96.6	42.1

Table 4.4 : Melting temperature, enthalpy and degree of crystallinity values of the fiber samples crystallized at a particular crystallization temperature.

Samples	Tcry (°C)	Tm (°C)	ΔHm (J/g)	ΔHc (J/g)	Xc (%)
PP	77.3	163.5	77.3	-91.6	36.9
3%POSS/PP	55.6	162.8	55.6	-63.4	27.4
5%POSS/PP	67.2	161.9	67.2	-102	33.8
8%POSS/PP	54.1	161.4	54.1	-59	27.1

Table 4.2 - 4.4 showed that the ΔHm (calculated from the thermograms by evaluating the area under the melting curves) vary depending on the POSS content. Both Tm and Tcry values decrease by increasing of POSS content. In light of this information it can be clearly seen that from the, addition of POSS reduces the melting and crystallisation temperature of PP. Increasing of POSS content also decrease degree of crystallinity. This indicates that chain movements restricted by presence of POSS molecules. Morover, fiber samples have higher degree of crystallinity values than film samples.

4.4 Thermogravimetric Analysis (TGA)

The influence of POSS content on the thermal stability and degradation behavior of PP were investigated by thermogravimetric analysis (TGA) for the PP/POSS nanocomposites. Specimens of ca. 5 mg were subjected to thermal scan from room temperature up to 800 °C, at a scan rate of 10 °C/min under nitrogen. The temperature at the onset of thermal degradation or 5 % mass loss (T1), and 10% mass loss (T2) was estimated from a mass versus temperature plot. T1 and T2 values for samples were given in Table 4.5.

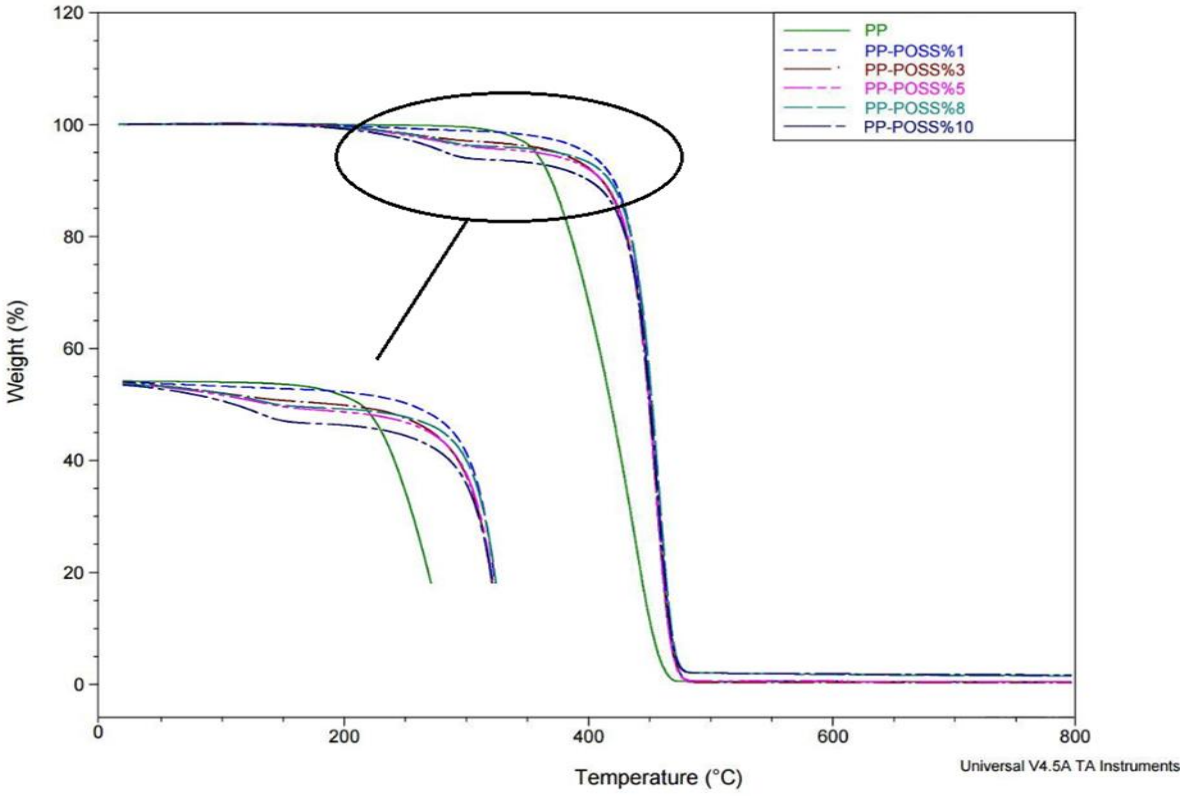

Figure 4.12 : TGA curves for PP/POSS nanocomposites under nitrogen atmosphere.

Table 4.5 : T1 and T2 temperatures for all compositions.

Samples	T1 (°C)	T2 (°C)
PP	358.23	370.84
1%POSS/PP	399.76	421.73
3%POSS/PP	375.71	411.88
5%POSS/PP	358.21	412.02
8%POSS/PP	375.25	418.29
10%POSS/PP	284.45	401.19

Thermograms of samples with varied POSS levels are shown in Figure 4.12. It is seen that POSS reinforced PP samples did not show weight loss until around 400 °C. However, for 10%POSS/PP sample, the weight loss was observed to begin at approximately 280 °C reaching a weight loss of 5 %. It can be attributed to the loss of moisture from the PP/POSS molecules. Additionally, neat PP matrix started degradation at around 350 °C under nitrogen. As can be observed, the TGA curves shift towards higher temperature with addition of POSS molecules on PP, indicating that the introduction of POSS group has a positive effect on the thermal stability of the materials.

4.5 Morphological Results

In order to characterize nanocomposite morphology and structures of 97 different fibers were characterized by using polarized optical microscope (Figures 4.13 - 4.21) according to the procedure given in the Section 3.4.5.1.

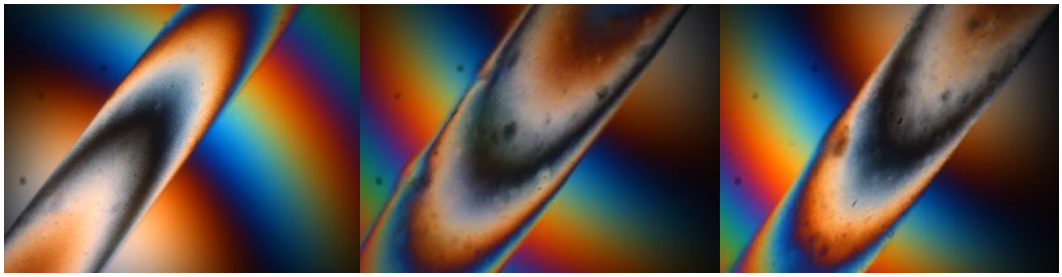

(a) (b) (c)

Figure 4.13 : POM micrographs of nanofibers in (a) 1%POSS/PP-0.5/20 and (b) 3%POSS/PP-0.5/20 and (c) 5%POSS/PP-0.5/20.

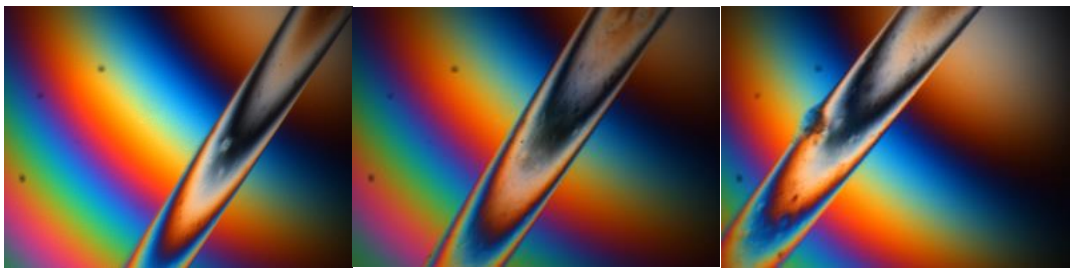

(a) (b) (c)

Figure 4.14 : POM micrographs of nanofibers in (a) 1%POSS/PP-0.5/60 and (b) 3%POSS/PP-0.5/60 and (c) 5%POSS/PP-0.5/60.

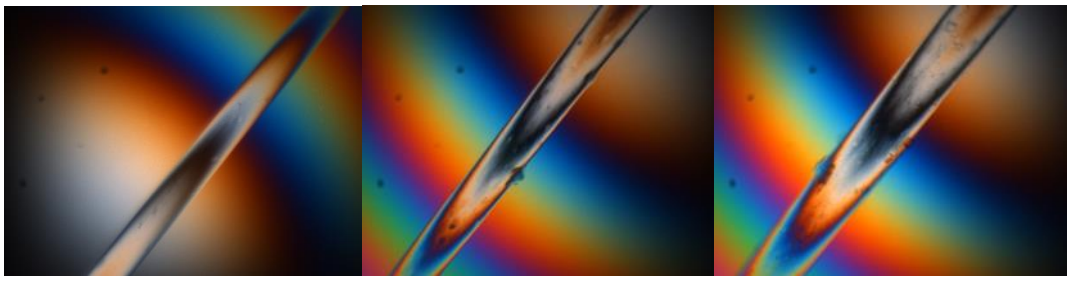

(a) (b) (c)

Figure 4.15 : POM micrographs of nanofibers in (a) 1%POSS/PP-0.5/120 and (b) 3%POSS/PP-0.5/120 and (c) 5%POSS/PP-0.5/120.

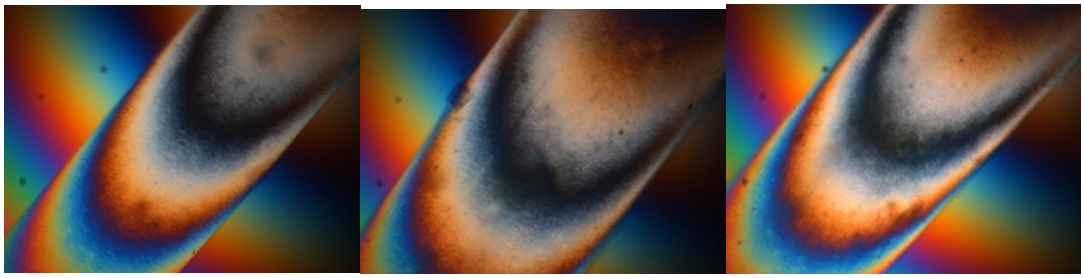

(a) (b) (c)

Figure 4.16 : POM micrographs of nanofibers in (a) 1%POSS/PP-1/20 and (b) 3%POSS/PP-1/20 and (c) 5%POSS/PP-1/20.

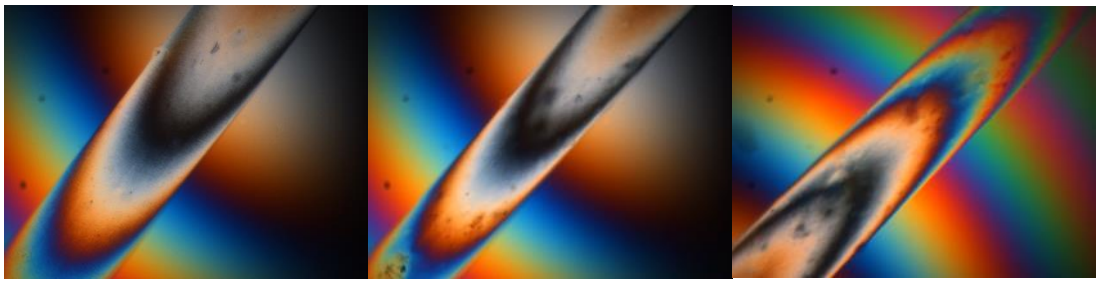

(a) (b) (c)

Figure 4.17 : POM micrographs of nanofibers in (a) 1%POSS/PP-1/60 and (b) 3%POSS/PP-1/60 and (c) 5%POSS/PP-1/60.

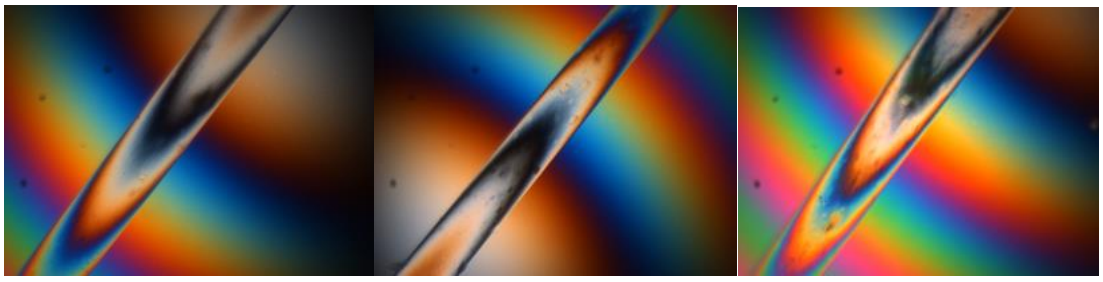

(a) (b) (c)

Figure 4.18 : POM micrographs of nanofibers in (a) 1%POSS/PP-1/120 and (b) 3%POSS/PP-1/120 and (c) 5%POSS/PP-1/120.

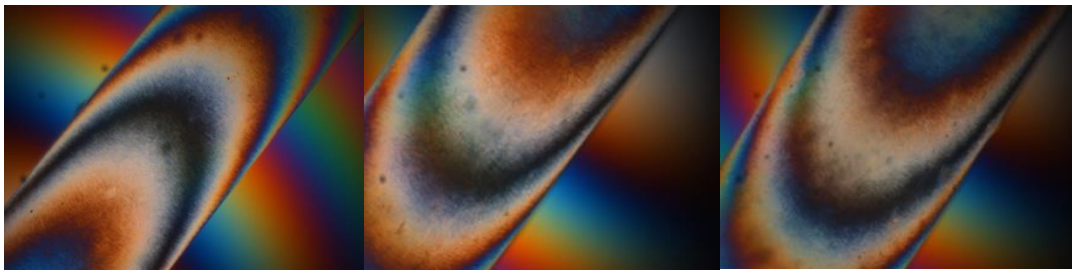

(a) (b) (c)

Figure 4.19 : POM micrographs of nanofibers in (a) 1%POSS/PP-2/20 and (b) 3%POSS/PP-2/20 and (c) 5%POSS/PP-2/20.

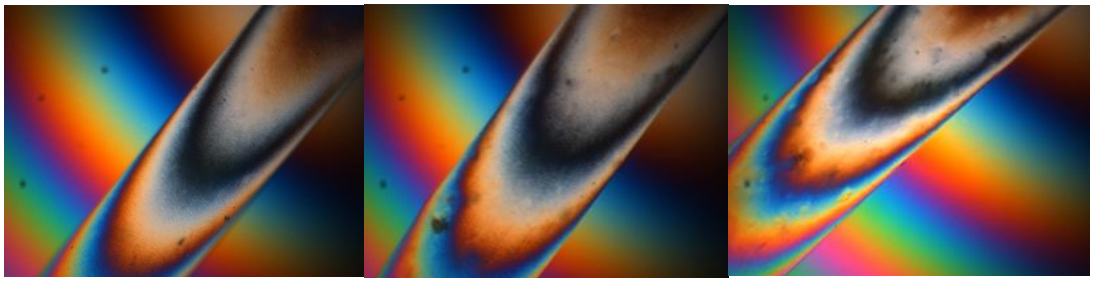

(a) (b) (c)

Figure 4.20 : POM micrographs of nanofibers in (a) 1%POSS/PP-2/60 and (b) 3%POSS/PP-2/60 and (c) 5%POSS/PP-2/60.

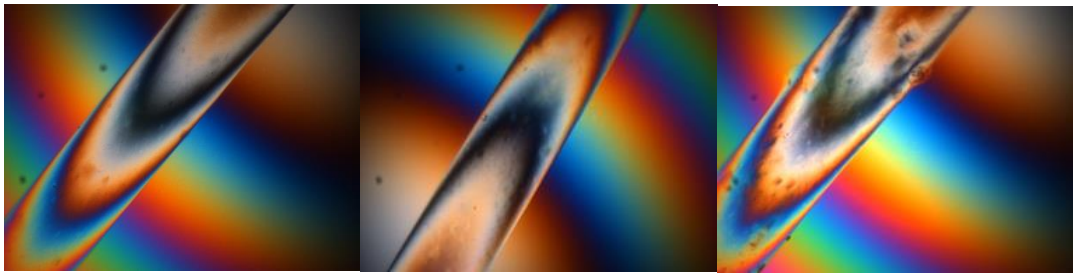

(a) (b) (c)

Figure 4.21 : POM micrographs of nanofibers in (a) 1%POSS/PP-2/120 and (b) 3%POSS/PP-2/120 and (c) 5%POSS/PP-2/120.

Birefringence (Δn_{12}) of solid fibers was measured using a polarized optical microscope equipped (POM) with 30 order Berek compensator. For the fiber birefringence, equations 2, 3, 4 and 5 must be taken to transform the raw data into the Hermans orientation factor, which is the wanted result. Birefringence values calculated by using Γ: retardation time and d: fiber diameter.

$$2i = i_{\text{black}} + i_{\text{red}} \quad (2)$$

$$\Gamma = 6.377^{*} \text{ value } (10000\, f\,(2i)) \quad (3)$$

$$\Delta n_{12} = \Gamma / d \quad (4)$$

$$f = \Delta n_{12} / \Delta n^{0} \quad (5)$$

Table 4.6 : Birefringence calculation for PP 80 rpm 2mm/min and 60 DDR.

Black	Red	B+R	2i	10000f(2i)	Γ	diameter(nm)	Δn_{12}
6.7	8.9	15.6	15.6	184.9	1179	129700	0.009

Example calculation for birefringence is seen in Table 4.6. All birefringence value were given in Table 4.7 which are calculated by the same method as shown in Table 4.6. Birefringence-DDR graphs were plotted (Figure 4.22 - 4.24) by using data in Table 4.7.

Table 4.7 : Birefringence values for all samples.

Plunger speed (mm/min) /take up speed(rpm)	PP	1% POSS/PP	3% POSS/PP	5% POSS/PP	8% POSS/PP	10% POSS/PP
2/20	0.0016	0.0041	0.0035	0.0042	0.0040	0.0021
2/40	0.0063	0.0047	0.0038	0.0057	0.0060	0.0021
2/60	0.0083	0.0046	0.0048	0.0079	0.0059	0.0023
2/80	0.0090	0.0058	0.0051	0.0074	0.0069	0.0023
2/100	0.0103	0.0059	0.0049	0.0095	0.0047	0.0032
2/120	0.0031	0.0084	0.0074	0.0125	0.0082	0.0033
1/20	0.0059	0.0029	0.0136	0.0048	0.0040	0.0014
1/40	0.0078	0.0052	0.0030	0.0064	0.0058	-
1/60	0.0094	0.0046	0.0043	0.0076	0.0082	-
1/80	0.0110	0.0061	0.0086	0.0101	0.0086	-
1/100	0.0122	0.0075	0.0110	0.0121	0.0089	-
1/120	0.0139	0.0091	0.0115	0.0126	0.0102	-
0.5/20	0.0059	0.0038	0.0052	0.0039	0.0031	-
0.5/40	0.0087	0.0072	0.0096	0.0069	0.0059	-
0.5/60	0.0116	0.0023	0.0123	0.0098	0.0091	-
0.5/80	0.0135	0.0114	0.0178	0.0115	0.0087	-
0.5/100	0.0131	0.0110	0.0127	0.0129	0.0108	-
0.5/120	0.0109	0.0050	0.0136	0.0133	0.0116	-

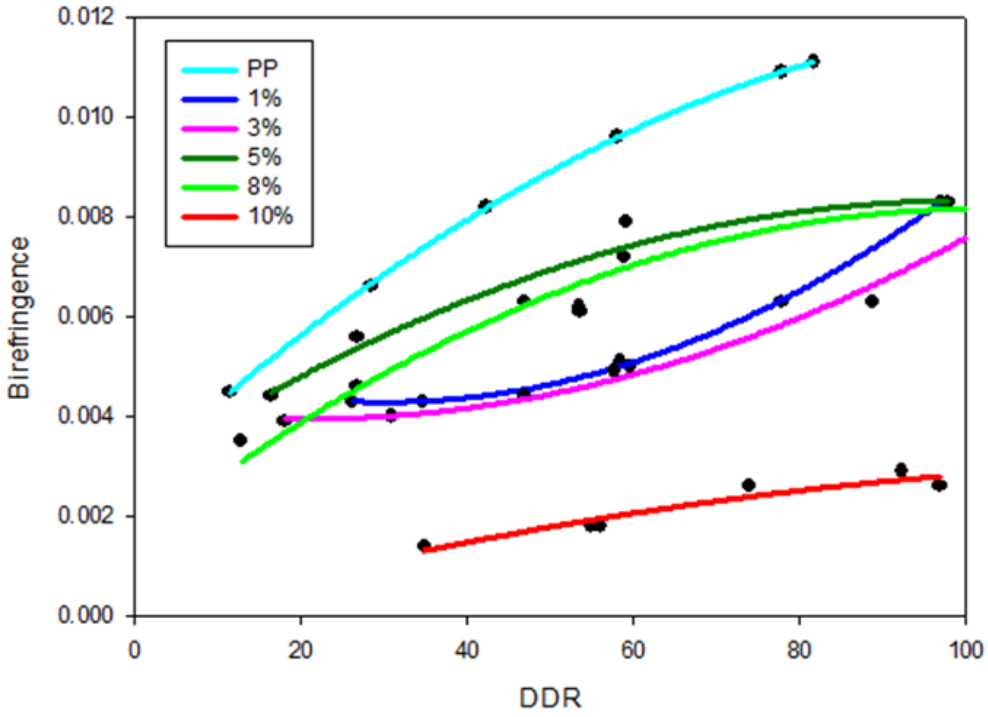

Figure 4.22 : The birefringence of PP/POSS nanofibers at selected DDR levels at 2 mm/min plunger speed.

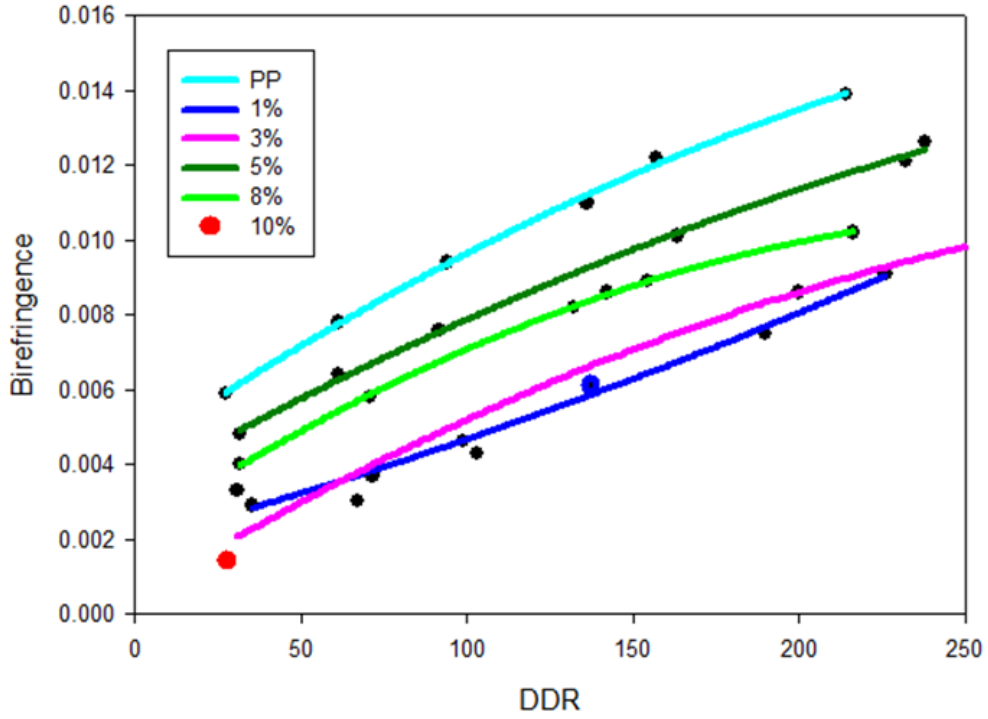

Figure 4.23 : The birefringence of PP/POSS nanofibers at selected DDR levels at 1 mm/min plunger speed.

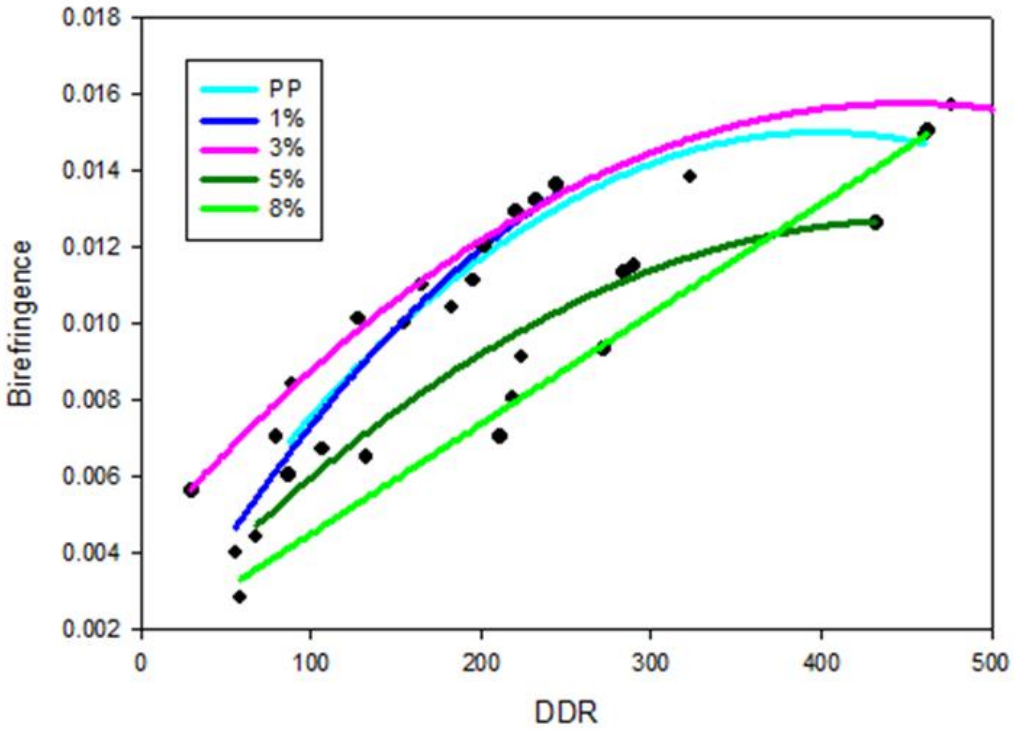

Figure 4.24 : The birefringence of PP/POSS nanofibers at selected DDR levels at 0.5 mm/min plunger speed.

Figure 4.22, Figure 4.23, and Figure 4.24 shows the increasing of birefringence value by increasing of DDR if it is compared with initial state. 10%POSS/PP nanofibers allows the melt spun process at maximum 1 mm/min plunger speed and 20 rpm take up speed conditions.

The birefringence of the as-spun filaments is plotted as a function of the draw-down ratio (DDR= D_{die}^2/D_{fiber}^2) in Figure 4.22-24. Comparison of PP and PP/POSS monofilament properties is also necessary because the POSS reinforced polypropylene has lower molecular weight, and thus its presence is expected to modify the orientation behavior of the PP fiber during spinning. In this graph, it is evident that the POSS reduces the molecular orientation of PP fibers for all spinning conditions employed in this study. Here, PP was characterized in non-extruded state. Extrusion process may lead to decrease molecular weight. Neat PP having higher MW contains an elevated number of entanglements that constrain the polymer chain mobility and consequently results in higher viscosity.

4.6 Small Angle X-ray Scattering (SAXS)

The lamellar structure of PP/POSS nanocomposite fibers was studied with two dimensional small-angle x-ray scattering (2DSAXS).

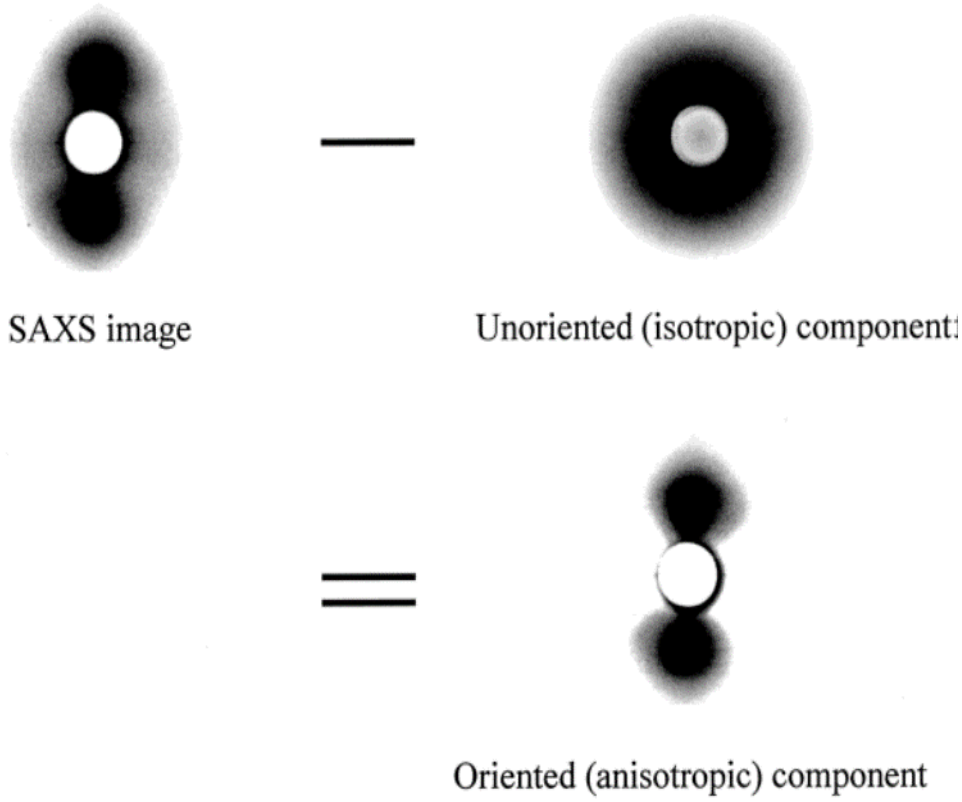

Figure 4.25 : Schematic diagram for the calculation of the oriented fraction from the SAXS pattern. The oriented fraction is obtained with the oriented component intensity divided by the total integrated SAXS intensity.

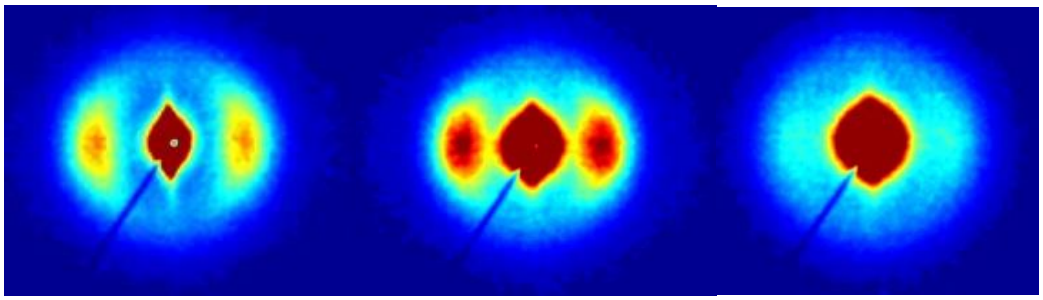

(a) (b) (c)

Figure 4.26 : Selected SAXS images of fibers at 20 rpm and 2 mm/min plunger speed values: (a) 1%POSS/PP, (b) 5%POSS/PP and (c) 10%POSS/PP for 1h explosure time.

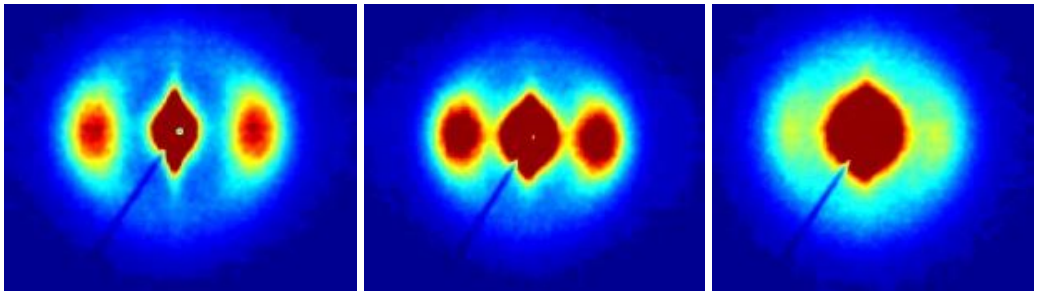

(a) (b) (c)

Figure 4.27 : Selected SAXS images of fibers at 60 rpm and 2 mm/min plunger speed values: (a) 1%POSS/PP, (b) 5%POSS/PP and (c) 10%POSS/PP for 1h explosure time.

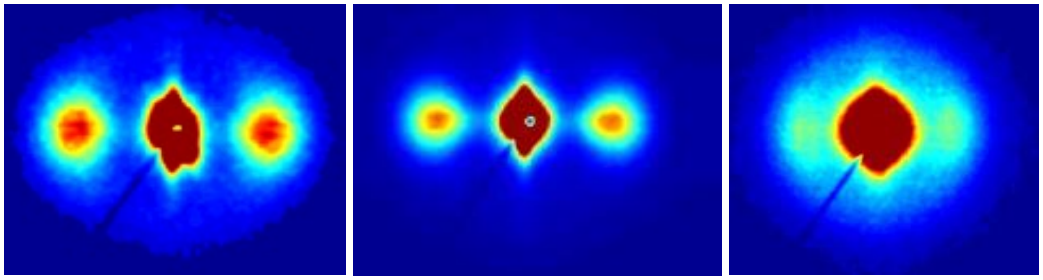

(a) (b) (c)

Figure 4.28 : Selected SAXS images of fibers at 120 rpm and 2 mm/min plunger speed values: (a) 1%POSS/PP, (b) 5%POSS/PP and (c) 10%POSS/PP for 1h explosure time.

The SAXS patterns showed scattering maxima along the shear direction, which corresponded to a lamellar structure developed perpendicularly to the flow direction. Increasing of take up speed remarkably increased the anisotropy of the samples. This means more oriented fibers were obtained at high take up speed values.

d-spacing is defined as the distance between adjacent planes and can be calculated for SAXS by Bragg's equation (Eqn. 6) where the q is scattering intensity. q values are obtained by the peak point of shoulder region of log intensity versus log q plot as seen in Figure 4.29. Remain part of the SAXS images were given in Appendix A.

$$q = 2\pi / d \tag{6}$$

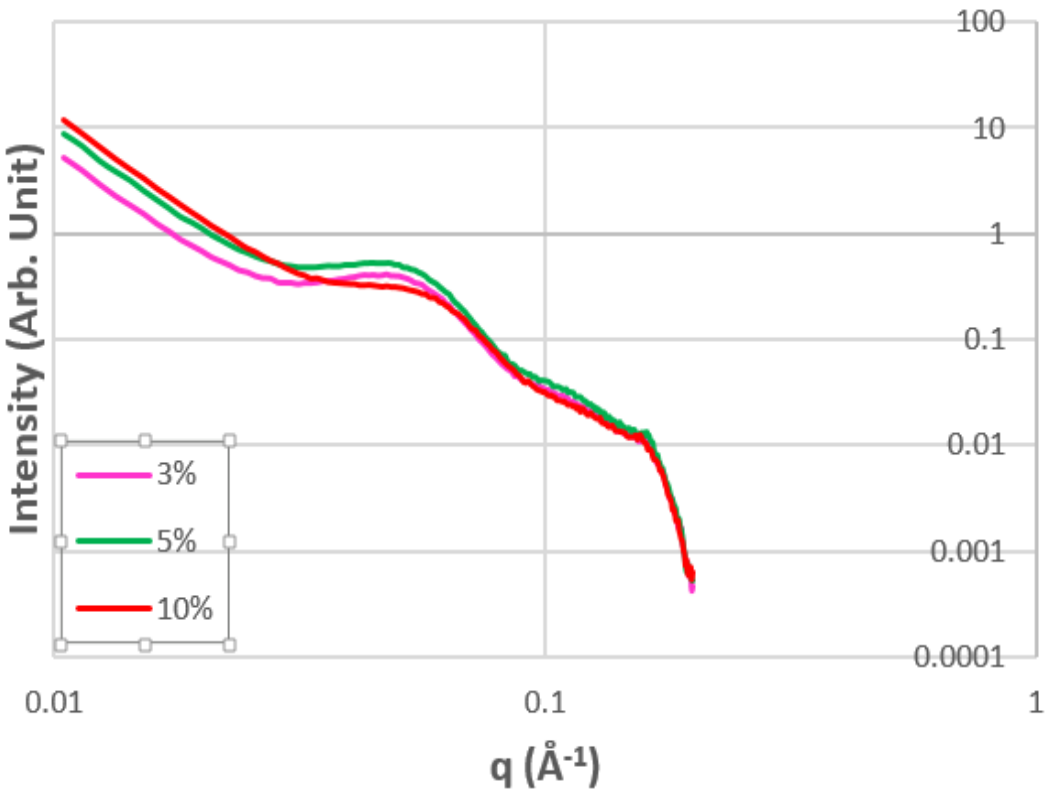

Figure 4.29 : Typical time evolution of linear SAXS plots of 3%, 5% and 10%POSS/PP-2/20 sample.

Table 4.8 : d-Spacing and scattering intensity values for various samples.

Sample	q	d
PP- 1/120	0.0496	126.7
PP- 2/20	0.0496	126.7
PP- 2/100	0.0496	126.7
PP- 1/120	0.0496	126.7
1%POSS/PP- 1/20	0.0534	117.7
1%POSS/PP- 1/60	0.0524	119.9
1%POSS/PP- 1/120	0.0505	124.4
1%POSS/PP- 2/20	0.0496	126.7
1%POSS/PP- 2/60	0.0524	119.9
1%POSS/PP- 2/120	0.0505	124.4
1%POSS/PP- 0.5/20	0.0515	122.0
3%POSS/PP- 1/60	0.0553	113.6
3%POSS/PP- 2/20	0.0515	122.0
3%POSS/PP- 2/120	0.0515	122.0
3%POSS/PP- 1/120	0.0515	122.0
3%POSS/PP- 0.5/80	0.0467	134.5
3%POSS/PP-0.5/120	0.0467	134.5
5%POSS/PP- 1/20	0.0534	117.7
5%POSS/PP- 1/120	0.0524	119.9
5%POSS/PP- 2/20	0.0534	117.7
5%POSS/PP- 2/60	0.0534	117.7
5%POSS/PP- 2/120	0.0515	122.0
5%POSS/PP- 0.5/20	0.0572	109.8
5%POSS/PP-0.5/120	0.0515	122.0
8%POSS/PP- 1/20	0.0563	111.6
8%POSS/PP- 1/100	0.0534	117.7
8%POSS/PP- 2/60	0.0543	115.7
8%POSS/PP- 2/20	0.0543	115.7
8%POSS/PP- 2/120	0.0534	117.7
8%POSS/PP- 0.5/40	0.0572	109.8
8%POSS/PP-0.5/120	0.0524	119.9
10%POSS/PP- 2/20	0.0601	104.5
10%POSS/PP- 2/40	0.0621	101.2
10%POSS/PP- 2/60	0.0572	109.8
10%POSS/PP- 2/80	0.0639	98.3
10%POSS/PP- 2/100	0.0581	108.1
10%POSS/PP- 2/120	0.0911	69.0

5. CONCLUSION

In this study, PP/POSS nanocomposites were prepared by melt blending via extrusion. Samples then were used for melt spinning process. The effects of POSS content and the draw down ratio (DDR) of fibers, on the mechanical, thermal, and the morphological properties of PP were investigated.

Mechanical property analysis of the samples showed that composition and DDR of the nanocomposites had a pronounced effect on the tensile properties of these materials. For PP it is found that as DDR increased the elongation to break increased, but modulus, and stress decrease. As a result, and increase in the fiber strength correlated well with increased crystallinity and polymer chain orientation.

Rheological analysis of nanocomposites indicate that increasing of frequency increases both storage modulus (G') and loss modulus (G'') for all temperatures. However, complex viscosity (η*) decreases with increasing frequency. The increase of frequency causes the restriction of chain movements and a stiffer behavior was observed. On the other side, complex viscosity is affected by temperature importantly. The value of complex viscosity showed large increase with reduction of temperature at high frequency.

Thermal properties of the samples were analyzed. Addition of POSS to PP reduces the melting temperature and the increases the width of the melting peaks. TGA curves indicate that the introduction of POSS group has a positive effect on the thermal stability of the PP. There was not seen dramatically changes in ΔHm value depending on the POSS content; however there only appears to be a slight decrease in 10%POSS/PP samples.

According to birefringence vs DDR graphs which are plotted depending on POM data as the DDR increase resulting birefringence increase for all samples. Contributing of POSS to samples decreased birefringence when it is compared with neat PP.

It is apparent from this work that fiber spinning dramatically changed the morphological properties of a polymer system according to SAXS patterns. As the

DDR increase anisotropy of fibers increase. Furthermore, it is observed that high POSS content fibers have more isotropic structure. In consideration of this observation it is clearly seen that POSS content effects the morphology of fibers significantly.

It is apparent from this study that fiber spinning dramatically changed the properties of a polymer system. Several apparent changes in the polymer properties are observed with increasing DDR, take up speed, plunger speed and POSS content.

REFERENCES

[1] **Kuo, Shiao-Wei, and Feng-Chih Chang.** (2011). POSS related polymer nanocomposites, *Progress in Polymer Science*, 36.12: 1649-1696.

[2] **Koo, Joseph H.** (2006). Polymer nanocomposites. McGraw-Hill Professional Pub.

[3] **Kawakami Y, Kakihana Y, Miyazato A, Tateyama S, Hoque MA.** (2010). Polyhedral oligomeric silsesquioxanes with controlled structure: formation and application in new Si-based polymer systems, *Adv Polym Sci*, 55:1–44.

[4] **Ramanathan H., Liu H., L.C.** (2005). Brinson Functionalized SWNT/polymer nanocomposites for dramatic property improvement, *J. Polym. Sci, B Polym. Phys.*, 43, pp. 2269–2279

[5] **Li G., Wang V., Ni H., Pittmann C.U.,** (2001). Polyhedral Oligomeric Silsesquioxane (POSS) Polymers and Copolymers: A Review, *J. Inorg.Organomet. Polym*. 11, 123.

[6] **Fu, Bruce X., et al.** (2001). Crystallization studies of isotactic polypropylene containing nanostructured polyhedral oligomeric silsesquioxane molecules under quiescent and shear conditions, *Journal of Polymer Science Part B: Polymer Physics*, 39.22: 2727-2739.

[7] **Lee, L.J. Zeng, C., Cao, X., Han, X., Shen, J., Xu, G.** (2005). Polymer nanocomposite foams, *Compos. Sci. Technol*, 65, 2344-2363.

[8] **Liu, H., Brinson, L.C.** (2008). Reinforcing efficiency of nanoparticles: A simple comparison for polymer nanocomposites, *Compos. Sci. Technol*, 68, 1502-1512.

[9] **Schadler, L.S., Brinson, L.C., Sawyer, W.G.** (2007). Polymer Nanocomposites: A Small Part of the Stroy, *J. Miner. Met. Mater. Soc.*, 59, 53-60.

[10] **Bao, S.P., Tjong, S.C.** (2008). Mechanical behaviors of polypropylene/carbon nanotube nanocomposites: The effects of loading rate and temperature, *Mater. Sci. Eng.*, A 485, 508-516.

[11] **Bellucci, F., Terenzi, A., Leuteritz, A., Pospiech, D., Frache, A., Traverso, G., Camino, G. (**2008). Intercalation degree in PP/organoclay nanocomposites: role of surfactant structure, *Polym. Advan. Technol*, 19, 547-555.

[12] **Rong, M.Z., Zhang, M.Q., Zheng, Y.X., Zeng, H.M., Walter, R., Friedrich, K.** (2001). Structure-property relationships of irradiation grafted nano-inorganic particle filled polypropylene composites, *Polymer*, 42, 167-183.

[13] **Huang, J., He, C., Liu, X., Xu, J., Tay, C.S.S., Chow, S.Y.** (2005). Organic-inorganic nanocomposites form cubic silsesquioxane epoxides: direct characterization of interphase, and thermomechanical properties, *Polymer*, 46, 7018-7027.

[14] **Joshi, M., Butola, B.S.** (2004). Polymeric nanocomposites- Polyhedral Oligomeric Silsesquioxanes (POSS) as hybrid naofiller, *J. Macromol. Sci.-Polym*, R 44, 389-410.

[15] **Pielichowski, K., Njuguna, J., Janowski, B., Pielichowski, J.** (2006). Polyhedral 12 Oligomeric Silsesquioxane (POSS)-Containg Nanohybrid Polymers, *Adv. Polym. Sci*, 201, 225-296.

[16] **Xu, H., Kuo, S.-W., Lee, J.-S., Chang, F.-C.** (2002). Preparation, Thermal Properties, and Tg Increase Mechanism of Inorganic/Organic Hybrid Polymers Based on Polyhedral Oligomeric Silsesquioxanes, *Macromolecules*, 35, 8788-8793.

[17] **Zheng, L., Farris, R.J., Coughlin, E.B.** (2001). Novel Polyolefin Nanocomposites: Synthesis of Characterization of Metallocene-Catalyzed Polyolefin Oligomeric Silsesquioxanes Copolymers, *Macromolecules*, 34, 8034-8039.

[18] **Fu, Bruce X., Andre Lee, and Timothy S. Haddad.** (2004). Styrene-butadiene-styrene triblock copolymers modified with polyhedral oligomeric silsesquioxanes, *Macromolecules*, 37.14: 5211-5218.

[19] **Baldi, F., Bignotti, F., Fina, A., Tabuani, D., Ricco, T.** (2007). Mechanical Characterization of Polyhedral Oligomeric Silsesquioxane/Polypropylene Blends, *J. Appl. Polym. Sci.* , 105, 935-943.

[20] **Chen, J.-H., Yao, B.-X., Su, W.-B., Yang, Y.-B.** (2007). Isothermal crystallization behavior of isotactic polypropylene blended with small loading of polyhedral oligomeric silsesquioxne, *Polymer*, 48, 1756-1769.

[21] **PAC.** (2007), 79, 1801. Definitions of terms relating to the structure and processing of sols, gels, networks, and inorganic-organic hybrid materials (IUPAC Recommendations), doi:10.1351/pac200779101801

[22] **Grala, M., Z. Bartczak, and M. Pracella.** (2013). Morphology and mechanical properties of polypropylene-POSS hybrid nanocomposites obtained by reactive blending, *Polymer Composites*, 34.6 929-941.

[23] **Pracella, Mariano, et al.** (2006). Polypropylene-POSS Nanocomposites: Morphology and Crystallization Behaviour, *Macromolecular symposia*, Vol. 234. No. 1. WILEY-VCH Verlag.

[24] **Carniato, Fabio, et al.** (2008). Polypropylene containing Ti-and Al-polyhedral oligomeric silsesquioxanes: crystallization process and thermal properties, *Nanotechnology*, 19.47: 475701.

[25] **Cromer, Brian M., et al.** (2015). In-situ polymerization of isotactic polypropylene-nanographite nanocomposites, *Polymer*, 80: 275-281.

[26] **Yamak, H. B.** (2013). Emulsion Polymerization: Effect of Polymerization Variables on the Properties of Vinyl Acetate Based Copolymer Latexes, *Polymer Science*, InTech.

[27] **Rauwendaal, C.** (1998). Understanding Extrusion. Munich: Hanser.

[28] **Giles, H. F. & Wagner, J. R. & Mount, E. M.** (2005). Extrusion: The Definitive Processing Guide and Handbook. USA: William-Andrew Publishing.

[29] **Crawford, R. J.** (2005). Plastics Engineering (3rd ed). Oxford: Butterworth-Heinemann.

[30] **Odian, G.** (2004). Principles of Polymerization. Hoboken, New Jersey: Wiley-Interscience.

[31] **McNally, Tony, and Petra Pötschke, eds.** (2011). Polymer-carbon nanotube composites: Preparation, properties and applications, *Elsevier*.

[32] **Nwabunma, D. & Kyu, T.** (Eds.). (2008). Polyolefin Blends. Hoboken, New Jersey: Wiley- Interscience.

[33] **Neissl, W and Gahleitner, M.** (2001). Tailor-made polymers through selective modification, *Macromol. Symp*, FIELD Full Journal Title:Macromolecular Symposia 2002;181(5th Oesterreichische Polymertage, Chemical and Physical Aspects of Polymer Science and Engineering):177-188

[34] **Kürkçü, P.** (2007). Modification of Polypropylene Films For Antistatic And Anti Scratch Properties, M.Sc., Department of Polymer Science and Technology, METU.

[35] **Baney, R.H.** (1995) Silsesquioxanes, *Chemical Reviews*, 95, 1409–1430.

[36] **Zheng L, Farris RJ, and Coughlin E.B.** (2001). Novel Polyolefin Nanocomposites: Synthesis and Characterizations of Metallocene-Catalyzed Polyolefin Polyhedral Oligomeric Silsesquioxane Copolymers, *Macromolecules*, 34(23):8034-8039.

[37] **Zheng L, Hong S, Cardoen G, Burgaz E, Gido SP, and Coughlin E.B.** (2004). Polymer Nanocomposites through Controlled Self-Assembly of Cubic Silsesquioxane Scaffolds, *Macromolecules*, 37(23):8606-8611.

[38] **Waddon AJ, Zheng L, Farris RJ, and Coughlin E.B. (**2002). Nanostructured Polyethylene-POSS Copolymers: Control of Crystallization and Aggregation, *Nano Letters*, 2(10):1149-1155.

[39] **Waddon AJ and Coughlin E.B.** (2003). Crystal Structure of Polyhedral Oligomeric Silsequioxane (POSS) Nano-materials: A Study by X-ray Diffraction and Electron Microscopy, *Chemistry of Materials*, 15(24):4555-4561.

[40] **Zheng L, Waddon AJ, Farris RJ, and Coughlin E.B.** (2002). X-ray Characterizations of Polyethylene Polyhedral Oligomeric Silsesquioxane Copolymers, *Macromolecules*, 35(6):2375-2379.

[41] **Fu BX, Gelfer MY, Hsiao BS, Phillips S, Viers B, Blanski R, and Ruth P. (**2003). Physical gelation in ethylene-propylene copolymer melts induced by polyhedral oligomeric silsesquioxane (POSS) molecules, *Polymer*, 44(5):1499-1506.

[42] **Fu BX, Yang L, Somani RH, Zong SX, Hsiao BS, Phillips S, Blanski R, and Ruth P.** (2001). Crystallization studies of isotactic polypropylene containing nanostructured polyhedral oligomeric silsesquioxane molecules under quiescent and shear conditions, *Journal of Polymer Science, Part B: Polymer Physics*, 39(22):2727-2739.

[43] **Zhang HX, Shin YJ, Yoon KB, Lee DH.** (2009). Preparation and properties of propylene/POSS copolymer with rac-Et(Ind)2ZrCl2 catalyst, *Eur Polym J*, 45:40–6.

[44] **Fu BX, Yang C, Somani RH, Zong SX, Hsiao BS, Phillips S, Blanski R, Ruth D.** (2001). Crystallization studies of isotactic polypropylene containing nanostructured polyhedral oligomeric silsesquioxane molecules under quiescent and shear conditions, *J Polym Sci Part B: Polym Phys*, 39:2727–39.

[45] **Pracella M, Chionna D, Fina A, Tabuani D, Frache A, and Camino G.** (2006). Polypropylene-POSS nanocomposites: morphology and crystallization behaviour, *Macromolecular Symposia*, 234(Trends and Perspectives in Polymer Science and Technology):59-67.

[46] **Fina A, Tabuani D, Frache A, and Camino G.** (2005). Polypropylene-polyhedral oligomeric silsesquioxanes (POSS) nanocomposites, *Polymer*, 46(19):7855-7866.

[47] **Byoung-Jo Lee**, Ph.D Dissertation, The University of Akron, Summer 2009

[48] **Nair T.M. et al.** (2009). Dynamic Mechanical Analysis of Ethylene-Propylene-Diene Monomer Rubber and Styrene Butadiene Rubber Blends, *Journal of Applied Polymer Science* , Vol. 112, pp. 72-81.

[49] **Durmus A. et al.** (2012). Effect of polyhedral oligomeric silsesquioxane (POSS) reinforced polypropylene (PP) nanocomposite on the microstructure and isothermal crystallization kinetics of polyoxymethylene (POM). *Polymer 53.23: 5347-5357*.

APPENDICES

APPENDIX A: Figures

APPENDIX B : Tables

APPENDIX A

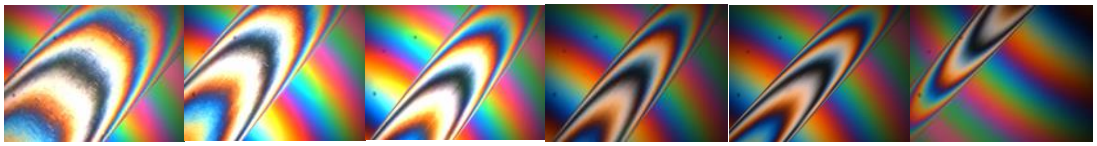

(a) (b) (c) (d) (e) (f)

Figure A.1 : POM micrographs of PP samples at 0.5 mm/min plunger speed and rpm of (a) 20, (b) 40, (c) 60, (d) 80, (e) 100, and (f) 120.

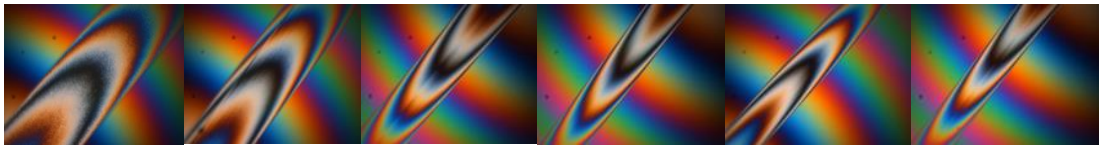

(a) (b) (c) (d) (e) (f)

Figure A.2 : POM micrographs of PP samples at 1 mm/min plunger speed and rpm of (a) 20, (b) 40, (c) 60, (d) 80, (e) 100, and (f) 120.

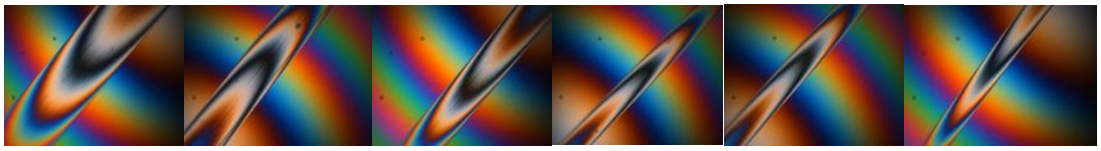

(a) (b) (c) (d) (e) (f)

Figure A.3 : POM micrographs of PP samples at 2 mm/min plunger speed and rpm of (a) 20, (b) 40, (c) 60, (d) 80, (e) 100, and (f) 120.

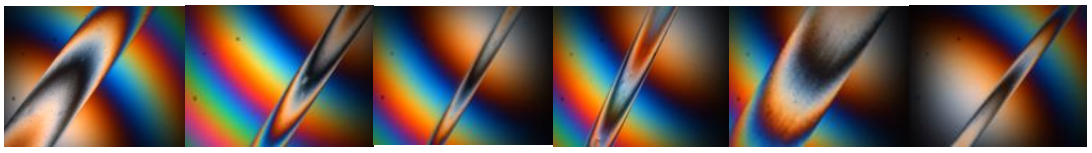

(a) (b) (c) (d) (e) (f)

Figure A.4 : POM micrographs of 1%POSS/PP samples at 0.5 mm/min plunger speed and rpm of (a) 20, (b) 40, (c) 60, (d) 80, (e) 100, and (f) 120.

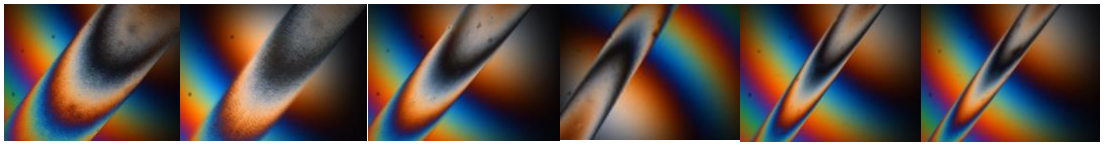

(a) (b) (c) (d) (e) (f)

Figure A.5 : POM micrographs of 1%POSS/PP samples at 1 mm/min plunger speed and rpm of (a) 20, (b) 40, (c) 60, (d) 80, (e) 100, and (f) 120.

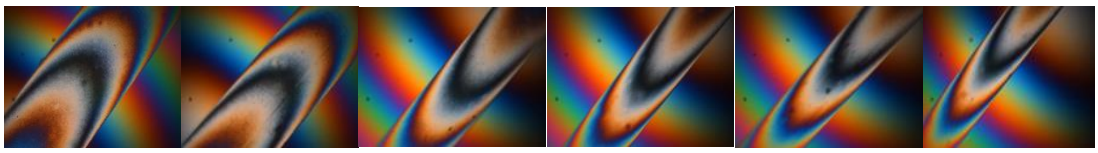

(a) (b) (c) (d) (e) (f)

Figure A.6 : POM micrographs of 1%POSS/PP samples at 2 mm/min plunger speed and rpm of (a) 20, (b) 40, (c) 60, (d) 80, (e) 100, and (f) 120.

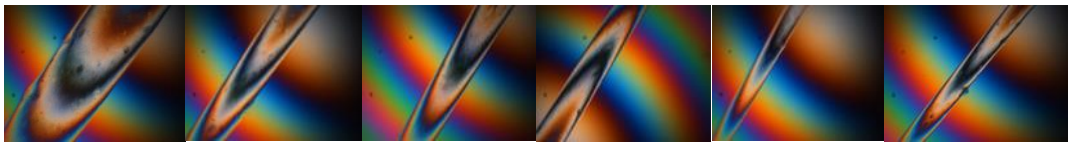

(a) (b) (c) (d) (e) (f)

Figure A.7 : POM micrographs of 3%POSS/PP samples at 0.5 mm/min plunger speed and rpm of (a) 20, (b) 40, (c) 60, (d) 80, (e) 100, and (f) 120.

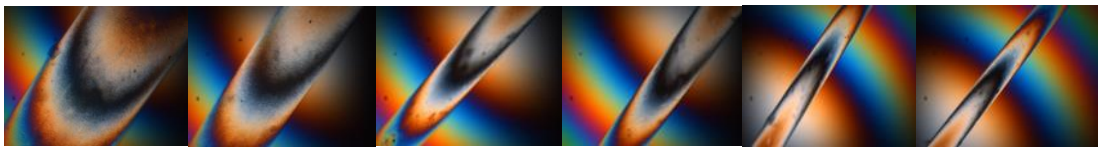

(a) (b) (c) (d) (e) (f)

Figure A.8 : POM micrographs of 3%POSS/PP samples at 1 mm/min plunger speed and rpm of (a) 20, (b) 40, (c) 60, (d) 80, (e) 100, and (f) 120.

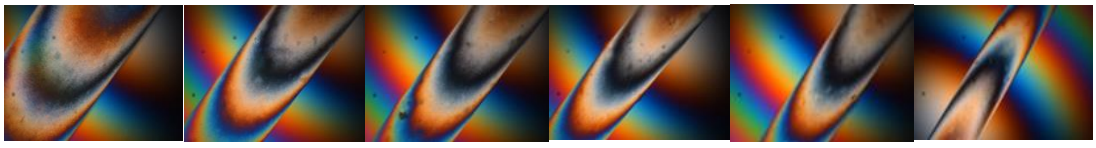

(a) (b) (c) (d) (e) (f)

Figure A.9 : POM micrographs of 3%POSS/PP samples at 2 mm/min plunger speed and rpm of (a) 20, (b) 40, (c) 60, (d) 80, (e) 100, and (f) 120.

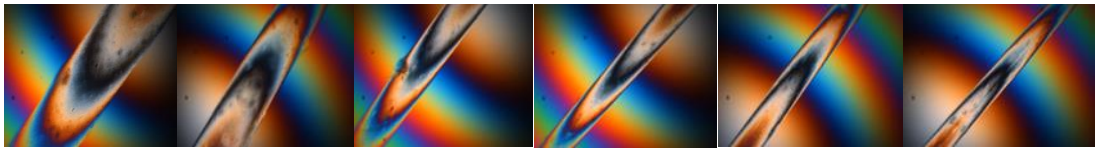

(a) (b) (c) (d) (e) (f)

Figure A.10 : POM micrographs of 5%POSS/PP samples at 0.5 mm/min plunger speed and rpm of (a) 20, (b) 40, (c) 60, (d) 80, (e) 100, and (f) 120.

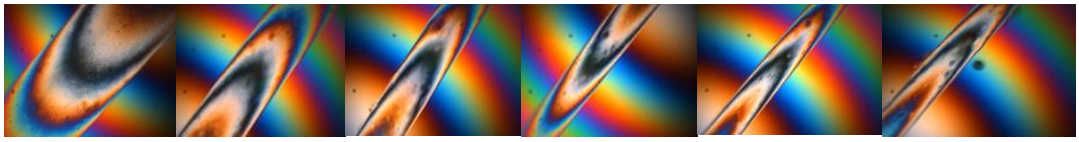

(a) (b) (c) (d) (e) (f)

Figure A.11 : POM micrographs of 5%POSS/PP samples at 1 mm/min plunger speed and rpm of (a) 20, (b) 40, (c) 60, (d) 80, (e) 100, and (f) 120.

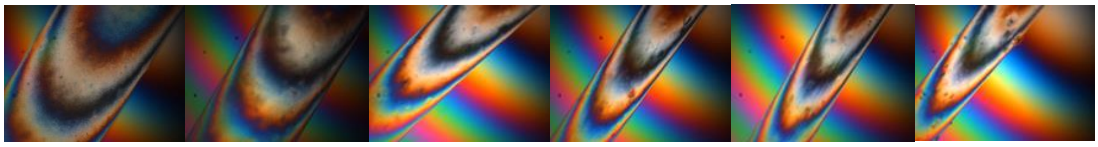

(a) (b) (c) (d) (e) (f)

Figure A.12 : POM micrographs of 5%POSS/PP samples at 2 mm/min plunger speed and rpm of (a) 20, (b) 40, (c) 60, (d) 80, (e) 100, and (f) 120.

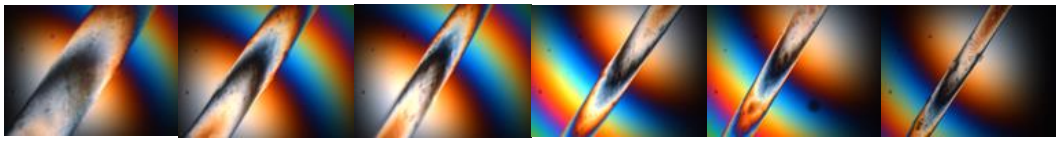

(a) (b) (c) (d) (e) (f)

Figure A.13 : POM micrographs of 8%POSS/PP samples at 0.5 mm/min plunger speed and rpm of (a) 20, (b) 40, (c) 60, (d) 80, (e) 100, and (f) 120.

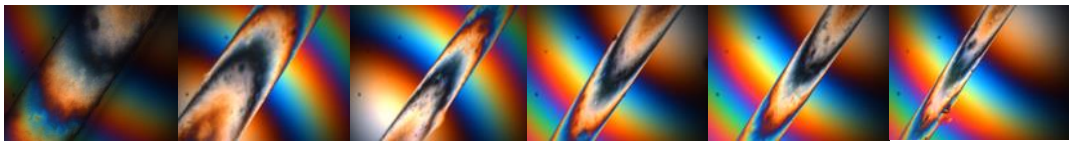

(a) (b) (c) (d) (e) (f)

Figure A.14 : POM micrographs of 8%POSS/PP samples at 1mm/min plunger speed and rpm of (a) 20, (b) 40, (c) 60, (d) 80, (e) 100, and (f) 120.

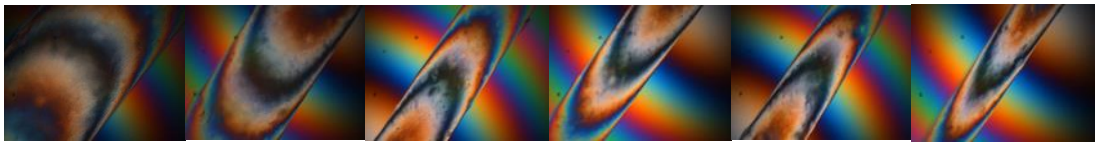

(a) (b) (c) (d) (e) (f)

Figure A.15 : POM micrographs of 8%POSS/PP samples at 2mm/min plunger speed and rpm of (a) 20, (b) 40, (c) 60, (d) 80, (e) 100, and (f) 120.

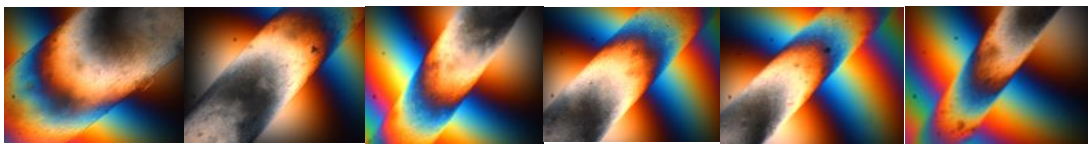

(a) (b) (c) (d) (e) (f)

Figure A.16 : POM micrographs of 10%POSS/PP samples at 2mm/min plunger speed and rpm of (a) 20, (b) 40, (c) 60, (d) 80, (e) 100, and (f) 120.

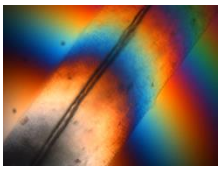

Figure A.17 : POM micrographs of 10%POSS/PP-1/20 sample.

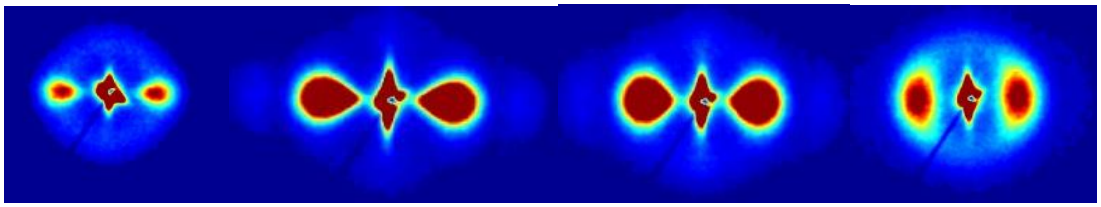

(a) (b) (c) (d)

Figure A.18 : SAXS images of samples (a) PP-0.5/120, (b) PP-1/120, (c) PP-2/100, (d) PP-2/20 for 15 min explosure time (a,b,c) and 30 min explosure time (d).

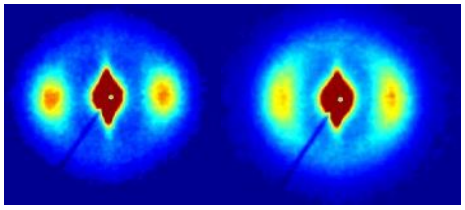

(a) (b)

Figure A.19 : SAXS images of samples, (a) 1%POSS/PP-1/60 for 30 min explosure time and, (b) 1%POSS/1/20 for 1h explosure time.

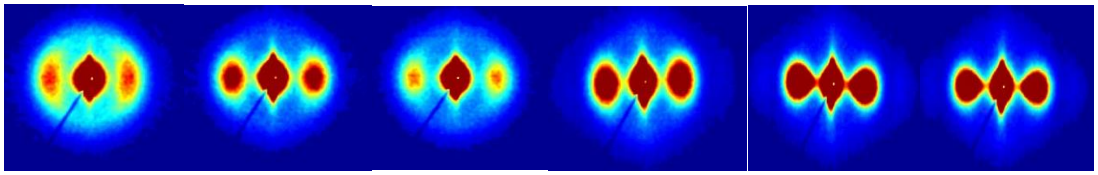

(a) (b) (c) (d) (e) (f)

Figure A.20 : SAXS images of samples (a) 3%POSS/PP-2/20, (b) 3%POSS/PP-2/120, (c) 3%POSS/PP-1/60, (d) 3%POSS/PP-1/120, (e)3%POSS/PP-0.5/80 (f)) 3%POSS/PP-0.5/120 for 30 min explosure time.

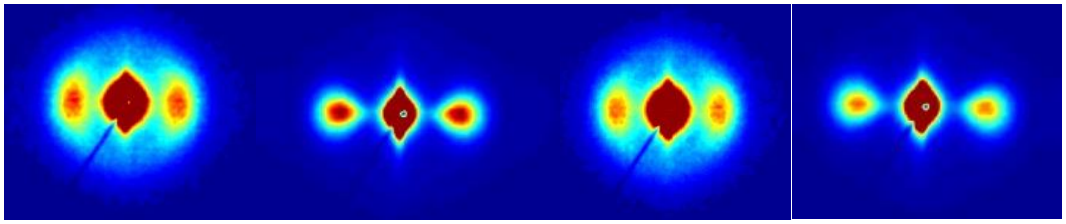

(a) (b) (c) (d)

Figure A.21 : SAXS images of samples (a) 5%POSS/PP-1/20, (b) 5%POSS/PP-1/120, (c) 5%POSS/PP-05/20, (d) 5%POSS/PP-05/120 for 1h explosure time.

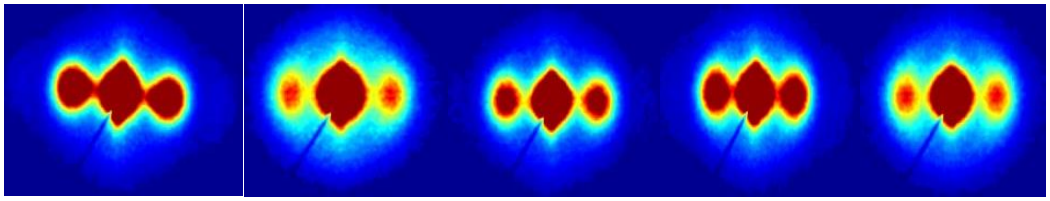

(a) (b) (c) (d) (e)

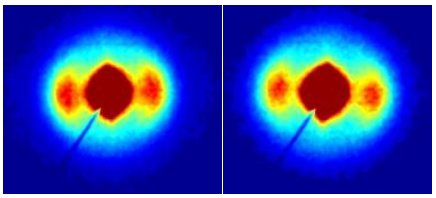

(f) (g)

Figure A.22 : SAXS images of samples (a) 8%POSS/PP-0.5/120, (b) 8%POSS/PP -0.5/40, (c) 8%POSS/PP-1/100, (d) 8%POSS/PP-2/120, (e) 8%POSS/PP-2/60 for 30 min explosure time and (f) 8%POSS/PP-2/20, (g) 8%POSS/PP-1/20 for 1h explosure time.

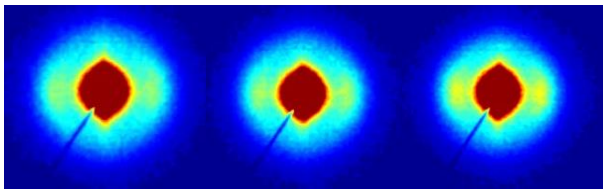

(a) (b) (c)

Figure A.23 : SAXS images of samples (a) 10%POSS/PP-0.2/40, (b) 10%POSS/PP -2/80, (c) 10%POSS/PP-2/100 for 1h explosure time.

SAXS GRAPHS

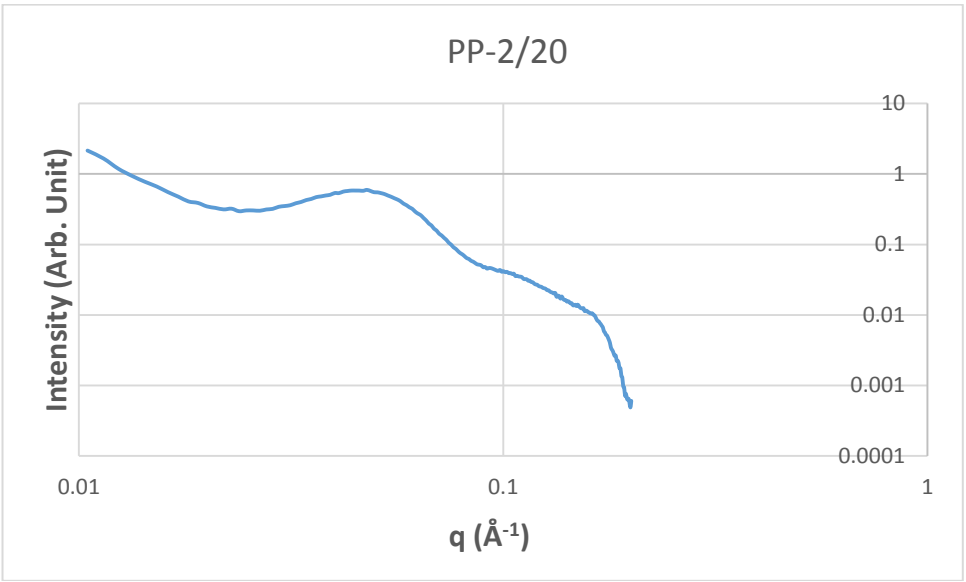

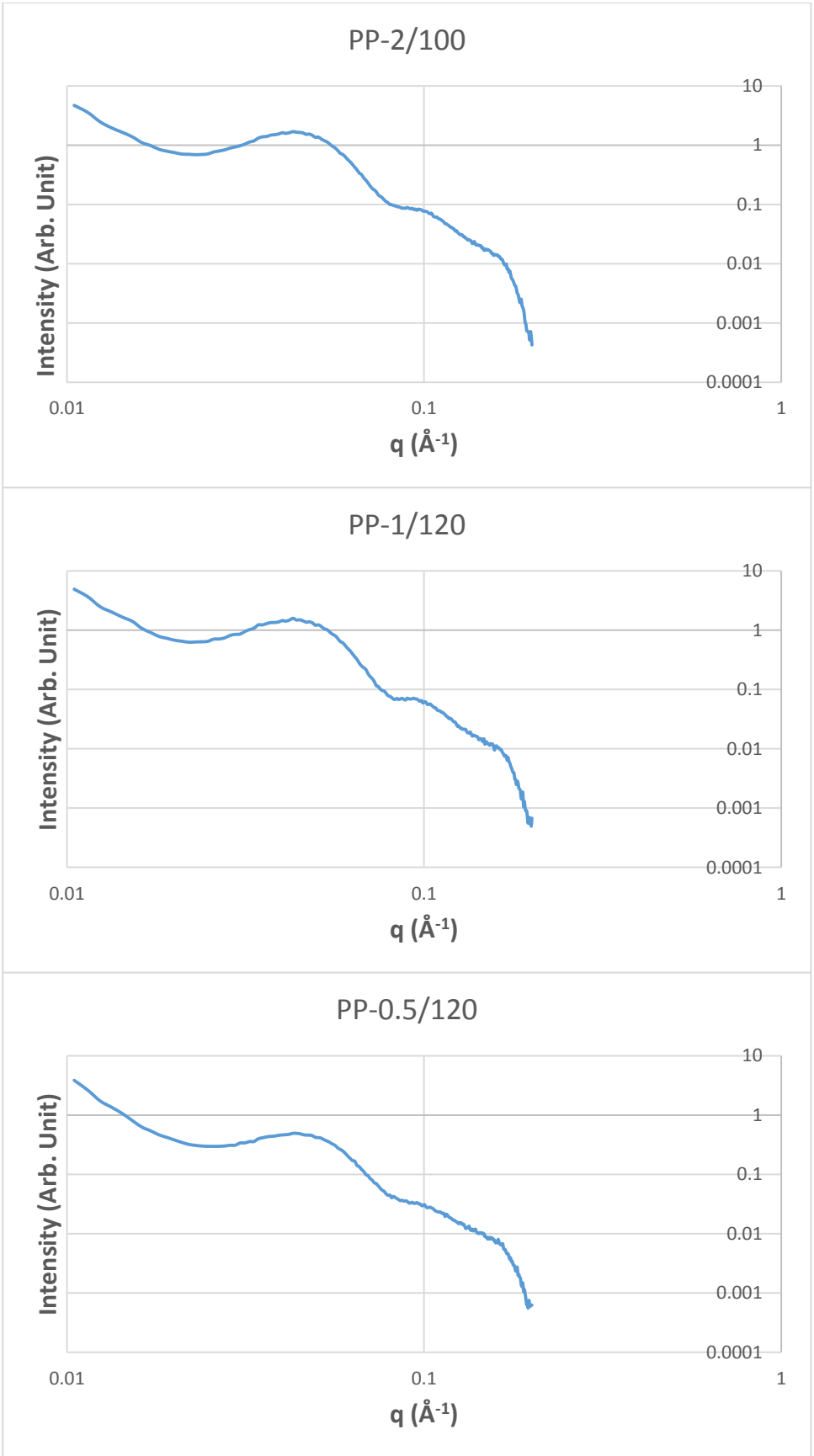
PP-2/100
Intensity (Arb. Unit)
10
1
0.1
0.01
0.001
0.0001
0.01
0.1
1
q (Å-1)
PP-1/120
Intensity (Arb. Unit)
10
1
0.1
0.01
0.001
0.0001
0.01
0.1
1
q (Å-1)
PP-0.5/120
Intensity (Arb. Unit)
10
1
0.1
0.01
0.001
0.0001
0.01
0.1
1
q (Å-1)

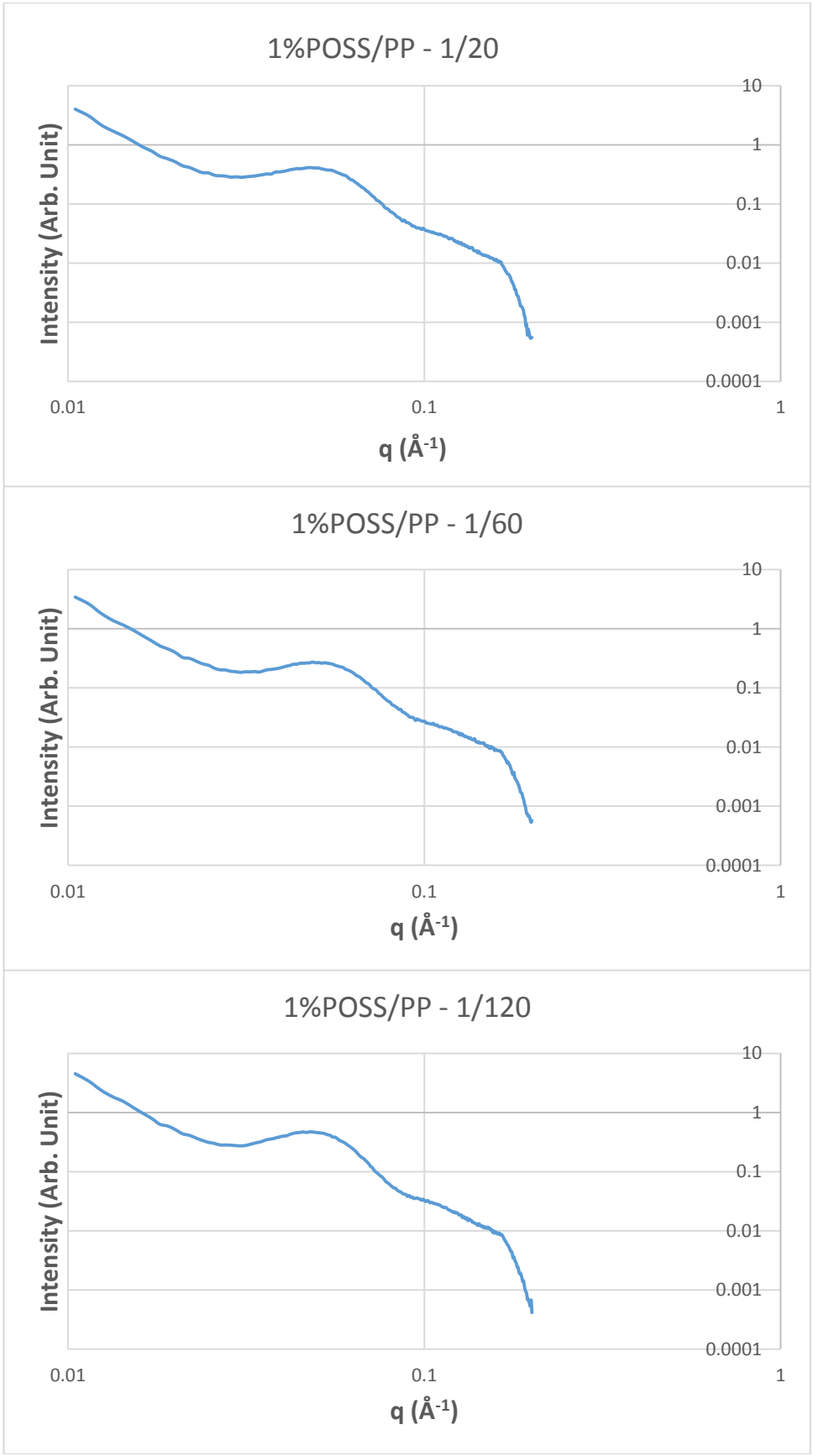
1%POSS/PP - 1/20
Intensity (Arb. Unit)
10
1
0.1
0.01
0.001
0.0001
0.01
0.1
1
q (Å-1)
1%POSS/PP - 1/60
Intensity (Arb. Unit)
10
1
0.1
0.01
0.001
0.0001
0.01
0.1
1
q (Å-1)
1%POSS/PP - 1/120
Intensity (Arb. Unit)
10
1
0.1
0.01
0.001
0.0001
0.01
0.1
1
q (Å-1)

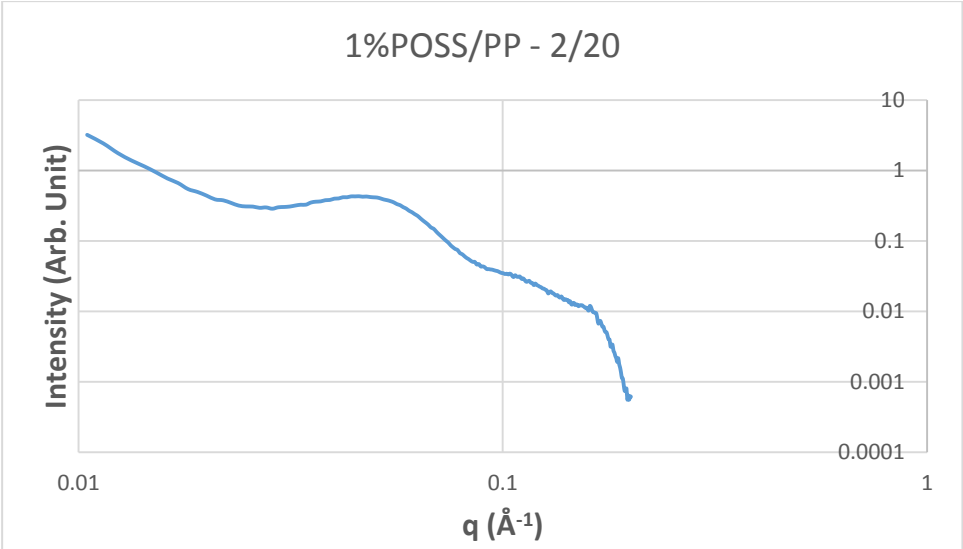
1%POSS/PP - 2/20
Intensity (Arb. Unit)
10
1
0.1
0.01
0.001
0.0001
0.01
0.1
1
q (Å-1)

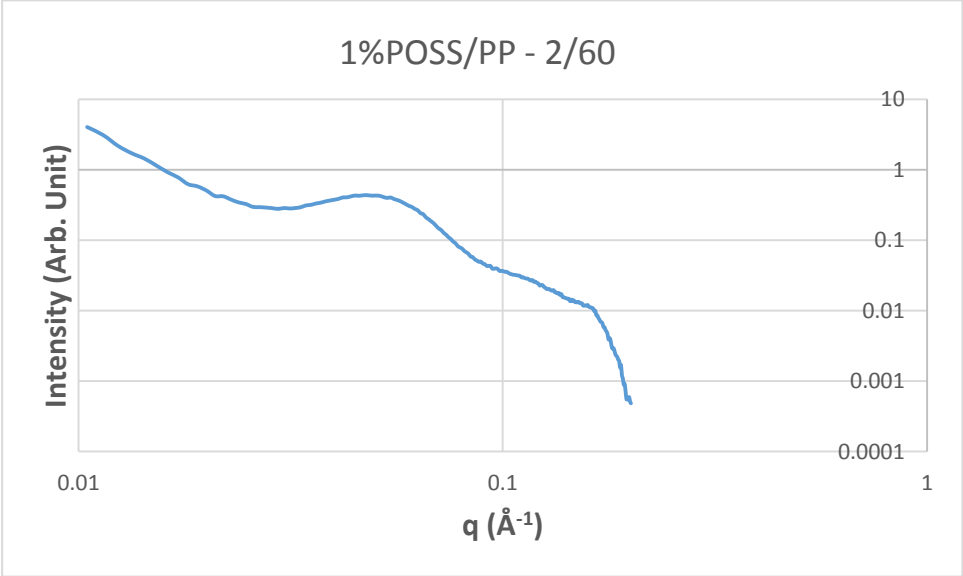
1%POSS/PP - 2/60
Intensity (Arb. Unit)
10
1
0.1
0.01
0.001
0.0001
0.01
0.1
1
q (Å-1)

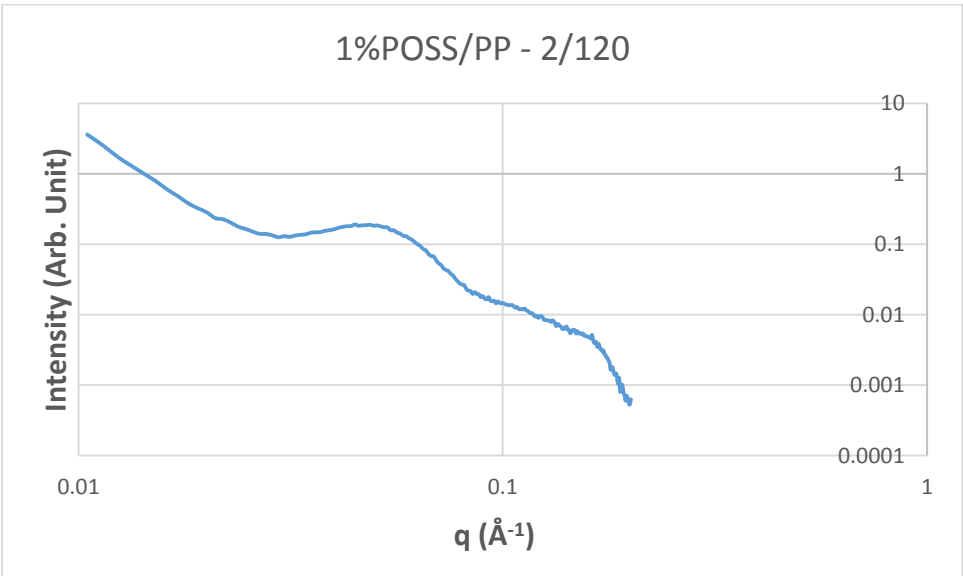
1%POSS/PP - 2/120
Intensity (Arb. Unit)
10
1
0.1
0.01
0.001
0.0001
0.01
0.1
1
q (Å-1)

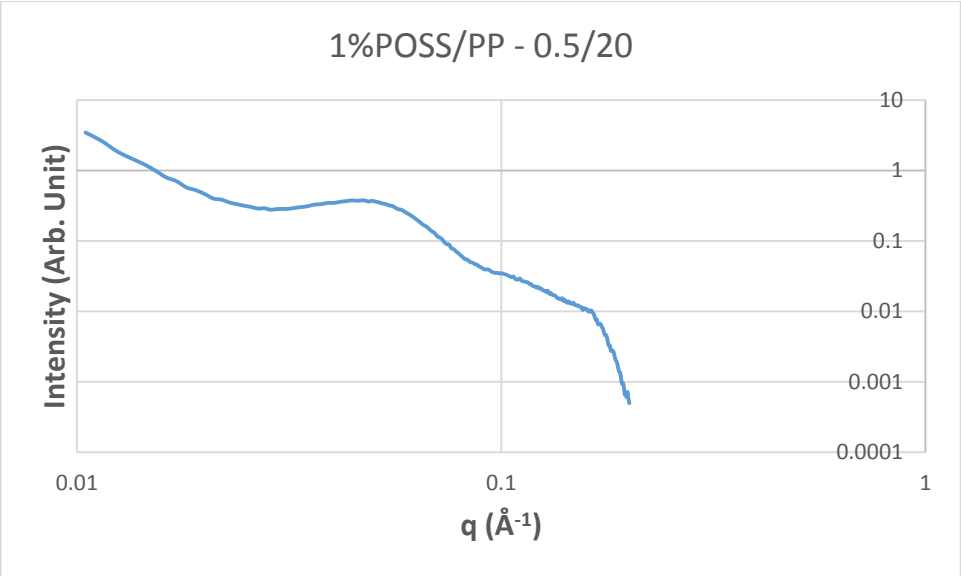
1%POSS/PP - 0.5/20
Intensity (Arb. Unit)
10
1
0.1
0.01
0.001
0.0001
0.01
0.1
1
q (Å-1)

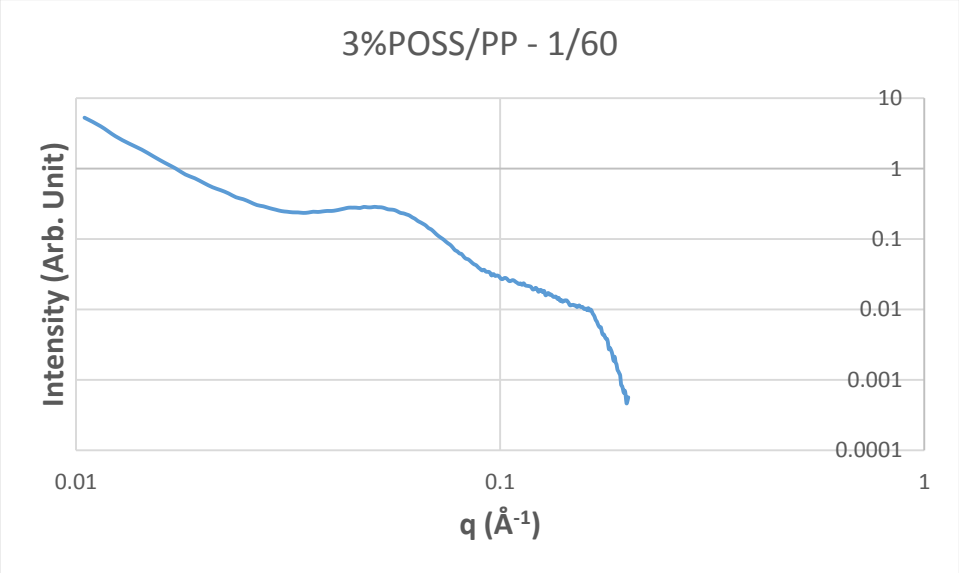
3%POSS/PP - 1/60
Intensity (Arb. Unit)
10
1
0.1
0.01
0.001
0.0001
0.01
0.1
1
q (Å-1)

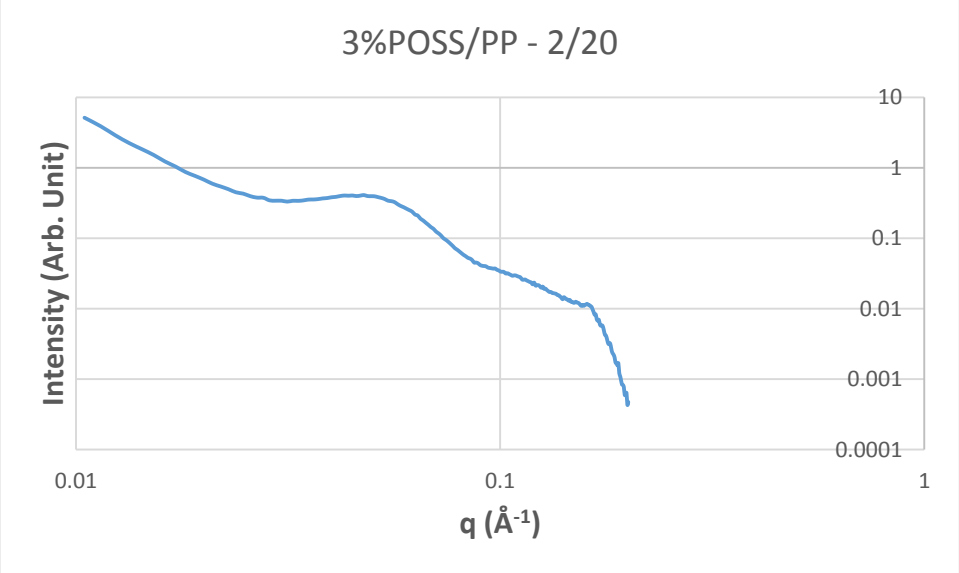
3%POSS/PP - 2/20
Intensity (Arb. Unit)
10
1
0.1
0.01
0.001
0.0001
0.01
0.1
1
q (Å-1)

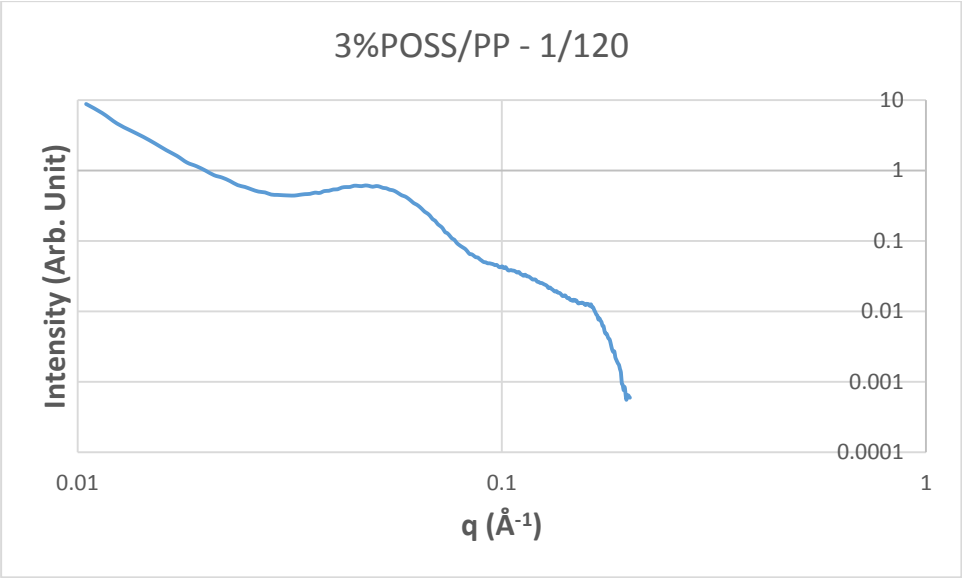
3%POSS/PP - 1/120
Intensity (Arb. Unit)
10
1
0.1
0.01
0.001
0.0001
0.01
0.1
1
q (Å-1)

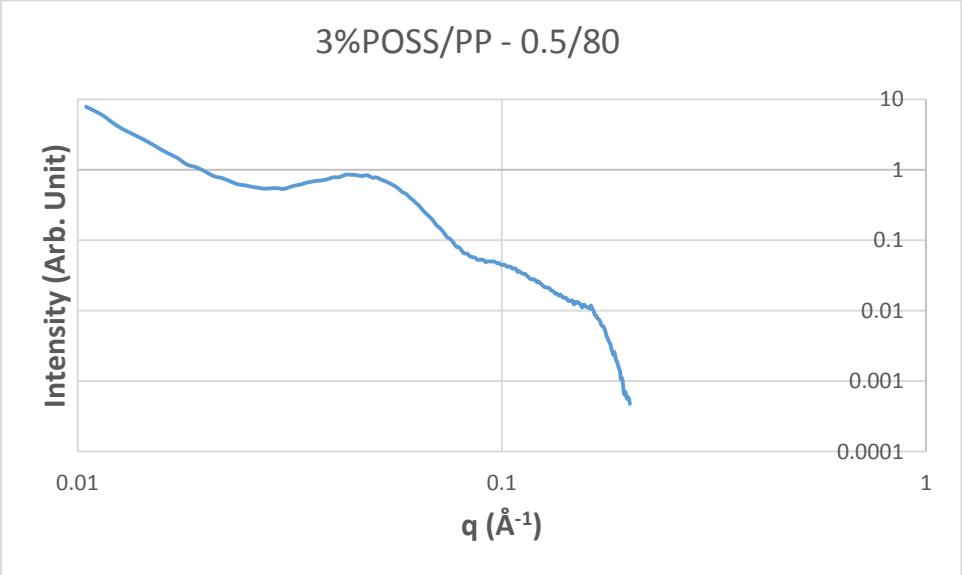
3%POSS/PP - 0.5/80
Intensity (Arb. Unit)
10
1
0.1
0.01
0.001
0.0001
0.01
0.1
1
q (Å-1)

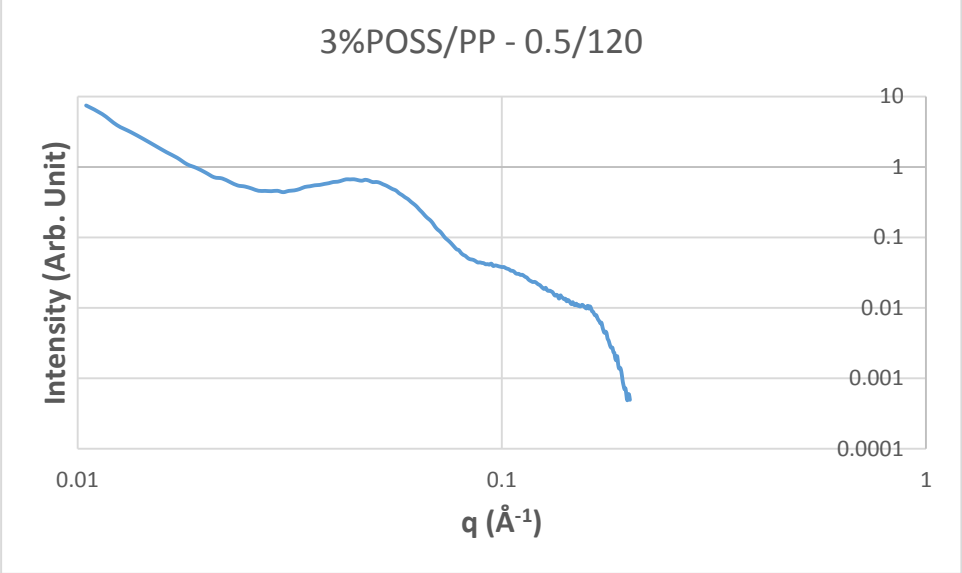
3%POSS/PP - 0.5/120
Intensity (Arb. Unit)
10
1
0.1
0.01
0.001
0.0001
0.01
0.1
1
q (Å-1)

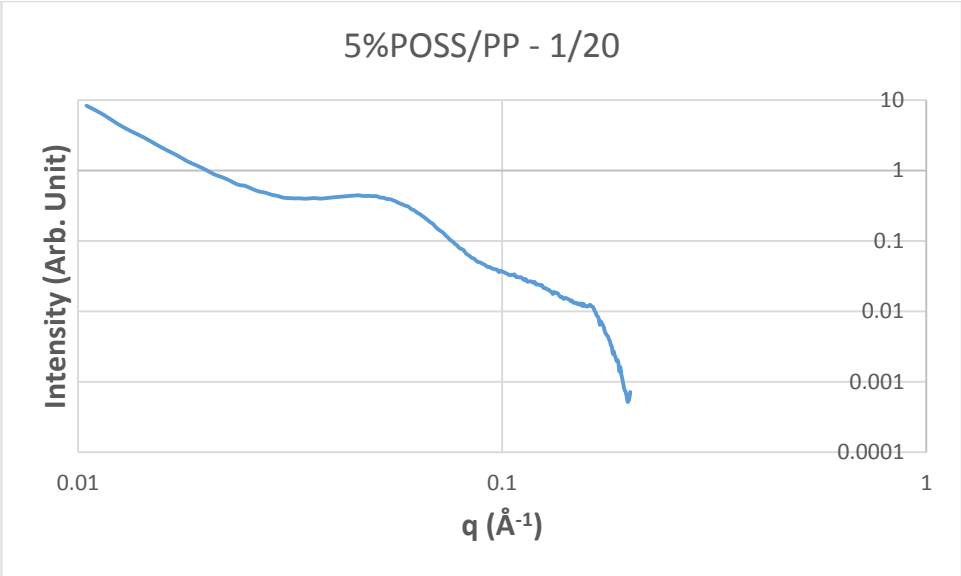
5%POSS/PP - 1/20
Intensity (Arb. Unit)
10
1
0.1
0.01
0.001
0.0001
0.01
0.1
1
q (Å-1)

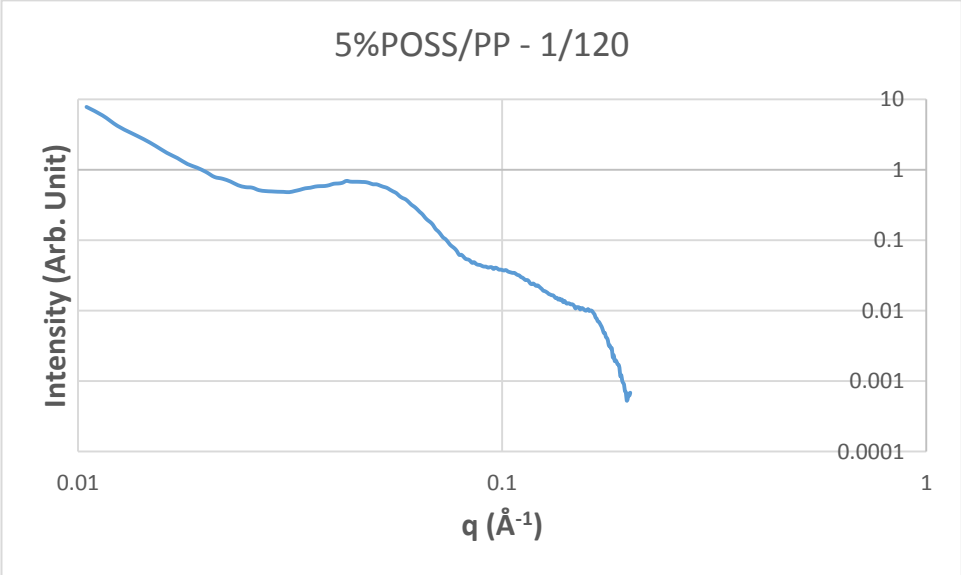
5%POSS/PP - 1/120
Intensity (Arb. Unit)
10
1
0.1
0.01
0.001
0.0001
0.01
0.1
1
q (Å-1)

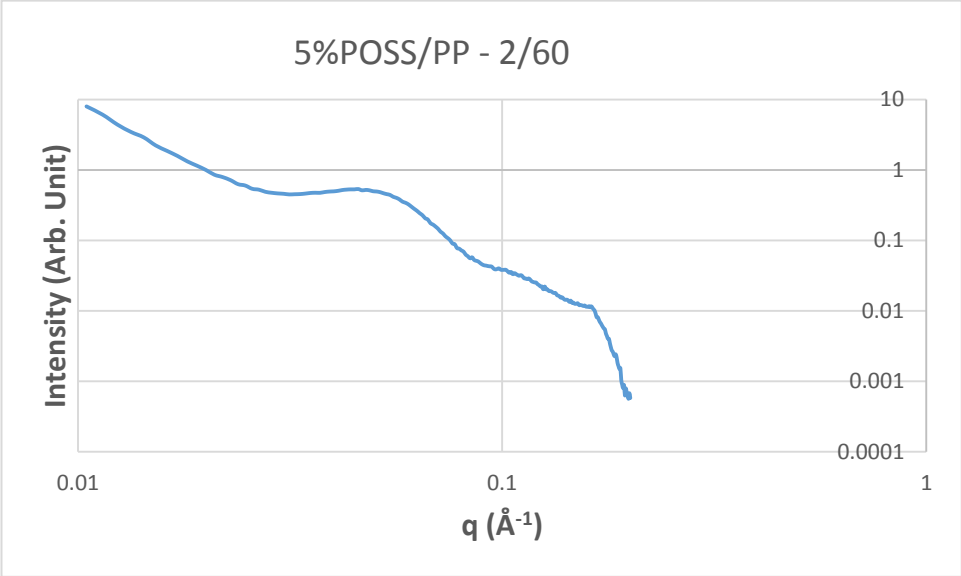
5%POSS/PP - 2/60
Intensity (Arb. Unit)
10
1
0.1
0.01
0.001
0.0001
0.01
0.1
1
q (Å-1)

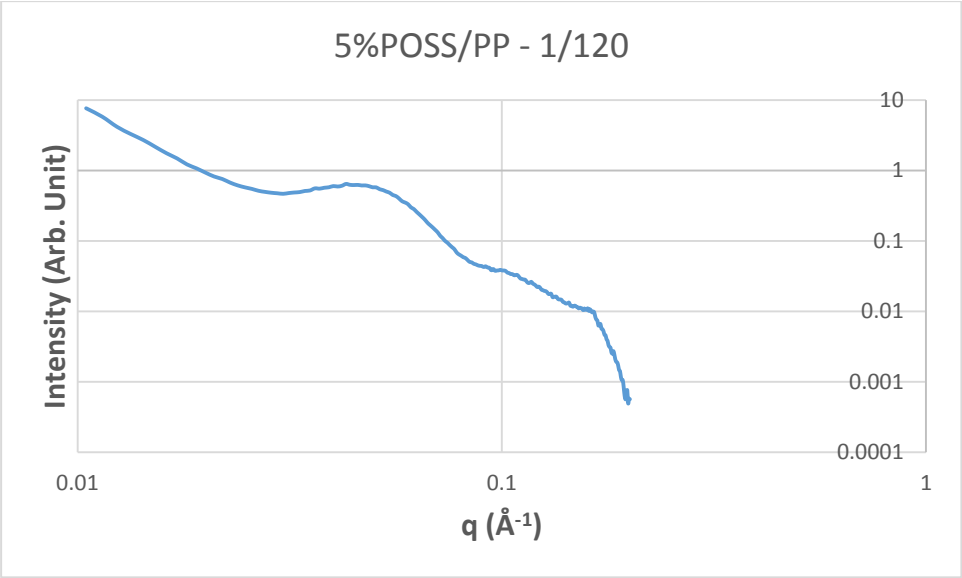
5%POSS/PP - 1/120
Intensity (Arb. Unit)
10
1
0.1
0.01
0.001
0.0001
0.01
0.1
1
q (Å-1)

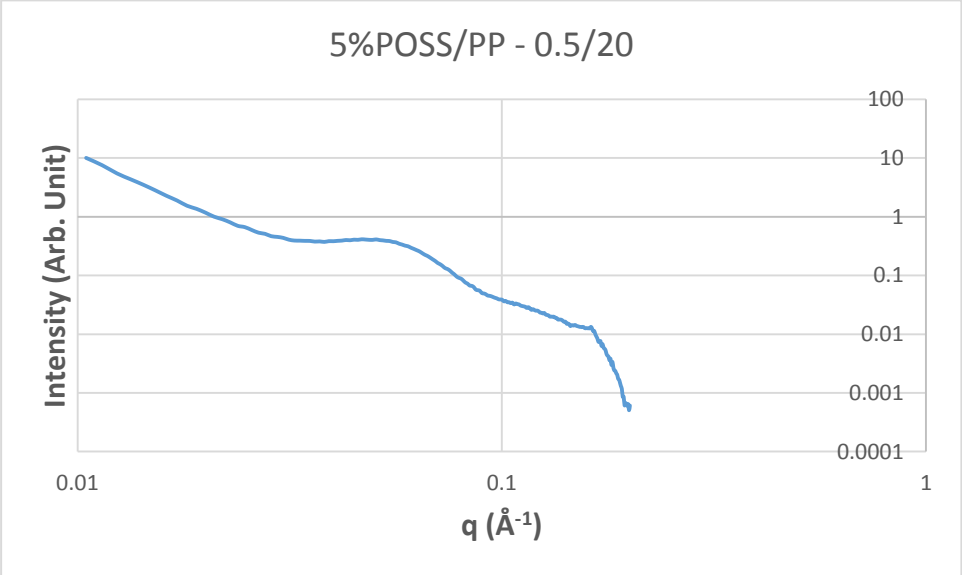
5%POSS/PP - 0.5/20
Intensity (Arb. Unit)
100
10
1
0.1
0.01
0.001
0.0001
0.01
0.1
1
q (Å-1)

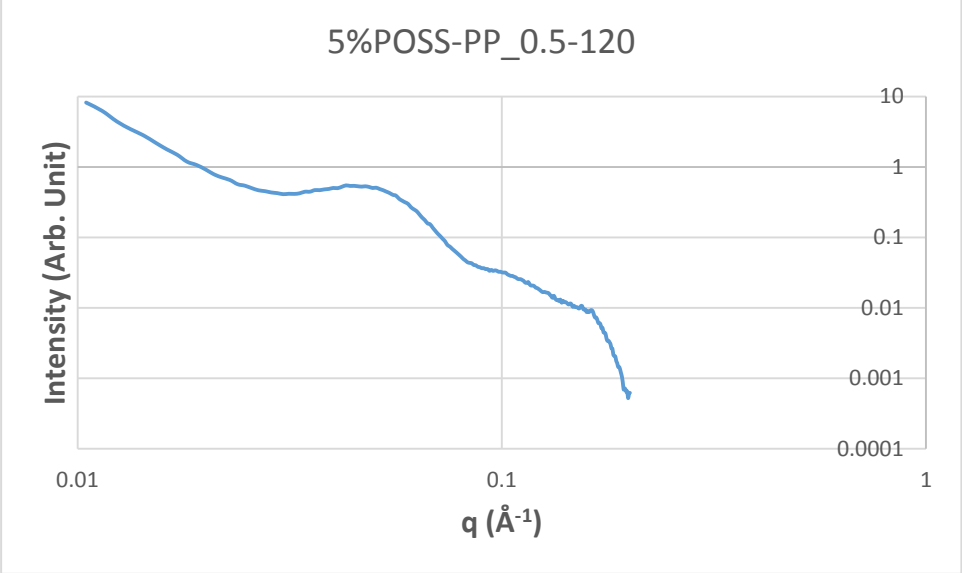
5%POSS-PP_0.5-120
Intensity (Arb. Unit)
10
1
0.1
0.01
0.001
0.0001
0.01
0.1
1
q (Å-1)

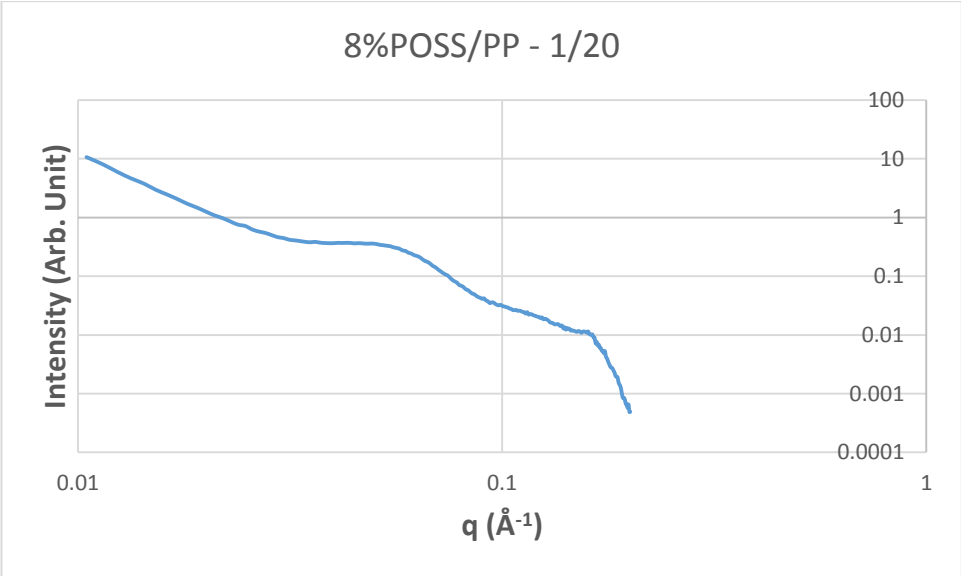
8%POSS/PP - 1/20
Intensity (Arb. Unit)
100
10
1
0.1
0.01
0.001
0.0001
0.01
0.1
1
q (Å-1)

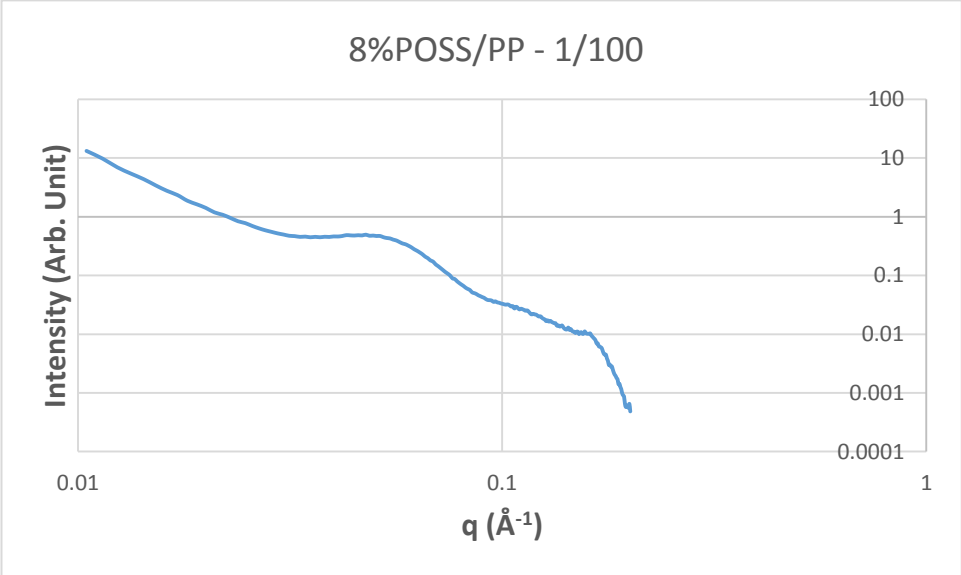
8%POSS/PP - 1/100
Intensity (Arb. Unit)
100
10
1
0.1
0.01
0.001
0.0001
0.01
0.1
1
q (Å-1)

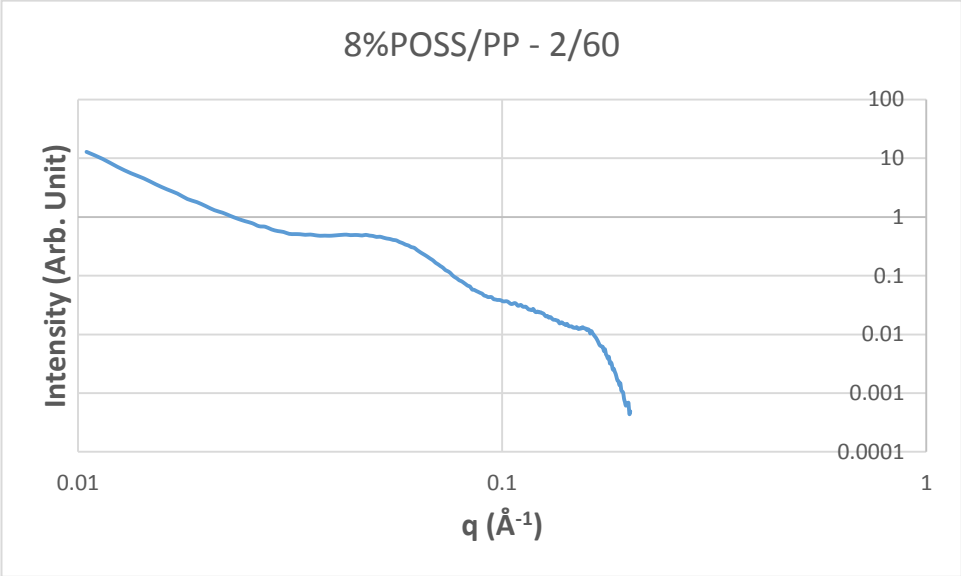
8%POSS/PP - 2/60
Intensity (Arb. Unit)
100
10
1
0.1
0.01
0.001
0.0001
0.01
0.1
1
q (Å-1)

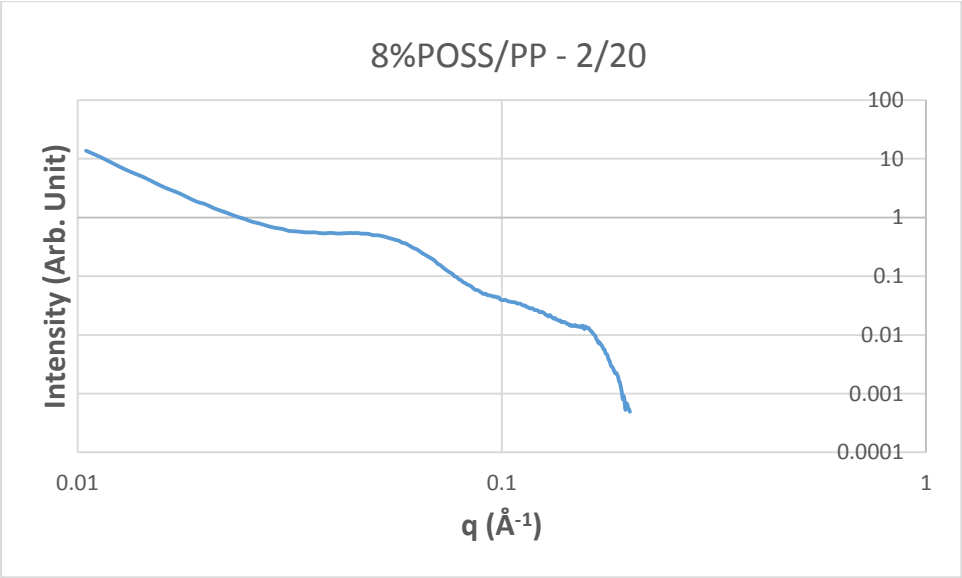
8%POSS/PP - 2/20
Intensity (Arb. Unit)
100
10
1
0.1
0.01
0.001
0.0001
0.01
0.1
1
q (Å-1)

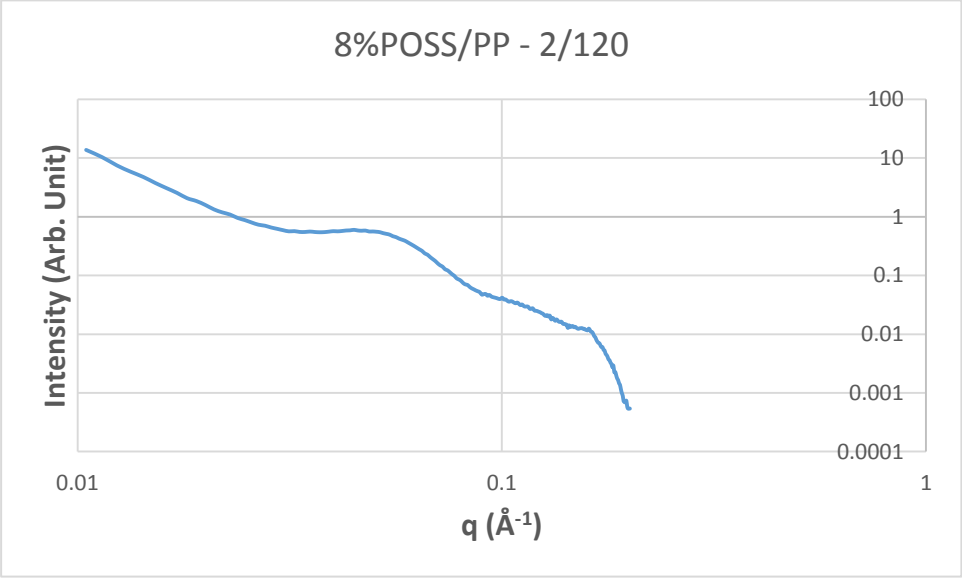
8%POSS/PP - 2/120
Intensity (Arb. Unit)
100
10
1
0.1
0.01
0.001
0.0001
0.01
0.1
1
q (Å-1)

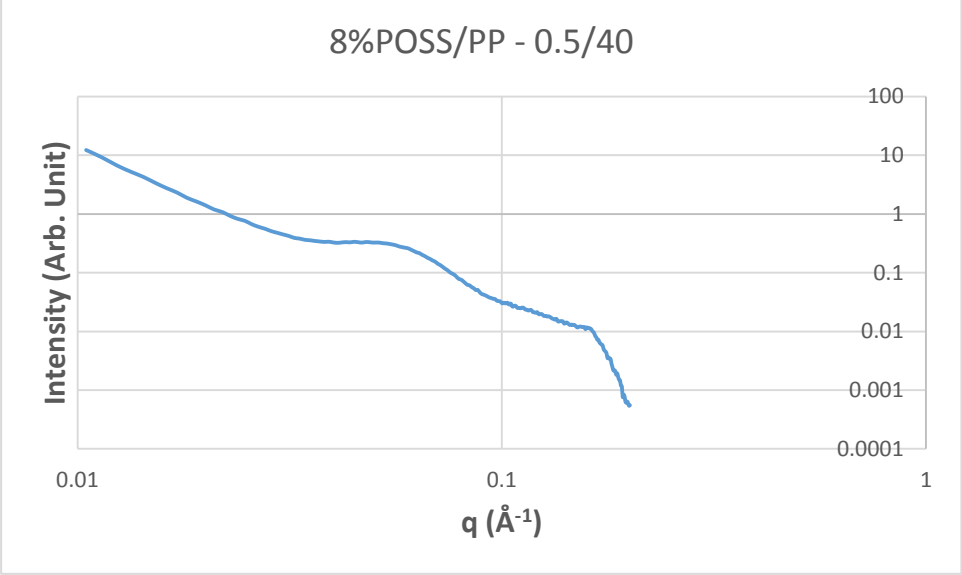
8%POSS/PP - 0.5/40
Intensity (Arb. Unit)
100
10
1
0.1
0.01
0.001
0.0001
0.01
0.1
1
q (Å-1)

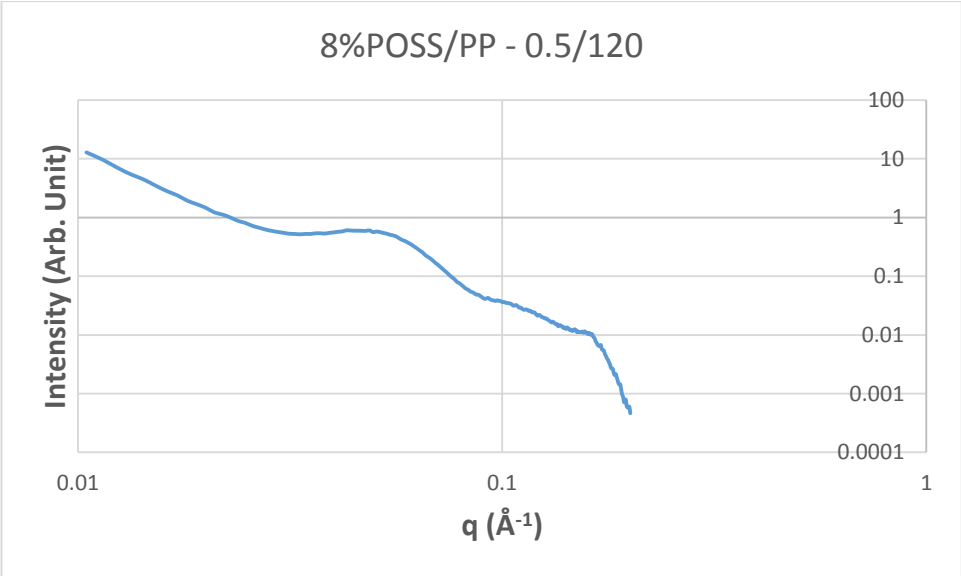
8%POSS/PP - 0.5/120
Intensity (Arb. Unit)
100
10
1
0.1
0.01
0.001
0.0001
0.01
0.1
1
q (Å-1)

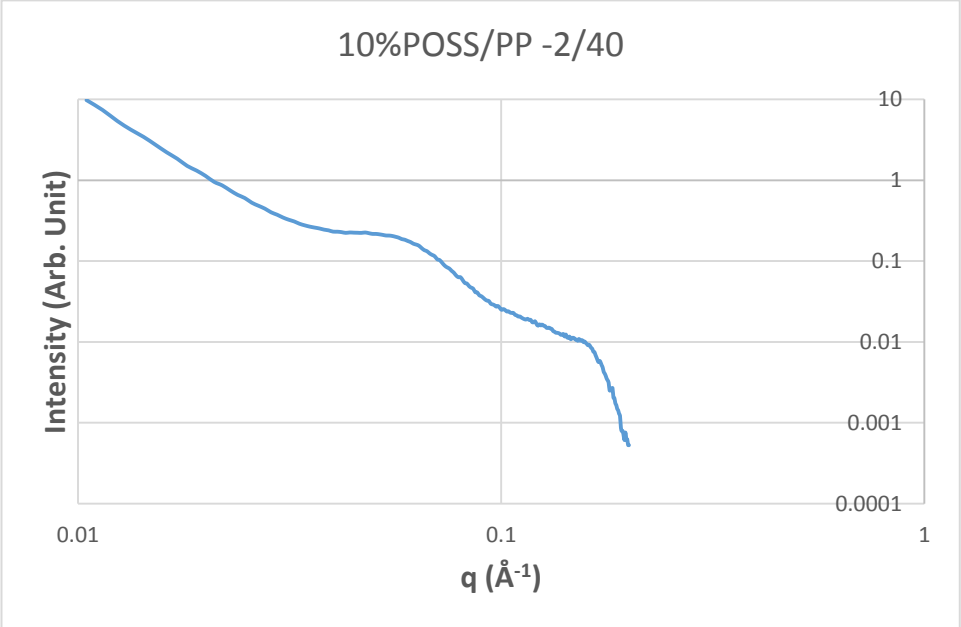
10%POSS/PP -2/40
Intensity (Arb. Unit)
10
1
0.1
0.01
0.001
0.0001
0.01
0.1
1
q (Å-1)

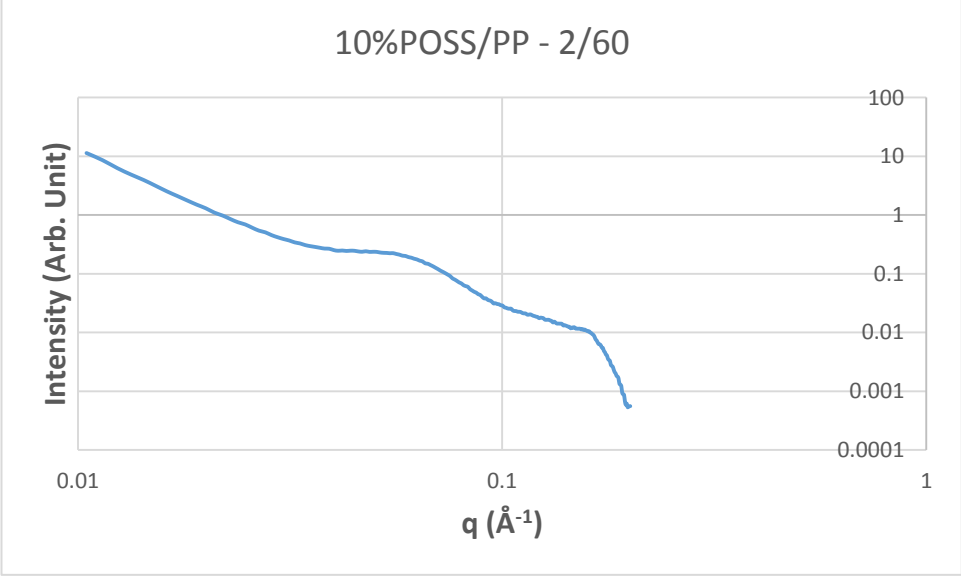
10%POSS/PP - 2/60
Intensity (Arb. Unit)
100
10
1
0.1
0.01
0.001
0.0001
0.01
0.1
1
q (Å-1)

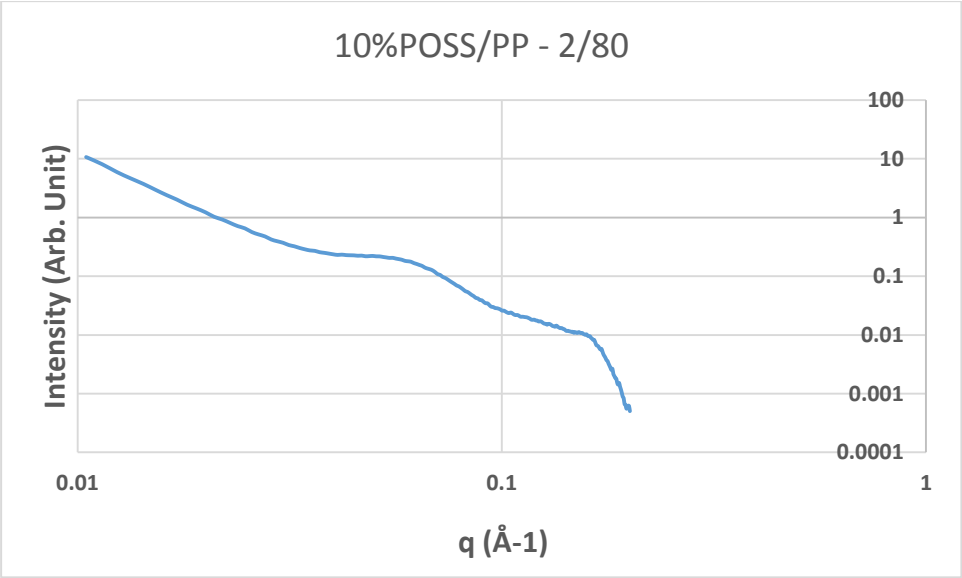
10%POSS/PP - 2/80
Intensity (Arb. Unit)
100
10
1
0.1
0.01
0.001
0.0001
0.01
0.1
1
q (Å-1)

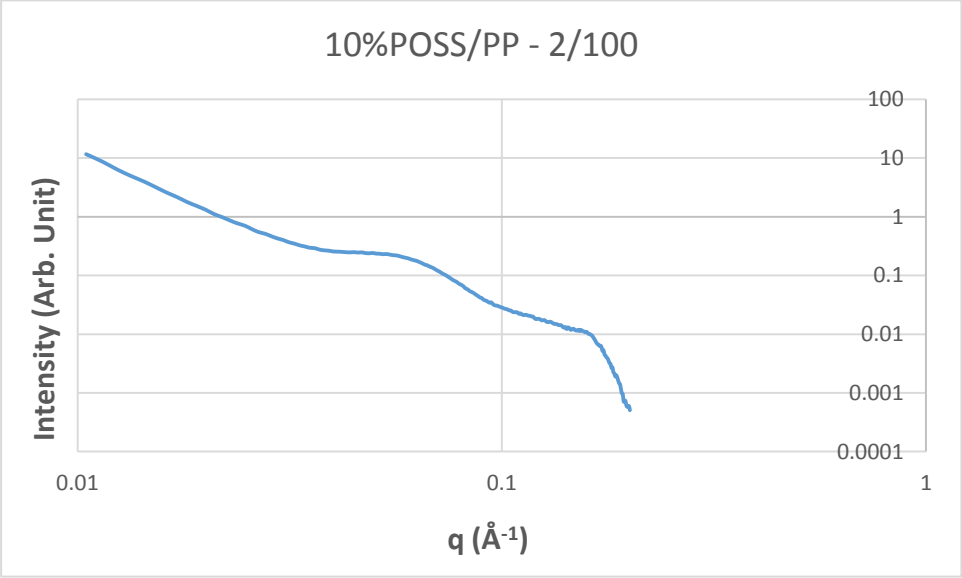
10%POSS/PP - 2/100
Intensity (Arb. Unit)
100
10
1
0.1
0.01
0.001
0.0001
0.01
0.1
1
q (Å-1)

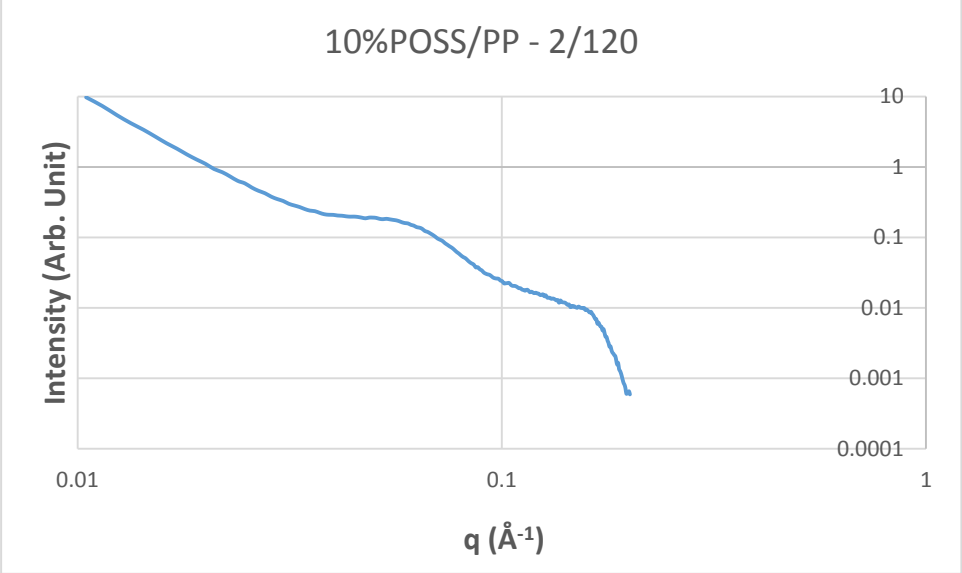
10%POSS/PP - 2/120
Intensity (Arb. Unit)
10
1
0.1
0.01
0.001
0.0001
0.01
0.1
1
q (Å-1)

APPENDIX B

Table B.1 : Tensile data for all samples

PP-0.5 (mm/min) plunger speed

rpm	Maximum Load (N)	Tensile stress at Max. Load (MPa)	Tensile strain at Max.	Tensile strain at Break (%)	Tensile stress at Yield (MPa)	Modulus (E-modulus) (MPa)
20	0.55	54	745	844	32	651
40	0.36	73	858	976	34	668
60	0.34	78	631	651	61	794
80	0.22	89	727	775	89	569
100	0.24	95	618	655	96	1357
120	0.27	95	609	670	95	1420

PP-1 (mm/min) plunger speed

rpm	Maximum Load (N)	Tensile stress at Max. Load (MPa)	Tensile strain at Max.	Tensile strain at Break (%)	Tensile stress at Yield (MPa)	Modulus (E-modulus) (MPa)
20	1.58	50	875	991	33	1452
40	0.69	64	721	867	49	1477
60	0.65	71	700	875	69	1008
80	0.41	61	578	751	34	880
100	0.44	73	670	850	73	906
120	0.41	84	690	764	84	872

PP-2 (mm/min) plunger speed

rpm	Maximum Load (N)	Tensile stress at Max. Load (MPa)	Tensile strain at Max.	Tensile strain at Break (%)	Tensile stress at Yield (MPa)	Modulus (E-modulus) (MPa)
20	2.11	46	929	1009	35	1423
40	1.21	51	742	924	36	1452
60	1.23	64	860	956	39	1675
80	0.82	63	805	900	38	1554
100	0.71	73	726	769	53	1699
120	0.62	76	684	1062	76	2479

1%POSS/PP-0.5 (mm/min) plunger speed

rpm	Maximum Load (N)	Tensile stress at Max. Load (MPa)	Tensile strain at Max.	Tensile strain at Break (%)	Tensile stress at Yield (MPa)	Modulus (E-modulus) (MPa)
20	0.39	33	477.	848	23	1008
40	0.25	79	604	729	72	461
60	0.65	33	459	650	28	1130
80	0.37	53	746	1048	34	1015
100	0.35	29	601	903	22	977
120	0.55	47	727	868	30	1039

1%POSS/PP- 1 (mm/min) plunger speed

rpm	Maximum Load (N)	Tensile stress at Max. Load (MPa)	Tensile strain at Max.	Tensile strain at Break (%)	Tensile stress at Yield (MPa)	Modulus (E-modulus) (MPa)
20	0.78	32	945	1112	31	1112
40	0.47	43	871	1088	27	1166
60	0.35	52	684	910	25	687
80	0.27	49	661	870	19	396
100	0.29	47	654	809	22	475
120	0.18	73	577	703	34	1165

1%POSS/PP-2 (mm/min) plunger speed

rpm	Maximum Load (N)	Tensile stress at Max. Load (MPa)	Tensile strain at Max.	Tensile strain at Break (%)	Tensile stress at Yield (MPa)	Modulus (E-modulus) (MPa)
20	1.39	29	1128	1299	24	636
40	0.68	27	671	1075	26	1078
60	0.58	33	661	914	27	1023
80	0.62	47	778	1059	27	1392
100	0.38	36	595	925	24	965
120	0.35	47	574	854	27	1126

3%POSS/PP-0.5 (mm/min) plunger speed

rpm	Maximum Load (N)	Tensile stress at Max. Load (MPa)	Tensile strain at Max.	Tensile strain at Break (%)	Tensile stress at Yield (MPa)	Modulus (E-modulus) (MPa)
20	0.68	44	866	958	30	1208
40	0.29	52	701	897	34	762
60	0.19	61	506	630	41	549
80	0.21	73	500	595	47	889
100	0.27	56	658	730	36	698
120	0.11	52	618	584	50	1130

3%POSS/PP-1 (mm/min) plunger speed

rpm	Maximum Load (N)	Tensile stress at Max. Load (MPa)	Tensile strain at Max.	Tensile strain at Break (%)	Tensile stress at Yield (MPa)	Modulus (E-modulus) (MPa)
20	0.76	30	816	1160	29	921
40	0.32	31	747	1034	27	1530
60	0.27	40	768	977	27	534
80	0.31	42	739	955	30	668
100	0.15	46	616	681	33	651
120	0.19	52	666	768	34	368

3%POSS/PP-2 (mm/min) plunger speed

rpm	Maximum Load (N)	Tensile stress at Max. Load (MPa)	Tensile strain at Max.	Tensile strain at Break (%)	Tensile stress at Yield (MPa)	Modulus (E-modulus) (MPa)
20	1.85	36	1122	1110	32	1239
40	0.74	32	838	1038	29	1242
60	0.66	43	857	1029	30	1287
80	0.61	43	773	1089	33	1309
100	0.51	48	47	931	32	1561
120	0.41	54	781	918	34	841

5%POSS/PP-0.5 (mm/min) plunger speed

rpm	Maximum Load (N)	Tensile stress at Max. Load (MPa)	Tensile strain at Max.	Tensile strain at Break (%)	Tensile stress at Yield (MPa)	Modulus (E-modulus) (MPa)
20	0.54	39	815	1176	29	1403
40	0.3	56	675	866	35	655
60	0.18	50	687	809	29	558
80	0.11	47	559	632	37	757
100	0.11	54	490	625	43	750
120	0.1	51	481	556	47	1306

5%POSS/PP-1 (mm/min) plunger speed

rpm	Maximum Load (N)	Tensile stress at Max. Load (MPa)	Tensile strain at Max.	Tensile strain at Break (%)	Tensile stress at Yield (MPa)	Modulus (E-modulus) (MPa)
20	0.73	35	845	986	28	1258
40	0.47	49	697	880	33	1564
60	0.29	46	609	802	29	726
80	0.25	69	582	636	39	556
100	0.27	64	564	634	40	928
120	0.22	61	580	686	34	538

5%POSS/PP-2 (mm/min) plunger speed

rpm	Maximum Load (N)	Tensile stress at Max. Load (MPa)	Tensile strain at Max.	Tensile strain at Break (%)	Tensile stress at Yield (MPa)	Modulus (E-modulus) (MPa)
20	1.73	37	826	1008	30	1157
40	1.03	43	814	1044	32	1259
60	0.68	46	661	1070	33	1404
80	0.65	51	736	984	33	1592
100	0.37	71	634	690	62	912
120	0.41	71	662	729	43	947

8%POSS/PP-0.5 (mm/min) plunger speed

rpm	Maximum Load (N)	Tensile stress at Max. Load (MPa)	Tensile strain at Max.	Tensile strain at Break (%)	Tensile stress at Yield (MPa)	Modulus (E-modulus) (MPa)
20	0.52	43	801	1168	39	1521
40	0.34	64	773	929	33	715
60	0.27	71	652	986	59	858
80	0.26	92	622	717	56	648
100	0.2	87	531	620	50	1794
120	0.17	107	476	562	107	520

8%POSS/PP-1 (mm/min) plunger speed

rpm	Maximum Load (N)	Tensile stress at Max. Load (MPa)	Tensile strain at Max.	Tensile strain at Break (%)	Tensile stress at Yield (MPa)	Modulus (E-modulus) (MPa)
20	0.95	35	913	1016	26	992
40	0.49	38	772	1066	28	1123
60	0.27	53	638	844	28	381
80	0.28	55	653	839	31	542
100	0.24	49	554	814	30	493
120	0.19	51	573	732	32	540

8%POSS/PP-2 (mm/min) plunger speed

rpm	Maximum Load (N)	Tensile stress at Max. Load (MPa)	Tensile strain at Max.	Tensile strain at Break (%)	Tensile stress at Yield (MPa)	Modulus (E-modulus) (MPa)
20	1.46	31	1201	956	26	667
40	0.92	35	871	1223	23	508
60	0.82	43	861	933	25	1034
80	0.52	35	705	938	23	759
100	0.4	41	732	776	21	421
120	0.41	37	695	889	21	407

10%POSS/PP-2 (mm/min) plunger speed

rpm	Maximum Load (N)	Tensile stress at Max. Load (MPa)	Tensile strain at Max.	Tensile strain at Break (%)	Tensile stress at Yield (MPa)	Modulus (E-modulus) (MPa)
20	1.06	26	867	793	23	600
40	0.53	33	864	969	20	747
60	0.31	24	704	865	19	417
80	0.46	38	945	1045	20	851
100	0.33	37	749	823	21	547
120	0.26	31	632	798	23	619

10%POSS/PP-1 (mm/min) plunger speed

rpm	Maximum Load (N)	Tensile stress at Max. Load (MPa)	Tensile strain at Max.	Tensile strain at Break (%)	Tensile stress at Yield (MPa)	Modulus (E-modulus) (MPa)
20	0.49	25	708	836	19	601

CURRICULUM VITAE

Name Surname: Sevil KAYNAR

Place and Date of Birth: Bursa – 19.07.1992

E-Mail: sevilkaynar@gmail.com

EDUCATION:

B.Sc.: Yıldız Technical University - Metallurgical and Material Engineering

M.Sc.: Istanbul Technical Univertsity - Polymer Science and Technology

EXPERIENCE:

Visiting Researcher, University of Akron, OH, USA. **(**June-Sept.2015)